TIGERBAY DEVELOPMENT

# Daisy, Thistle, and Gravel Creeks Hazard and Risk Assessment

**Final REV 2**
**December 12, 2022**

**BGC Project No.: 2143002**

Prepared by BGC Engineering Inc. for:
**Tigerbay Development Corporation**

BGC ENGINEERING INC. 500-980 Howe Street, Vancouver, BC Canada V6Z 0C8
Tel: 604.684.5900 Fax: 604.684.5909

# TABLE OF REVISIONS

| ISSUE | DATE | REV | REMARKS |
|---|---|---|---|
| DRAFT | July 20, 2022 | A | Original draft issue of hazard assessment report. |
| FINAL | August 9, 2022 | 0 | Final issue of hazard assessment. Risk assessment to follow. |
| DRAFT | August 22, 2022 | B | Draft issue of hazard and risk assessment. |
| FINAL | August 25, 2022 | 1 | Final issue of hazard and risk assessment. |
| FINAL | December 12, 2022 | 2 | Final issue of hazard and risk assessment with revisions in response to Piteau Associates (Piteau) and SLRD review comments. |

# LIMITATIONS

# EXECUTIVE SUMMARY

At the request of Tigerbay Development Corp (Tigerbay), BGC Engineering Inc. (BGC) completed a detailed assessment of steep creek hazards on Daisy, Thistle, and Gravel creeks through the proposed development south of Britannia Beach, BC. Steep creek processes include floods, debris floods, and debris flows that all result from a combination of steep terrain, rain, and debris (Figure E-1).

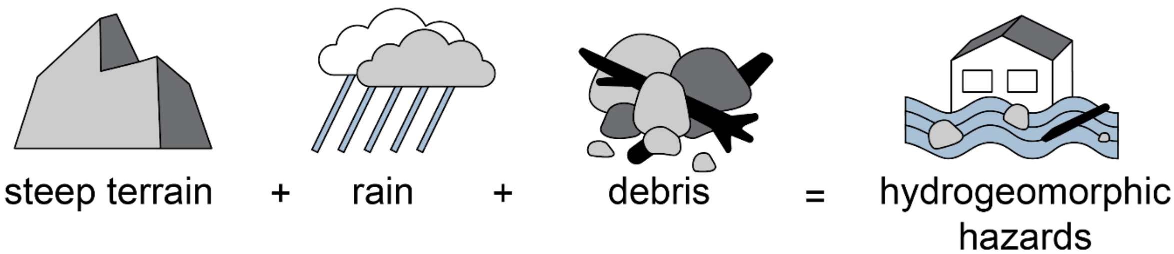


**Figure E-1-1.Illustration of steep creek hazards.**

Individual creeks can be susceptible to a range of these process types. This is the case for the study creeks as summarized in Table E-1.

**Table E-1. Dominant process types on study creeks.**

| Dominant Process Type Classification | Daisy Creek | Thistle Creek | Gravel Creek |
|---|---|---|---|
| BGC classification | Debris flows and debris floods | Floods and debris floods | Floods and debris floods |

This study builds on BGC's previous assessment of Gravel Creek (BGC, November 13, 2020). It is a baseline (pre-mitigation) assessment and will inform future phases of site and channel layout along with mitigation planning, as required. Using a combination of aerial imagery, desktop analysis, and field observations, BGC developed a relationship for each creek to describe how often (frequent) events of this nature are expected and at what size (magnitude) for a range of representative return periods (Table E-2). Each of these F-M relationships includes consideration of climate change impacts to the end of the century (2100). For Daisy Creek, BGC also considered the potential impacts of wildfires on debris-flow size and frequency and completed radiocarbon dating of samples from the proposed development area.

**Table E-2. Summary of best estimate F-M relationships for each study creek. Sediment volumes are reported as those arriving at the fan apex. For each return period the highest magnitude event is reported.**

| Representative Return Period (years) | Daisy Creek | | Thistle Creek | | Gravel Creek | |
|---|---|---|---|---|---|---|
| | Sediment Volume ($m^3$) | Peak Discharge ($m^3/s$) | Sediment Volume ($m^3$) | Peak Discharge ($m^3/s$) | Sediment Volume ($m^3$) | Peak Discharge ($m^3/s$) |
| 20 | 1,600 | 28 | 1,300 | 16 | - | 8 |
| 50 | 1,900 | 31 | 1,800 | 18 | - | 9 |
| 200 | 8,000 | 170 | 3,000 | 20 | 1,000 | 10 |
| 500 | 13,000 | 250 | 4,000 | 22 | 1,400 | 11 |
| 2,500 | 20,000 | 350 | 5,000 | 26 | 2,000 | 12 |
| 5,000 | 24,000 | 410 | - | - | - | - |

The F-M relationships were the foundational input for numerical modelling of the steep creek hazards. BGC used the numerical modelling program HEC-RAS to model floods, debris floods and debris flows on the creeks. The results illustrate that:

- Daisy Creek
  - The debris basin is effective at retaining debris-flow sediment volumes up to 2,500-year return period flows.
  - The culvert below Highway 99 is undersized to convey debris floods and debris flows for all return periods considered and overflow along Highway 99 is expected.
  - The CN Rail bridge has insufficient capacity and is expected to experience additional sedimentation which will further reduce the capacity.
- Thistle and Gravel creeks
  - Significant inundation (up to 3 m) will occur in all modelled return periods.
  - Most overbank flow stems from Gravel Creek which has a poorly defined channel within the proposed development area.
  - Water flow and ponding is expected on the upstream (east) side of Highway 99.

BGC created a composite hazard map to illustrate the hazard associated with steep creek processes within the proposed development area for baseline conditions (Drawing 08). The areas of highest hazard are within the creek channels. Moderate to low hazard was identified for areas along Daisy Creek where flow leaves the channel at the Highway 99, CN Rail, and downstream culvert crossings. Gravel Creek is poorly confined and overland flow contributes to low to moderate hazard in areas north of the main channel.

For the hazard scenarios considered in this assessment, modelled flows associated with floods, debris floods, and debris flows on the study creeks did not result in sufficient intensities that life loss is expected at any of the proposed building locations. BGC did not assess life safety risk to motorists on Highway 99. Flow depths are sufficient to result in economic damages within the proposed development in absence of channel improvements and mitigation works.

# TABLE OF CONTENTS

## LIST OF TABLES

## LIST OF FIGURES



## LIST OF APPENDICES



## LIST OF DRAWINGS

## ACKNOWLEDGEMENT

This report was originally completed in August 2022 with the final revisions completed after the untimely passing of Dr. Matthias Jakob, P.Geo., P.L.Eng., one of the leading international experts in steep creek hazards and risk. Dr. Jakob was engaged in the hazard and risk assessment throughout the project, including as part of field work. The project team is grateful for his contributions and acknowledges that the findings presented herein and report benefitted from his contribution and review.

# 1. INTRODUCTION

## 1.1. General

Tigerbay Development Corporation (Tigerbay) has proposed a mixed-use development in South Britannia, British Columbia (BC). The site is located approximately 10 km south of Squamish, BC along Highway 99 (Drawing 01). The proposed development includes land designations for multi-family residential dwellings, recreational facilities, tourism infrastructure, commercial facilities, natural spaces, and a 2.4 ha surf park (Figure 1-1).


**Figure 1-1. Proposed land use map (Ekistics, 2021).**

The proposed development intersects four creeks: from south to north these are Minaty Creek, Daisy Creek, Thistle Creek, and Gravel Creek (Drawing 01). At the request of Tigerbay, BGC Engineering Inc. (BGC) has completed a steep creek hazard and risk assessment for Daisy and Thistle creeks and updated BGC's 2020 hazard assessment for Gravel Creek (BGC, November 13, 2020). Minaty Creek is not included in the scope of this project.

This study forms part of the technical studies required as part of Tigerbay's application to amend the Squamish-Lillooet Regional District (SLRD) Official Community Plan (OCP) and Zoning Bylaw (540) to accommodate the proposed development.

## 1.2. Scope of Work

BGC's scope of work is outlined in the proposed work plan (BGC, January 24, 2022). The project was carried out under the terms of professional services agreement between Tigerbay and BGC dated February 16, 2022.

The scope of work includes:

- Steep creek geohazard assessment for Daisy and Thistle creeks and refinement of the hazard assessment at Gravel Creek, including:
  - Desktop analysis of Daisy and Thistle creeks to supplement the BGC (November 13, 2020) assessment of site conditions
  - Field study to assist in geohazard characterization and assessment of Daisy and Thistle creeks
  - Detailed frequency-magnitude analysis of Daisy, Thistle, and Gravel creeks
  - Numerical modelling on Daisy, Thistle, and Gravel creeks
  - Development of a composite hazard map for the study area.
- Quantitative individual and group life-loss risk assessments based on the hazard assessment results and proposed development layout.

BGC evaluated clearwater floods, debris floods, and debris flows. BGC did not assess additional geohazards that could threaten the study area which may include snow avalanches, sea level rise, earthquakes, tsunamis (generated by subaerial or submarine landslides, or earthquakes), liquefaction failures, delta front landslides or meteorological events. While landslides (debris slides, rock slides) were identified as part of the study area characterization, they were only considered in the hazard assessment if they contributed to the frequency and magnitude of debris flows and debris floods in the study area.

The study scope was informed by and followed guidance by Engineers and Geoscientists of British Columbia (EGBC, 2017) guidelines for flood map preparation, EGBC professional practice guidelines for Legislated Flood Assessments in a Changing Climate in BC (EGBC, 2018) and Landslide Assessments in British Columbia (EGBC, 2022). BGC also reviewed the BC Ministry of Transportation and Infrastructure (MoTI) Subdivision Preliminary Layout Review – Natural Hazard Risk directive (MoTI, 2015).

## 1.3. Study Team

The study team that contributed to this scope of work is summarized in Table 1-1.

**Table 1-1. Study team. Professional designations are for practice in British Columbia.**

| Project Role | Team Member |
|---|---|
| Project Manager, Technical Lead | Lauren Hutchinson, M.Sc., P.Eng. |
| Technical Reviewers | Matthias Jakob, Ph.D., P.Geo., P.L.Eng.<br>Hamish Weatherly, M.Sc., P.Geo. |
| Project Geoscientists / Engineers | Hazel Wong, M.Eng., P.Geo.<br>Hilary Shirra, B.A.Sc., E.I.T.<br>Sophia Zubrycky, M.A.Sc., E.I.T. |

## 1.4. Report Outline

This report summarizes the steep creek hazard and risk assessments at Daisy, Thistle, and Gravel creeks. Technical terminology related to steep creek hazard and risk pertinent to this study is summarized in Appendix A. This report is organized into the following sections:

- Section 2 (Steep Creek Hazards) provides an overview of steep creek hazards (debris floods and debris flows) and how they differ from floods. Additional detail on these hazards is provided in Appendix C.
- Section 3 (Study Area) describes the study area examined in this study. A summary of the data compiled and reviewed in support of this study is included in Appendix B.
- Section 4 (Hazard Assessment) presents the hazard assessment for Daisy, Thistle, and Gravel creeks. Additional details on the technical methods are provided in Appendix D. Section 4 also describes the results of the composite hazard mapping, which is generated from numerical flow modelling (Appendix E) and methods outlined in Appendix F.
- Section 5 (Risk Assessment) presents the results of the quantitative risk assessment.
- Section 6 (Conclusions) outlines the conclusions and considerations for hazard management.

Photographs of the study creeks collected by BGC as part of the field work are included in the Photographs Attachment.

# 2. STEEP CREEK HAZARDS

## 2.1. Introduction

Steep creek or hydrogeomorphic hazards are natural hazards that involve a mixture of water and debris or sediment (Figure 2-1). These hazards typically occur on creeks and steep rivers with small watersheds (usually less than 100 km$^2$) in mountainous terrain, usually after intense or long rainfall events, sometimes aided by snowmelt and worsened by forest fires.

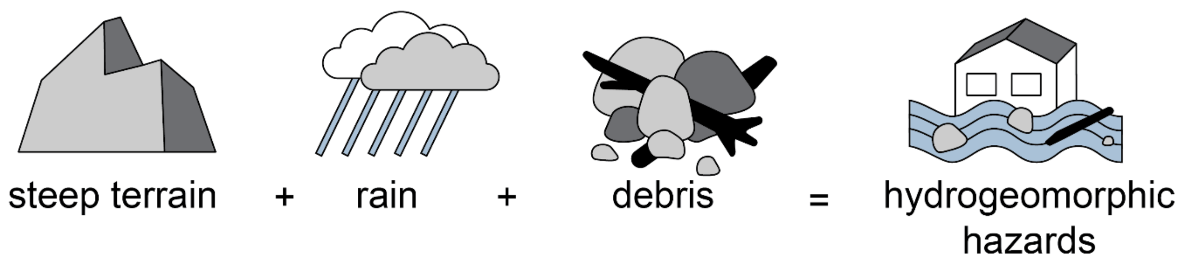


**Figure 2-1. Illustration of steep creek hazards.**

Steep creek hazards span a continuum of processes from clearwater floods (flood) to debris flows (Figure 2-2).

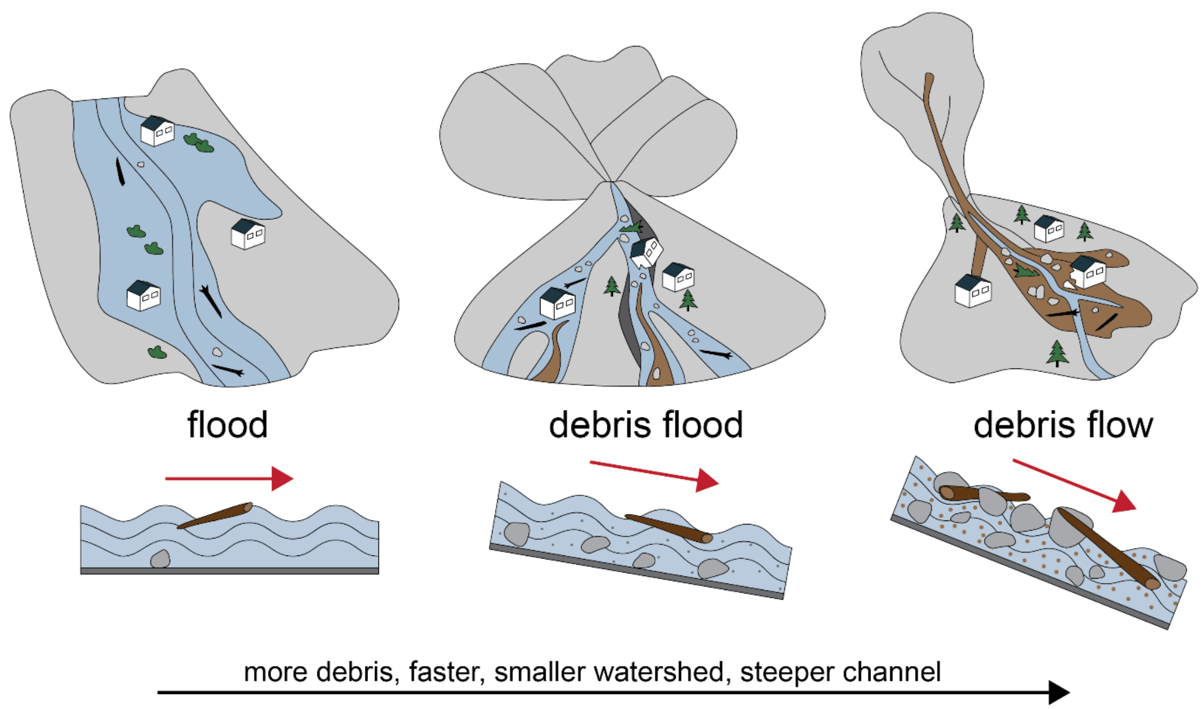


**Figure 2-2. Simplified illustration summarizing the hazards associated with each hydrogeomorphic process. BGC-created figure.**

The following two sections describe some general characteristics about debris floods and debris flows and how they differ from floods. More detail and the implications of these processes are provided in Appendix B.

## 2.2. Debris Floods

Debris floods occur when large volumes of water in a creek or river entrain the gravel, cobbles, and boulders on the channel bed; this is known as "full bed mobilization". Debris floods can occur from different mechanisms. BGC has adopted the definitions of three different sub-types of debris floods per Church and Jakob (2020):

- Type 1 – Debris floods that are generated from rainfall or snowmelt runoff resulting in sufficient water depth to result in full bed mobilization.
- Type 2 – Debris floods that are generated from diluted debris flows (e.g., a debris flow that runs into a main channel in the upper watershed).
- Type 3 – Debris floods that are generated from natural (e.g., landslide dam, glacial lake outbursts, moraine dam outbursts) or artificial dam (e.g., water retention or tailings dam) breaches.

Sediment and woody debris become entrained in floods leading to an increase in the volume of organic and mineral debris flowing down a channel, and an ensuing increase in peak discharge. This process is referred to as flow bulking. This phenomenon can be visualized by imagining a bucket of water spilled down a children's slide. When the bucket only contains water and a small amount of debris, that's a clearwater flood. If the bucket is refilled with 10 litres of water and subsequently a shovelful of sand and twigs is added, such that the water-sediment mixture occupies 12 litres, the mixture has been bulked by 20%. It has a bulking factor of 1.2. The water-sand mixture spilled down the slide represents a debris flood. The experiment can be repeated with increasing volumes of sediment until it becomes a debris flow (see Section 2.3).

The effects of debris floods can range from relatively harmless to catastrophic depending on their magnitude and duration. Debris floods can be relatively harmless if of short duration and low magnitude. In contrast, they can be damaging when they cause bank erosion and channel change but do not jeopardize major infrastructure or threaten lives. A catastrophic level is reached when major infrastructure and building damage occurs due to erosion, sediment and water entering buildings, building and bridge foundation collapse, culvert blockage, and road surfaces being eroded. While relatively rare, injuries and/or fatalities can occur when people try to escape these events.

## 2.3. Debris Flows

Debris flows have higher sediment concentrations than debris floods and can approach consistencies similar to wet concrete. Using the example of a bucket again, if sand is added to the bucket of water and fills it to the top, so that the fluid is half sand, half water, it is bulked by 100%, and has a bulking factor of 2. If you spill it down the slide, you now have a debris flow that behaves more like liquid concrete than water.

Debris flows are typically faster than debris floods and have substantially higher velocities and flow depths, resulting in higher peak discharges and impact forces. They are particularly threatening to life and properties due to these characteristics.

## 2.4. Comparing Steep Creek Processes

Individual steep creeks can be subject to a range of process types and experience different peak discharges depending on the process, even within the same return period class. Figure 2-3 demonstrates this concept with an example cross-section of a steep creek, including representative flood depths for the peak discharge ("Q") of the following processes:

- $Q_2$; Clearwater flow with 2-year return period
- $Q_{200}$; Clearwater flow with 200-year return period (i.e., a clearwater flood)
- $Q_{\text{max debris flood (full bed mobilization)}}$; Type 1 debris flood generated by full bed mobilization
- $Q_{\text{max debris flood (outburst flood)}}$; Type 3 debris flood generated by an outburst flood
- $Q_{\text{max debris flow}}$; Debris flow.

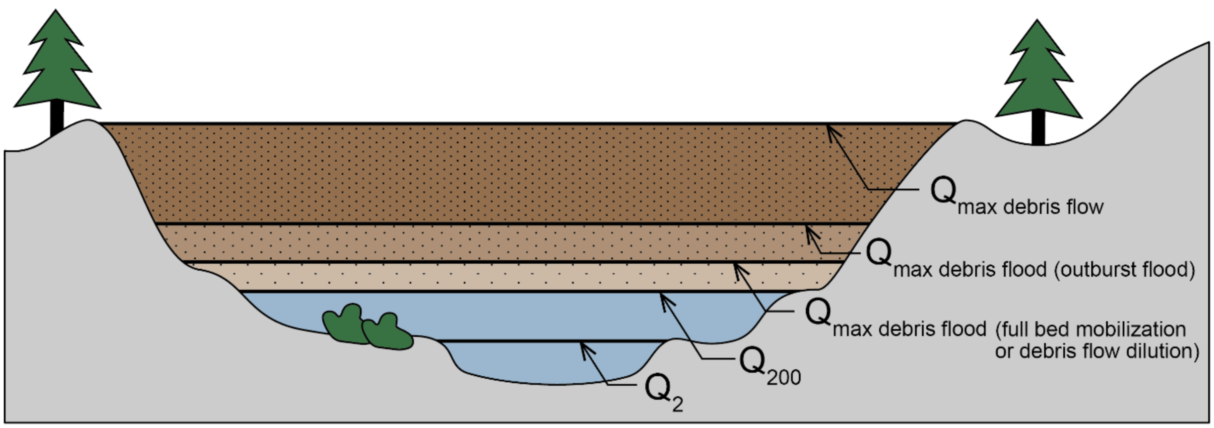


**Figure 2-3. Conceptual steep creek channel cross-section showing peak discharge levels for different events. Note that for some outburst floods or debris flows the discharge may exceed what is shown here.**

This difference in peak discharge is one of the reasons that process-type identification is critical for steep creeks. For example, if a bridge is designed to accommodate a 200-year clearwater flood, but the creek experiences a debris flow with a much larger peak discharge, the bridge would likely be damaged or destroyed. For floods, a longer duration is more likely to saturate protective dikes, increasing the likelihood for piping and dike failure prior to, or instead of, the structure being overtopped. For debris floods, the duration of the event will also affect the total volume of sediment transported and the amount of bank erosion occurring.

## 2.5. Impacts of Forestry on Watersheds

Logging activities, including cutblocks and road construction, influence landslide activity within watersheds (Jakob, 2000; Jordan, 2001). Jordan (2001) found that landslide frequencies were increased by roughly ten times by forest development in the Arrow and Kootenay Lake Forest Districts of BC with 95% of development-related landslides being the result of roads or skid trails. On older roads, road-fill failures were the most common cause of failure while on newer roads, drainage concentration and diversion by roads was found to be the most common cause (Jordan, 2001). Jordan (2001) also identified the influence of "gentle-over-steep" situations where a road is constructed on gentle sloping, low-hazard terrain and landslides occur on steeper terrain below. Jakob (2000) similarly found that landslide activity was nine times higher than in undisturbed forest on the west coast of Vancouver Island, BC. Moreover, Jakob (2000) found that failures in logged terrain occurred in gentler slopes than in natural terrain. The most common failure mechanisms were debris slides and debris flows initiating from road fill failures. These studies illustrate the importance of sound forestry management practices on landslide activity.

## 2.6. Wildfire Effects on Watersheds

Wildfires impact the hydrology and stability of a slope through loss of vegetation and modification of soil properties. During a fire, hydrophobic compounds accumulate below the soil surface, causing an increase of water repellency and reducing water storage capacity of the soil (Shakesby & Doerr, 2006). The removal of soil-mantling vegetation and litter reduces evapotranspiration and infiltration rates in the soil and changes the soil moisture dynamics (Rengers et al., 2020; Moody & Martin, 2001), as well as causing reduction in root strength, thus reducing the apparent cohesion of the soil (Rengers et al., 2020). There is also an increase of precipitation reaching the ground surface through loss of vegetative canopy (Rengers et al., 2020; Parise & Cannon, 2012). Figure 2-4 outlines some of the effects of wildfires on slope hydrology and stability.

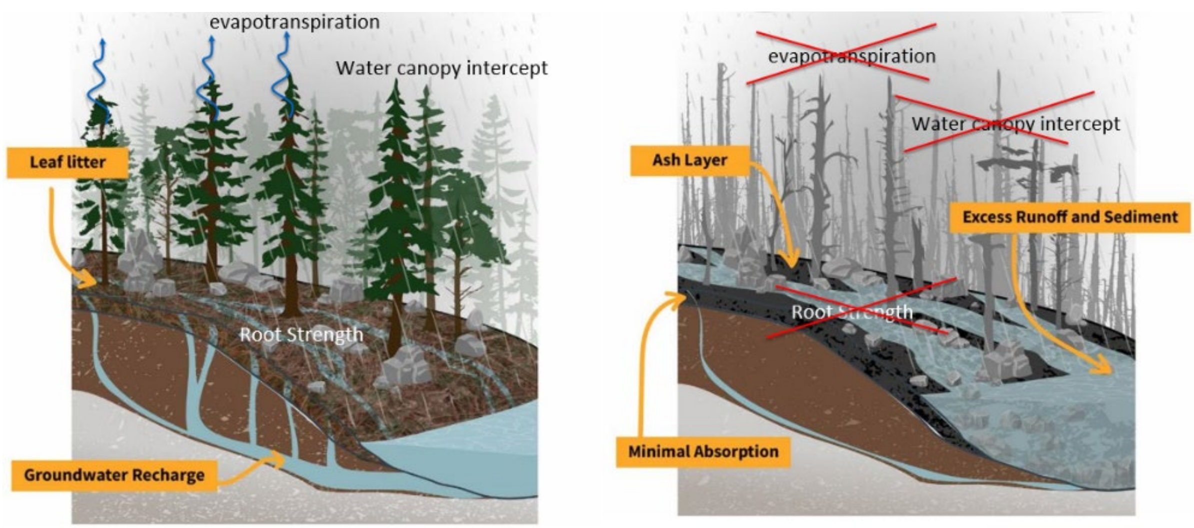


**Figure 2-4. Schematic showing hydrology on a slope in unburned conditions (left) and the potential effects of wildfires on slope hydrology, which influences slope stability (right). Figure adapted from United States Geological Survey (2020).**

As a result, burned slopes are often more susceptible to debris flows, debris floods, floods, and other slope hazards. The largest events are most often triggered by the first major storm following the wildfire event and the hazard remains elevated in the first two years following a fire (Cannon & Gartner, 2005; Staley et al., 2020; De Graff et al., 2015). Landscape recovery is usually reached after five to ten years, depending upon the rate of vegetation regrowth in the fire area (Bartels et al., 2016).

# 3. STUDY AREA

This section describes the physical setting of the Daisy, Thistle, and Gravel Creek watersheds. Observations of the study area are supported by data compiled by BGC and previous assessments provided by Tigerbay (Appendix B) as well as from field work completed by BGC (Lauren Hutchinson, Matthias Jakob, and Hilary Shirra) on May 11, 2022 and June 7, 2022. Representative photographs of the study area are provided in the Photographs Attachment.

## 3.1. First Nations

Daisy, Thistle, and Gravel creeks are within the traditional and unceded territory of the Skwxwú7mesh-ulh Úxwumíx̱w Nation.

## 3.2. Watershed Characterization

### 3.2.1. Physical Setting

The study creeks are located on west-facing slopes on the east side of Howe Sound (Drawing 01). The proposed development is on the heavily human-altered fan areas of the three study creeks. Modification of the fan areas associated with gravel mining has substantially changed the morphology and altered drainage of the individual fans, with a majority of the fan areas removed by mining. BGC delineated historic fan areas using the 1932 air photos that pre-date the gravel mining activities. A CN Rail line parallels the east coast of Howe Sound on the west side of the proposed development. Upstream of the proposed development, the BC Hydro right-of-way (RoW) transects the lower watersheds (Drawing 01). The watersheds are also transected by relict and active logging/access roads as described in Section 3.3.

The Daisy Creek watershed is underlain by quartz diorite intrusive rocks (Bellefontaine et al., 1994). A normal fault that trends southeast to northwest forms the bedrock geology contact between with the marine sedimentary and volcanic rocks of the Gambier Group that underlie the Thistle and Gravel Creek watersheds (Bellefontaine et al., 1994; Cui et al., 2017). The orientation of the normal fault is evident as a structural control on the orientation of main tributaries to Daisy Creek (Drawing 03). Parallel faults were observed in the upper watershed as well as at the inlet of the existing Daisy Creek debris basin (Photo 10). The bedrock has a strong structural influence on the watersheds and drives the orientation of lineaments and gullies (Drawing 03). The importance of the fault and associated structural elements is twofold. First, they provide a zone of structural weakness which allows fractured and possibly altered rocks to be preferentially eroded. Second, and because of the first point, creeks follow the fault traces thereby accentuating sediment recruitment.

The study creek watersheds are underlain by competent bedrock. This material type is less prone to rapid erosion that could produce significant amounts of sediment as may be expected from more friable sedimentary rocks (for example in much of the Canadian Rocky Mountains). Erosion is further reduced by tree cover reaching mountain tops in the study areas.

Surficial materials in the study watersheds are comprised of colluvial and till veneers (generally less than 1 m thick) overlying bedrock at mid-slope and bedrock outcrops surrounded by colluvium in the upper slopes. The colluvial veneer is comprised of rock fragments in a matrix of boulders, gravel, sand, and silt (Figure 3-1, Blais-Stevens, 2008). In lower reaches, the creeks extend downstream through mapped proglacial deltaic sediments, thick (> 10 m) glaciomarine terrace sediments, and fan sediments (Blais-Stevens, 2008). Detailed descriptions of these materials are provided in Table 3-1.

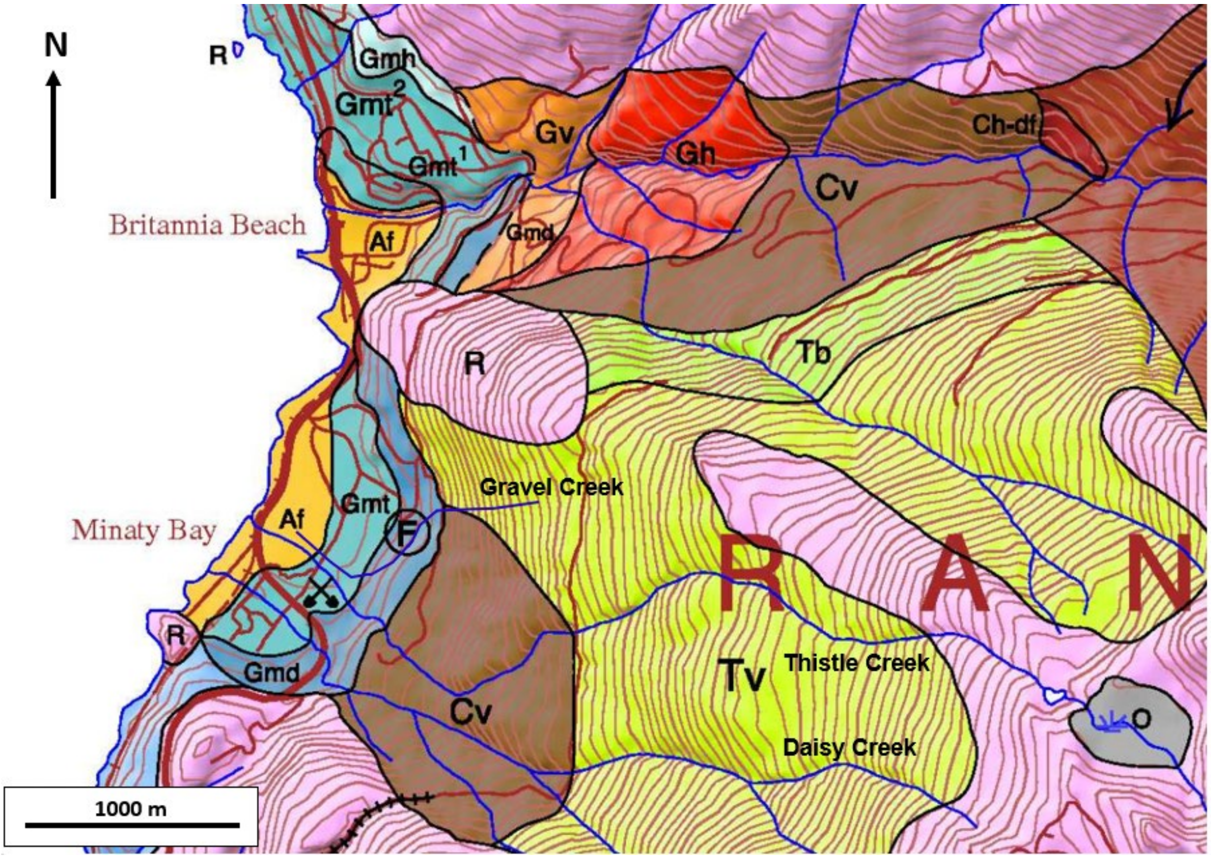


**Figure 3-1. Schematic of surficial geology of the study watersheds (Blais-Stevens, 2008). The approximate creek alignments were added by BGC. Table 3-1 provides a legend for the materials.**

**Table 3-1. Description of surficial materials in the study creek watersheds (Figure 3-1, Blais-Stevens, 2008).**

| Symbol | Description |
|---|---|
| Af | **Fan sediments:** poorly sorted sand and gravel, with diamicton; generally 2 to 15 m thick; forming fans at the toe of slopes. |
| Gmt | **Glaciomarine terrace sediments:** sand and gravel, stratified to massive; 1 to 10 m thick; forming flat surfaces perched well above alluvial deposits or associated with meltwater channels. |
| Gmd | **Proglacial deltaic sediments:** sand and gravel with minor silt and clay; on average 10 m thick, but can be >10 m; commonly overlie glaciomarine silt and clay; may form, in part, includes surfaces. |
| Cv | **Colluvial veneer:** rock fragments in a matrix of boulders, gravel, sand, silt; usually <3 m thick; formed by bedrock weathering or reworking of unconsolidated deposits. |
| Tv | **Till veneer:** discontinuous till cover with abundant bedrock outcrops; 1 m thick on average; reflecting topography of underlying bedrock |
| R | **Bedrock:** sedimentary, low-grade metamorphic[1], volcanic, and intrusive rocks of Jurassic to Quaternary age; including, in places, till veneer, drift, and colluvium. |
| O | **Organic deposit:** peat and muck, 1 to 10 m thick (typically 2 to 3 m), forming fens and bogs, organic deposits too small to be shown at this scale occur within other units; common within abandoned meltwater channels. |
| Gh | **Ice-contact deposit:** sand and gravel, stratified to massive and commonly faulted, generally >3 m thick, forming hummocky surfaces. |
| Ch-df | **Debris flow deposit:** mostly unconsolidated sediments with texture dependent on source materials, generally 1 to 10 m thick, but may exceed 10 m near the toe of large landslides, forming hummocky accumulations on lower slopes and valley floor. |

#### 3.2.1.1. Daisy Creek

Daisy Creek originates as two main tributary channels that join downstream of a logging road (Drawings 01, 03). The area immediately up and downstream of this crossing was logged in 2016 (Section 3.3). Downstream, the channel is deeply incised into a valley with till overlying bedrock. Sediment and organic debris availability in the channel is likely exacerbated by past and ongoing logging activities (Photos 1, 5; Section 3.3). BGC traversed the length of the channel or along the north channel bank, where required for access, up to elevation 450 m during a site visit on June 7, 2022. Between elevation 55 m and 325 m, BGC observed a sequence of wide (>30 m) lower angle (12-13°) depositional reaches between steeper (>15°) reaches (e.g., Photo 9) (Drawing 05a). BGC expects that substantial deposition and flow attenuation would occur in these reaches upstream of the existing debris basin (Drawing 01) because coarse-matrix debris flows tend to deposit at angles of < 14° (e.g., Hungr et al. 1984, VanDine, 1985). Within the channel, BGC estimated that the depth of erodible material overlying bedrock ranged from 0.5 m and 2 m thick. Moss cover on boulders and logs that cross the channel suggest that outside of the main

[1] Low-grade metamorphic rocks are those that have experienced metamorphism with a small increase in temperature under significant directional pressure leading to recrystallization of mineral constituents into leaf-like and elongated minerals.

wetted area the channel configuration within the forested area has been stable for a number of years.

Thurber (October 21, 2016) indicated that at approximate elevation 280 m, a 1.2 m high dam was identified. Thurber described the dam as a concrete structure which appeared to have been used to divert water to a wood stave culvert running along the north bank of the creek. At elevation 280 m, BGC reviewed channel conditions and then traversed along the north bank upstream to the logging road crossing at approximate elevation 370 m. BGC did not observe the structure during the field visit or identify evidence in the lidar. However, BGC did observe evidence of an old water pipeline (metal bracing) to this approximate location and the structure, if it exists, could be between BGC's field observation point and the logging road. BGC did observe a similar structure on Thistle Creek (Section 3.2.1.2).

BGC's field observations of the Daisy Creek watershed, (largely competent bedrock overlain with shallow soils without major sources of debris from talus slopes or Quaternary sediment deposits) are consistent with a channel supply-limited watershed (Jakob et al., 2005, Jakob, 2021). This means that it takes time for the watershed to 'recharge' sediment in the creek channel following a debris flow or debris flood. An exception could be an extremely rare event in which debris avalanches on open slopes contribute sediment to the channel system. This was captured by allowing multiple point sources in the frequency-magnitude analysis (see Section 4.3.4).

Daisy Creek has been previously identified as being subject to debris flows. The Daisy Creek debris retention basin was constructed in 2008[2] as part of the Sea to Sky Highway Improvement Project. It has a design volume of 25,000 m$^3$ based on an impoundment (deposition) angle of 5°[3] (Thurber, May 4, 2006). The design volume was informed by Thurber Consultants Ltd. (Thurber)'s 1983 debris-flow volume estimate of 24,000 m$^3$ based on estimated channel debris yield rate and contributing debris areas within the watershed as well as debris-flow volume data from similar creeks along the corridor. The inlet and stilling basin were designed by Northwest Hydraulic Consultants (NHC) and included an additional 1 m freeboard above the expected impoundment height for potential debris runup. The inlet of the basin is a steep (25°) 10 m tall bedrock waterfall. From the inlet, the creek turns 90° to the north. The basin is approximately 90 m long with a channel gradient of 5° (10%). The basin outlet is a 3 m diameter corrugated steel pipe (CSP) with a 2 m diameter CSP overflow culvert set into Class 25 kg riprap (Thurber, May 4, 2006). A hinged steel grillage structure is installed in front of the main culvert. As shown on the as-built drawings, the bars have a diameter of 30 mm. At the time of BGC's site visit on May 11, 2022, approximately 5 out of 12 bars of the steel grillage had been cut or broken (Photo 11). An approximately 10 m wide and 20 m long overflow spillway with Class 2,000 kg riprap was constructed at the basin outlet to convey flows that overtop the culverts into the main channel. Immediately downstream of the basin outlet, Daisy Creek turns 90° to the west before discharging below Highway 99 in an approximate 3.5 m (horizontal) by 2.2 m (vertical) oval CSP culvert (Photo 12).

---

2 As-built documentation from Kiewit shows a record drawing date of September 28, 2009. Design documentation is available from 2006. Turje (2020a) listed a construction date of 2008 and (2020b) listed a construction date of 2007.

3 An impoundment (deposition) angle, usually ½ to 2/3 of the channel slope is used to estimate the angle at which debris will deposit upstream of a structure for the purposes of estimating total stored volume.

BGC requested details on maintenance or debris clean-out works on the Daisy Creek debris basin from the Ministry of Transportation and Infrastructure (MoTI). At the time of writing, BGC has not received such details from MoTI. Thurber (June 13, 2016) report that in January 2016, a storm led to a debris flow on Daisy Creek that blocked the lower culvert in the debris basin resulting in water and sediment spilling through the upper culvert and clearwater flowing down Highway 99 and into lands to the north. Thurber (June 13, 2016) further indicates that a May 2016 inspection estimated the sediment volume of the January event at 2,000 to 3,000 m$^3$.

As part of their detailed debris-flow hazard assessment and preliminary evaluation of mitigation options, Thurber evaluated the efficacy of the Daisy Creek debris basin using numerical modelling of debris flows with DAN3D. Thurber identified three potential scenarios that could occur if the basin does not function as intended due to improper basin maintenance and cleanout, variations in the nature of debris flows, very high sediment volumes, or a combination thereof. These are:

- Deposit in the flat area to the north of the basin and east of the highway
- Travel northbound along the highway, flowing down the Highway 99 embankment in the direction of Thistle Creek
- Travel across Highway 99 along the general alignment of the Daisy Creek channel.

Thurber (2016) further recommended mitigation approaches to minimize the risks associated with the above scenarios and Turje (2020b) proposed alternate approaches. It is outside of the scope of the current assessment to review either Thurber's or Turje's proposed mitigation approaches.

The existing (estimated 2.2 m in diameter) road crossing downstream of Highway 99 experienced significant damage in the November 2021 atmospheric river events and was clogged with debris with debris buildup and roadway slumping at the inlet (Photo 13 and 14). Downstream, Daisy Creek is conveyed below the CN Rail line by a concrete bridge approximately 5 m wide and 1 m deep (Photo 15). Turje (2020b) estimated that the crossing has inadequate capacity to convey flows associated with debris floods and debris flows on Daisy Creek in the present condition due to sedimentation. Turje (2020b) recommended excavation of sediment or replacement with a wider bridge. BGC notes that excavation of sediment is likely only a short-term solution as continued aggradation is expected through this reach.

#### 3.2.1.2. Thistle Creek

Thistle Creek originates at two small lakes (approximately 4,800 m$^2$ and 8,100 m$^2$) below a cirque[4] in the upper watershed (Drawing 01). Downstream of the cirque, the main (southern) channel has an average of slope of 20° (35%) to the fan apex (Drawing 05b). Between elevation 730 m and 280 m, Thistle Creek is composed of two poorly confined branches that flow over bedrock-controlled steps (e.g., Photo 18) and waterfalls (e.g., Photo 19). Similar to Daisy Creek, the bedrock control in the Thistle Creek watershed is consistent with a channel supply-limited watershed. Portions of the upper watershed are presently logged, and a main logging road crosses the two branches of Thistle Creek at approximately 400 m elevation (Photo 17). Further description of logging activities in the study watersheds is provided in Section 3.3.

[4] A steep-sided depression at the head of a valley or mountainside, often formed through glacial erosion.

At the confluence of the two channels (280 m elevation), BGC observed a historic concrete gravity dam approximately 7.5 m wide and up to 4 m tall with a front face inclined at 60° (Photo 20). Material retained upstream of the structure is consistent with the other channel material[5] ($D_{84}$ of 250 mm to 400 mm; $D_{50}$ of 50 mm to 10 mm) with some woody debris rafted onto the surface. BGC believes that this dam was likely built to convey water for mine processing at the Britannia Mine. The dam creates a local depositional area and currently stabilizes the channel. BGC observed only minor evidence of abrasion over the lip of the structure indicating that since installation there has not been debris impact of sufficient intensity to damage the lip of the structure. BGC is not aware of a dam safety assessment for this structure. Turje (2020b) indicated that Thurber had advised the Ministry of Forests (MoF) of the location of the structure and MoF had indicated that the dam would likely be decommissioned in the near future. Such decommissioning of the dam would release the sediment stored upstream and should be reviewed in light of what the sediment release would mean for downstream hazards.

Downstream of the confluence, a historic debris slide was noted by BGC in low-angle terrain on the right (north) bank that crosses the channel at approximately 245 m elevation. The debris slide covers an area of approximately 3,400 $m^2$ (approximately 100 m long (NE-SW) and 30 m wide (N-S)). Based on the Blais-Stevens (2008) mapping shown in Figure 3-1, this slide is located in an area of colluvial veneer. This slide was first evident in 1932 based on BGC's air photo review (Section 4.3.1, Appendix D). BGC did not observe any evidence that would suggest ongoing or future instability in this location that would contribute to downstream hazards on Thistle Creek.

In the lower watershed (40 m to 280 m elevation), Thistle Creek has an average slope of 18°. The channel is well confined in the valley (Photo 21). A short reach (100 m to 130 m elevation) over a bench formed by the pro-glacial deltaic sediments (Figure 3-1) is poorly confined with the potential for flow to overtop the channel banks leading to localized diffuse overland flooding. BGC did not observe any evidence of boulder lobes, levees, or tree scars on Thistle Creek within the watershed. Such features would be expected within a watershed of a creek that had a history of debris flows.

Immediately upslope of the proposed development, a tributary to Thistle Creek was noted that joins the main channel on the right (north) bank at approximately 20 m elevation (Drawing 02). The tributary is heavily incised into the highly erodible, poorly sorted, sand and gravel terrace sediments (Figure 3-1). The channel banks are largely unvegetated, and BGC expects they may continue to erode (Photo 23).

Within the proposed development area, Thistle Creek has an average slope of 1° (2%). The creek is conveyed below any existing roadway by an approximately 10 m wide by 1.65 m high bridge (Photo 24). Thistle Creek is conveyed below Highway 99 and the CN Rail line through a concrete box culvert approximately 3 m wide by 2.2 m tall with a 1.8 m tall headwall and wingwalls set at approximately 45° (Photos 25, 26). At the time of BGC's site visit (May 11, 2022), the Highway 99/CN Rail culvert was clear of debris.

---

5 $D_{84}$ and $D_{50}$ are used to describe the grain size distribution of a channel and relate to the 85th and 50th percentiles of the grain sizes within the channel.

#### 3.2.1.3. Gravel Creek

As described by BGC (November 13, 2020), the Gravel Creek upper watershed (above 110 m elevation) is steep (30°-50°) with bedrock outcrops (Photo 27). The lower watershed (below 110 m elevation) is less steep (10° to 30°) (Drawing 05c). Surface water drainage in the Gravel Creek watershed is heavily influenced by the presence of active and relict logging/access roads. Upstream of the proposed development, Gravel Creek flows in the upstream (eastern) ditch of a logging / access road (22 m to 40 m elevation). BGC observed rilling and erosion along this access road in 2020 (June 16, 2020) and 2022 (June 7, 2022) field inspections (Photos 28, 29). As observed in June 2022, flow directed to the east side of the logging access road intersects the heavily erodible terrace sediments (Figure 3-1, Photo 29) with the potential for substantial erosion and gullying if flow is uncontrolled.

Detailed description of the channel morphology and existing infrastructure is provided in BGC's Gravel Creek Hazard Assessment (BGC, November 13, 2020). Debris source areas described in BGC (November 13, 2020) are included in the present assessment. As with the other study creeks, the Gravel Creek fan apex and boundaries have been altered due to anthropogenic modification associated with gravel mining. Gravel Creek is an ephemeral (seasonal flow) creek. No flow was observed in the creek during BGC inspections in 2020 (June 16) or 2022 (May 11; June 7).

### 3.2.2. Desktop-Level Process Classification

Table 3-2 summarizes the study creeks watershed and fan characteristics. Figure 3-2 shows a desktop-level steep creek process classification based on watershed stream length and Melton ratio (Wilford et al., 2004). This preliminary classification suggests that Thistle Creek is prone to debris flows, while Daisy Creek and Gravel Creek are prone to debris floods and debris flows. Importantly, the classification shown in Figure 3-2 does not account for the continuum of processes that a watershed may be subject to at different return periods, nor does it account for sediment availability. BGC supplemented this desktop-level classification with air photo and field observations to assess the dominant process types (Section 4.2).

**Table 3-2. Watershed characteristics of Daisy, Thistle, and Gravel creeks.**

| Characteristic | Daisy Creek | Thistle Creek | Gravel Creek |
|---|---|---|---|
| Watershed area ($km^2$) | 2.86 | 1.81 | 0.73 |
| Maximum watershed elevation (m) | 1320 | 1458 | 533 |
| Minimum watershed elevation (m) | 53 | 44 | 35 |
| Watershed relief (m) | 1267 | 1414 | 498 |
| Melton Ratio (km/km)[1] | 0.75 | 1.05 | 0.58 |
| Average channel gradient of mainstem above fan apex (%) | 41 | 35 | 30 |
| Fan area ($km^2$)[2] | 0.22 | 0.03 | 0.05 |
| Average channel gradient on fan (%) | 4.3 | 1.6 | 1.8 |
| Average fan gradient (%) | 4.5 | 3.5 | 2.5 |

Notes:

1. BGC updated the watershed area and associated morphometric characteristics of Gravel Creek from those presented in 2020 (BGC, November 13, 2020) based on refinements with the improved lidar coverage.
2. BGC delineated the fan areas based on air photos from 1932. These fan areas differ from the modern fans which are not observable due to the level of anthropogenic modification. Construction of access/logging roads has modified the creek drainage patterns since the 1932 air photo. BGC did not delineate the subaqueous portions of the Daisy or Thistle Creek watersheds as bathymetric data was not available. For this reason, the fan areas identified for Daisy and Thistle creeks may be considered lower than the full fan-deltas.

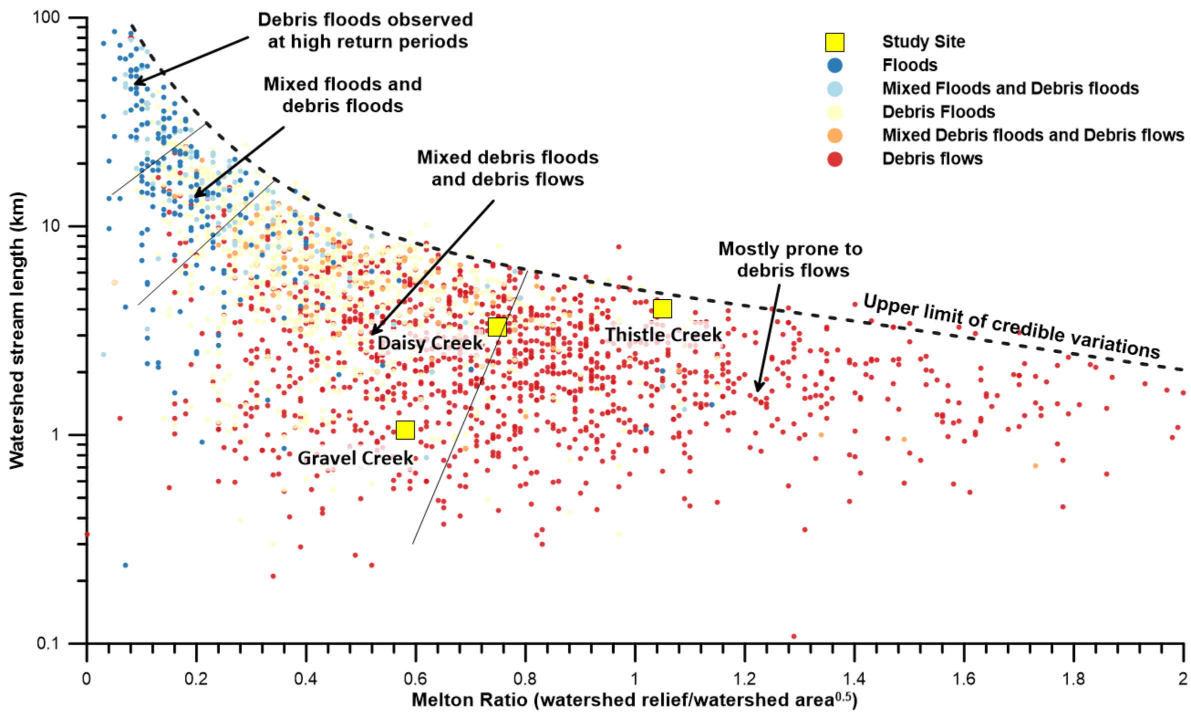


**Figure 3-2. Classification of Daisy, Thistle, and Gravel creeks with respect to hydrogeomorphic processes, based on stream length and Melton Ratio[6]. Note that this representation is simplistic because it does not include the dimension of return period. Some creeks are subject to different processes at different return periods**

## 3.3. Forestry

The study creek watersheds are all forested with past and ongoing logging activities. Evidence of logging or a burn is evident south of and adjacent to the Daisy Creek watershed in the 1940 air photo (Drawing 04). Construction of a logging road south of the study watersheds is first evident in the 1952 air photo. This logging road is evident in the 1994 air photo and was extended to the north through the study creek watersheds in the 2003 air photo (Drawing 04). This remains the main logging artery today with bridge crossings on the Daisy Creek tributaries (Photos 2, 4; DSQ 3148, 3149 in MoF system) and culverts on the Thistle Creek tributaries (Photo 17; DSQ 3151, DSQ 3152).

Clear cut logging is evident in all three study creek watersheds in 2003 with increased areal extent in the 2020 image (Drawing 04). Active and retired[7] forest cut blocks within the study creek watersheds are shown in Figure 3-3.

[6] Stream length is measured upstream along the stream extending farthest from the debris fan apex, and Melton Ratio is watershed relief divided by the square root of the watershed area.

[7] Retired is the 'life cycle status code' available in iMapBC. A specific definition is not provided. BGC interprets this to mean that no future logging activities are anticipated in the cut block.

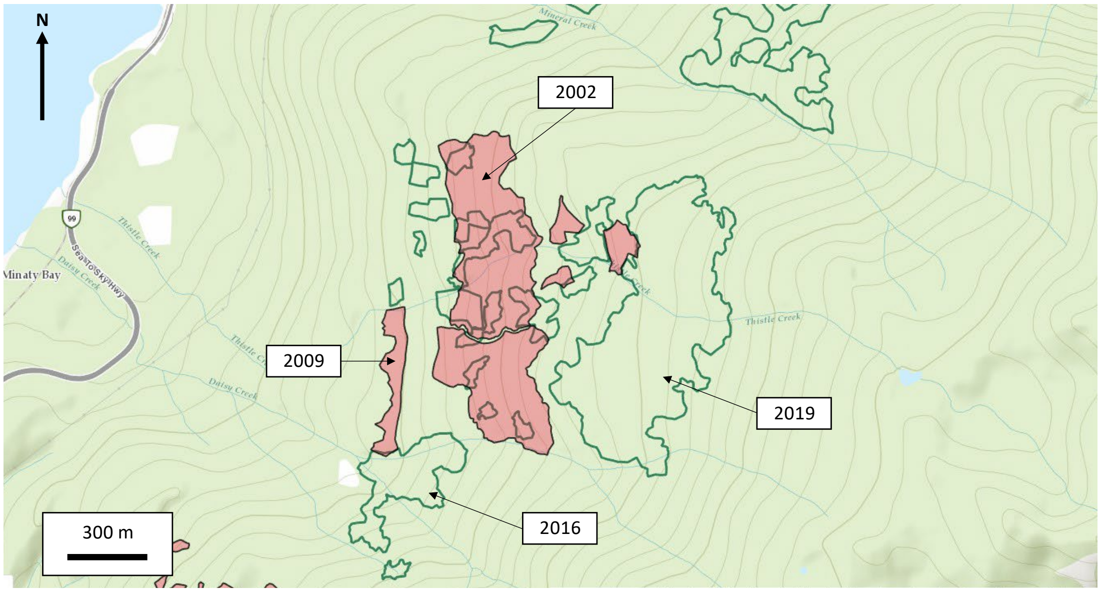


**Figure 3-3. Active (black) and retired (red) cut blocks in the study creek watersheds. The logging date of the largest cut blocks is annotated in the text boxes. Map source: iMap BC.**

The study area is within Black Mount Logging (Black Mount) and Richply Plywood Corporation Limited (Richply) logging areas. Black Mount provided a logging plan for the study area (Figure 3-4) and indicated that blocks T8 and T6 in the Thistle Creek watershed are engineered[8] and that blocks T9 and T10 in and south of the Daisy Creek watershed are representative of a potential future helicopter-supported logging program once visuals can be met[9] (email from Dave Rollins, personal communication, June 15, 2022). From the logging plans provided, no additional cutblocks are planned in the study area watersheds than those identified.

The logging plan shown in Figure 3-4 also demonstrates the number and extent of roads (private and permitted) within the study area. Logging / access roads influence local surface water drainage by providing preferential flow paths in the ditches that parallel the roads and along the roads themselves when flow overtops the ditches. The impacts of forestry on watersheds are further discussed in Section 2.5

In the study watersheds, logging road fill and slash management have the potential to influence sediment availability. BGC observed increased sediment and organic debris in the Daisy Creek channels within the cutblock at and upstream of the confluence of the main tributaries (Figure 3-5). In these areas, the logging extended to the edge of the creek without a riparian buffer. BGC also observed flow concentration and erosion along roads above the Gravel and Thistle watersheds (Photos 28, 29). Given the highly erodible nature of the sand and gravel deposits in the proposed development, in particular in the vicinity of Thistle and Gravel creeks, surface water management is of particular importance to manage downstream erosion.

[8] Engineered refers to a block where the falling boundary and roads are physically located in the forest (flagging ribbons hung) (email from Dave Rollins, personal communication, July 14, 2022).

[9] This term refers to meeting the Visual Quality Objectives outlined by the government which require the visual impact of older cut blocks to improve before new cut blocks can be started (email from Dave Rollins, personal communication, July 14, 2022).

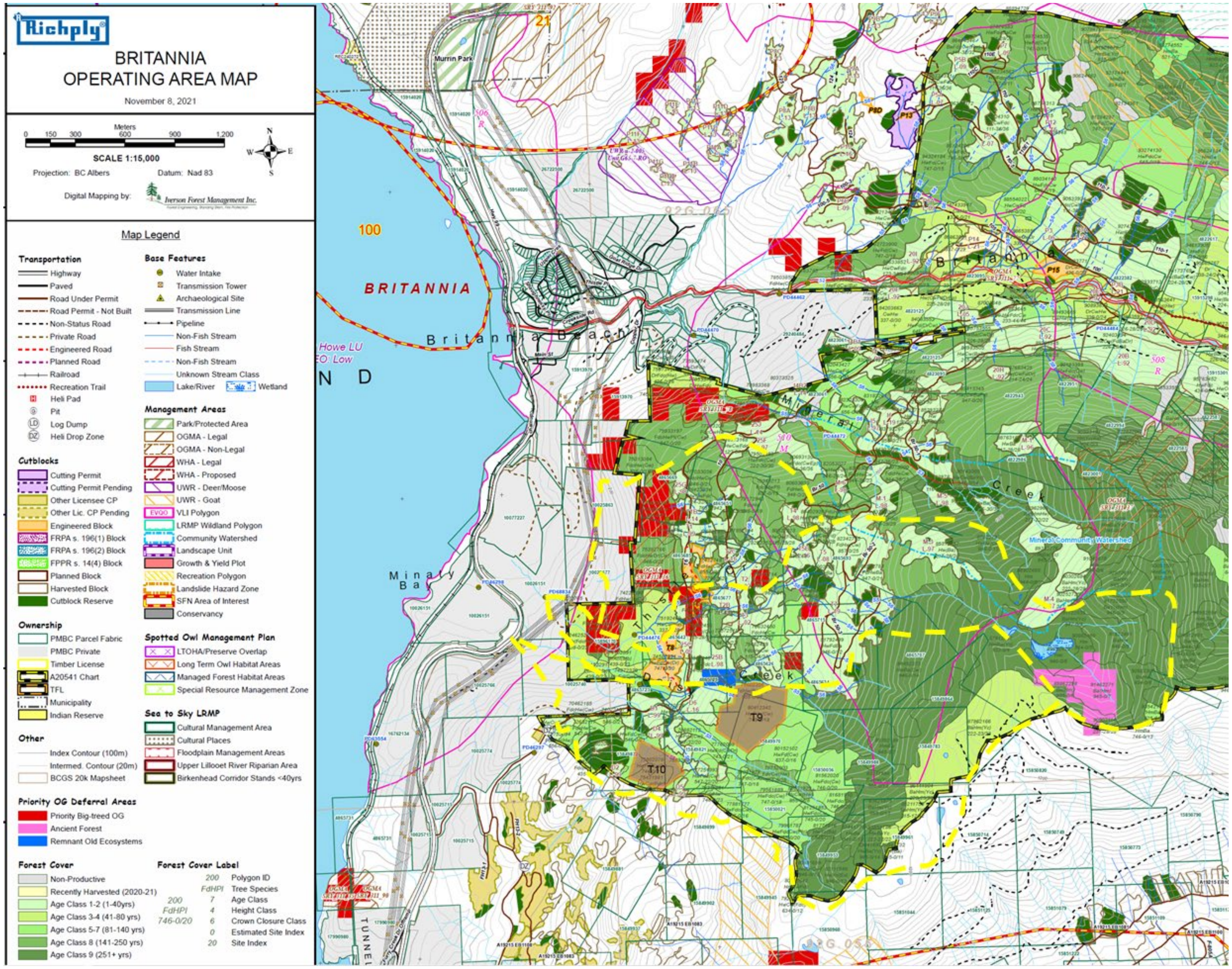


**Figure 3-4. Logging plan provided by Black Mount (1:20,000). Blocks T8, T6 are engineered; blocks T9, T10 are potential heli programs. Approximate watersheds delineated in yellow.**

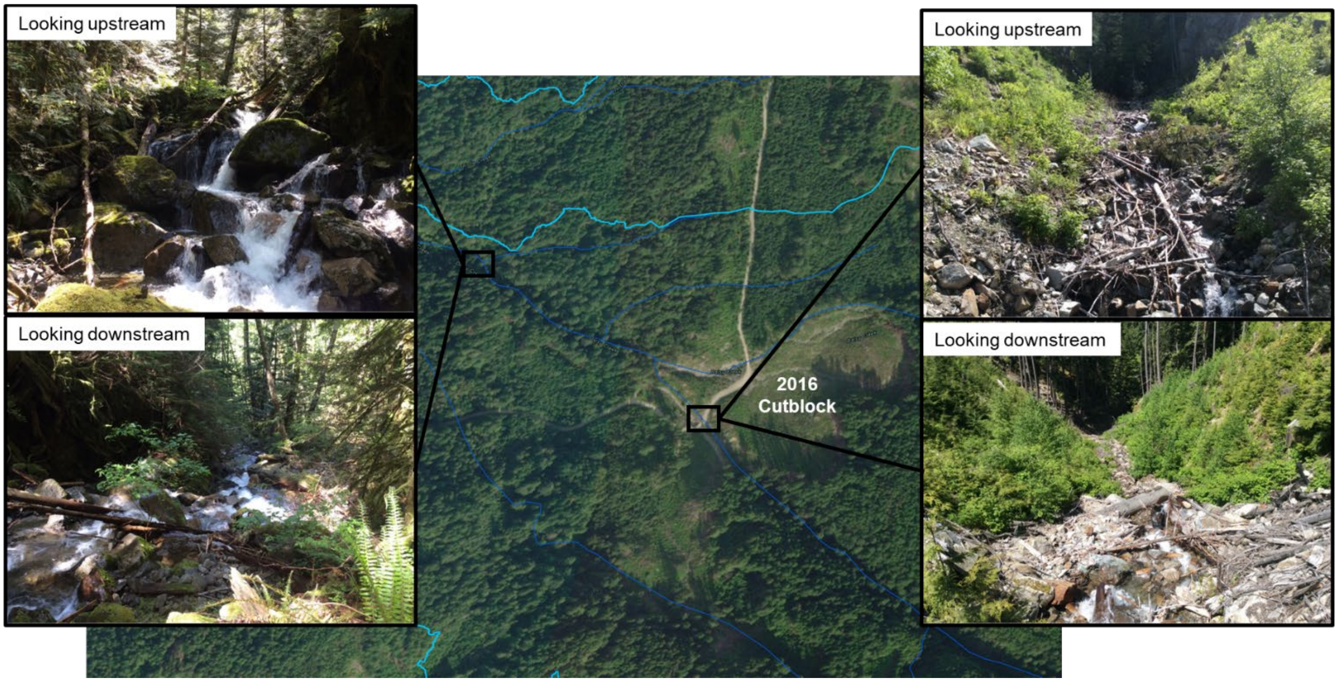


**Figure 3-5. Comparison of available sediment and organic debris in forested (left) and logged (right) reaches on Daisy Creek. Note the considerable organic debris loading in the logged reaches. Base map is ESRI World Imagery. Photos: BGC, June 7, 2022.**

## 3.4. Wildfire History

The BC Wildfire Service (2022) has recorded no wildfire activity in the Daisy, Thistle, and Gravel creeks watersheds. BGC reviewed the wildfire history in the Sea to Sky corridor as a proxy for the study area which extends from Shannon Falls to Lions Bay and from the Howe Sound shoreline eastwards to ridge crests (approximately 8 to 13 km). Within this area, 14 historical fires were recorded between 1922 and 2012 with burned areas ranging between 0.01 $km^2$ to 3.4 $km^2$. The influence of wildfires on watersheds is discussed in Section 2.6. Frequency and magnitude of post-fire debris flows are discussed in Appendix D.

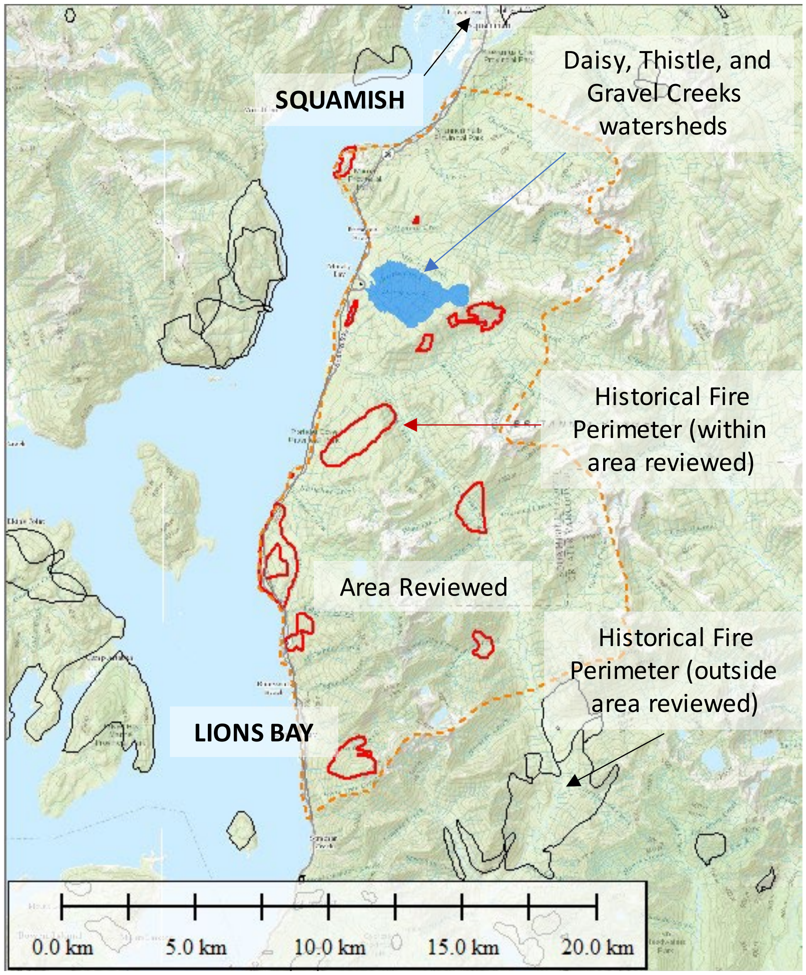


**Figure 3-6. Historical fire perimeters (red) in the area reviewed (orange) in proximity to the Daisy, Thistle, and Gravel Creek watersheds (blue).**

## 3.5. Climate

Table 3-3 provides a summary of the historical (1981 to 2010) climate normals for Squamish (airport). Monthly precipitation is highest in the winter (November to January), and lowest in the summer (July to August) (Figure 3-7). The highest temperatures occur in June and August with average temperatures between 16°C and 18°C (Table 3-3). The lowest temperatures occur in December and January, with a 30-year mean of 3°C (Table 3-3).

The critical months for debris-flood and debris-flow initiation are October to December, though these hazards can occur at other months of the year. In those months, antecedent moisture conditions (i.e., how much rain or snowmelt has occurred prior to a potentially debris-flow initiating storm) and high intensity and prolonged rain coincide. Particularly dangerous are situations in which a relatively thin (< 0.5 m) layer of wet snow exists followed by rapid rise in freezing level and heavy and prolonged precipitation, typical for atmospheric rivers originating in the subtropics or tropics and affecting the BC Coast, or sequences of standard north Pacific cyclones. Rainfall is still high in January, but some of it may be absorbed by accumulated snow at higher elevation that acts as a sponge delaying or hindering transfer of rain water into the underlying forest soils.

With climate change, however, the debris-flow prone season will prolong with debris flows becoming more likely in all winter months as snow depth decreases in conjunction with heavier and more frequent heavy rain (Jakob and Owen, 2021).

**Table 3-3. 1981 to 2010 climate normals at the Squamish STP Central D[1] station (ID 1047671).**

| Variable | Month | | | | | | | | | | | |
|---|---|---|---|---|---|---|---|---|---|---|---|---|
| | Jan | Feb | Mar | Apr | May | Jun | Jul | Aug | Sep | Oct | Nov | Dec |
| Temperature (°C) | 3 | 5 | 7 | 10 | 13 | 16 | 18 | 18 | 15 | 10 | 6 | 3 |
| Rainfall (mm) | 300 | 180 | 198 | 153 | 116 | 83 | 59 | 66 | 83 | 256 | 382 | 268 |
| Snowfall (mm) | 26 | 13 | 8 | 0 | 0 | 0 | 0 | 0 | 0 | 0 | 9 | 31 |
| Precipitation[2] (mm) | 326 | 193 | 207 | 153 | 116 | 83 | 59 | 66 | 83 | 256 | 391 | 299 |

Notes:

1. "D" represents that there is 15 years of data.
2. Precipitation is a combination of rainfall and snowfall amounts.

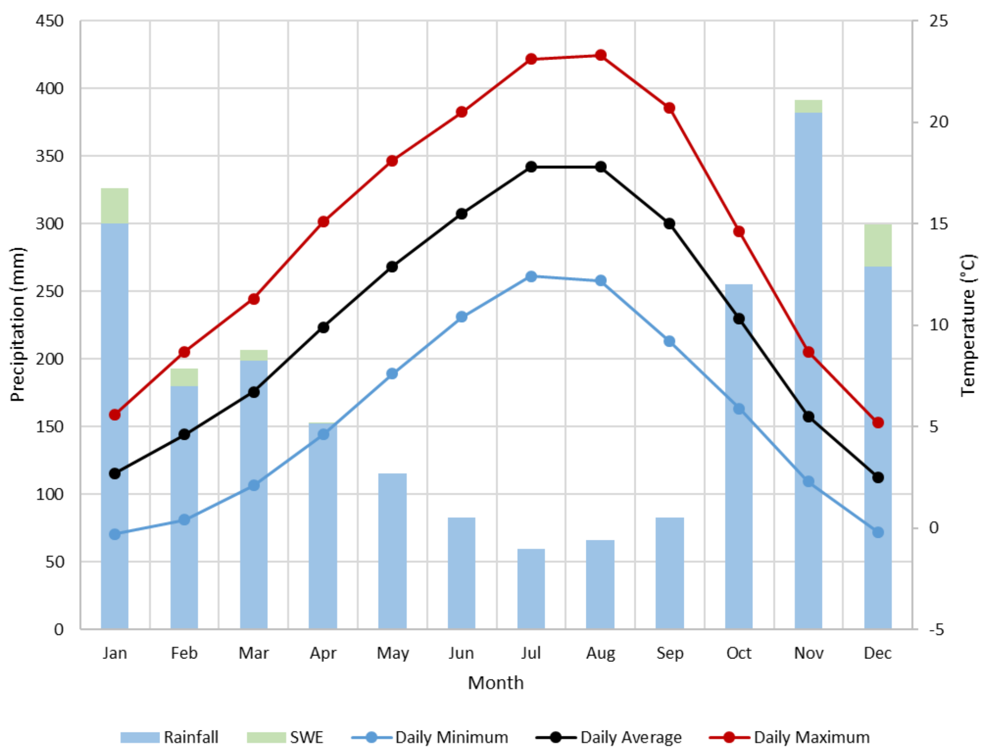


**Figure 3-7. Climate normals at the Squamish STP Central D climate station for 1981 to 2010.**

BGC considered climate change impacts on the frequency and magnitude of steep creek hazard processes on Daisy, Thistle, and Gravel creeks as part of the hazard assessment (Section 4.3.2).

## 3.6. Proposed Development

The proposed development includes land designations for multi-family residential dwellings, recreational facilities, tourism infrastructure, commercial facilities, natural spaces and a 2.4 ha (six acre) surf park (Figure 1-1, Drawing 02). Development is proposed in three phases (Turje, May 31, 2020a):

- Phase 1 (present – 2025): the "Wavegarden" surf park, recreation area, brewpub and up to 20 cabins and glamping sites configured as a surfing village around the surf park
- Phase 2 (2026 – 2030): construction of permanent core utilities and the initial phases of residential development and tourist accommodations
- Phase 3: remaining infrastructure as required.

# 4. HAZARD ASSESSMENT

## 4.1. Introduction

Hazard assessment is the process of identifying and evaluating the hazards in an area of interest. The results of a hazard assessment inform subsequent evaluation of the risks associated with the hazards and design of risk-control measures, if required.

In this section, we summarize the steep creek processes on Daisy, Thistle, and Gravel creeks (Section 4.2) and documented historical steep creek events (Section 4.3.1), describe how these events may change with climate change (Section 4.3.2), and summarize the results of the frequency-magnitude (F-M) analysis for the creek (Sections 4.3.3 and 4.3.4) that was used for numerical modelling (Section 4.4) to generate the composite hazard map (Section 4.5). The results presented in this section are supported by methods described in Appendices D, E, and F.

Graphical overviews of the general methodologies for assessment of flood- and debris flood processes (Figure 4-1) and debris-flow processes (Figure 4-2) are shown below. These methodologies were customized for application to the study area based on the dominant process types, unique site characteristics, and available information and budget. Test trenching and application of historical area-volume relationships were not included in this study due to the substantial anthropogenic modification on the study fans. In relation to bank erosion, human modification prevents accurate delineation of historic bank extents to inform calibration and modelling of projected future bank erosion along the channels. BGC understands that bank erosion potential will be integrated in future designs of the study creek channels.

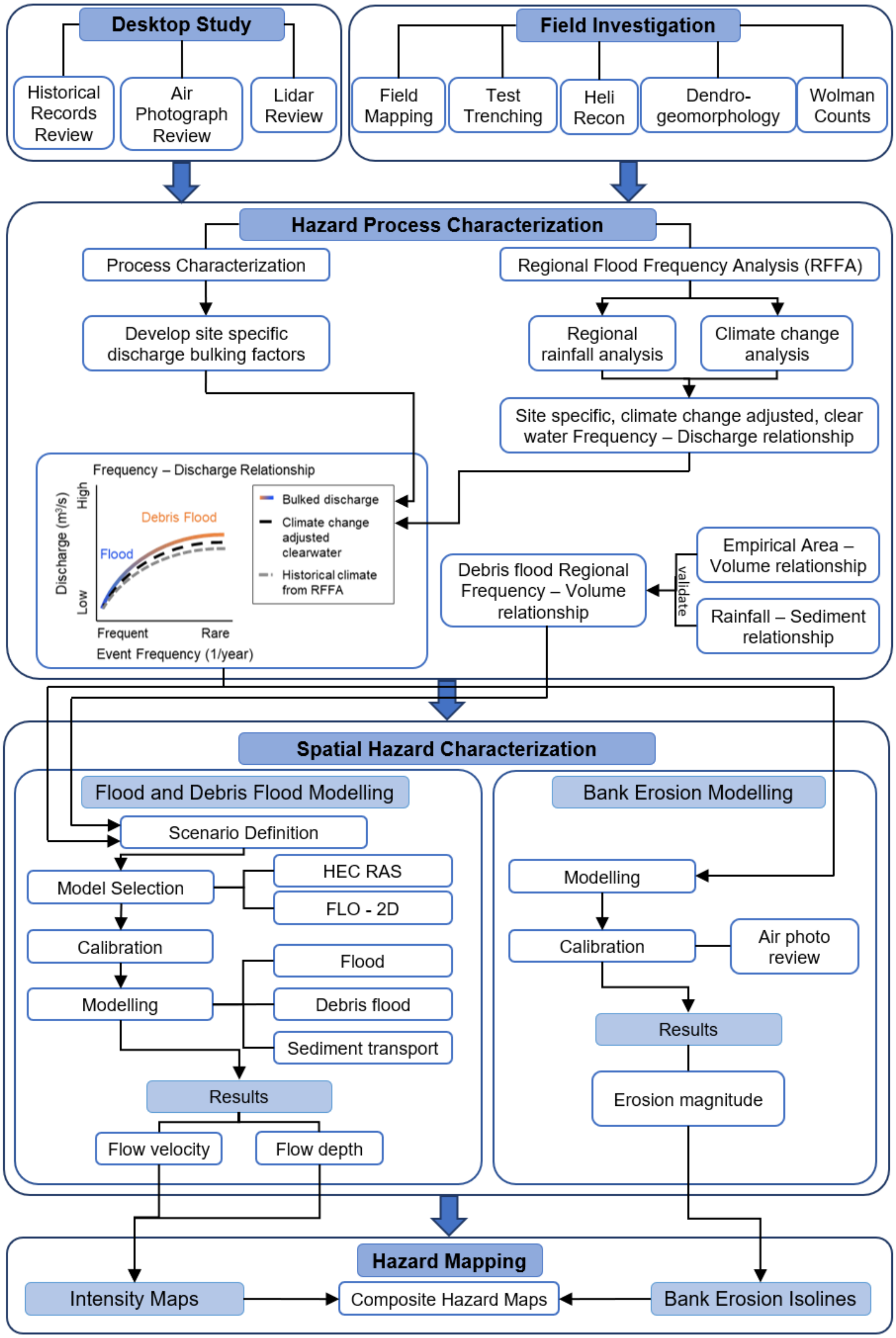


**Figure 4-1. Flood and debris-flood prone steep creek assessment workflow (Jakob et al., 2022). BGC applied this workflow to Thistle and Gravel creeks.**

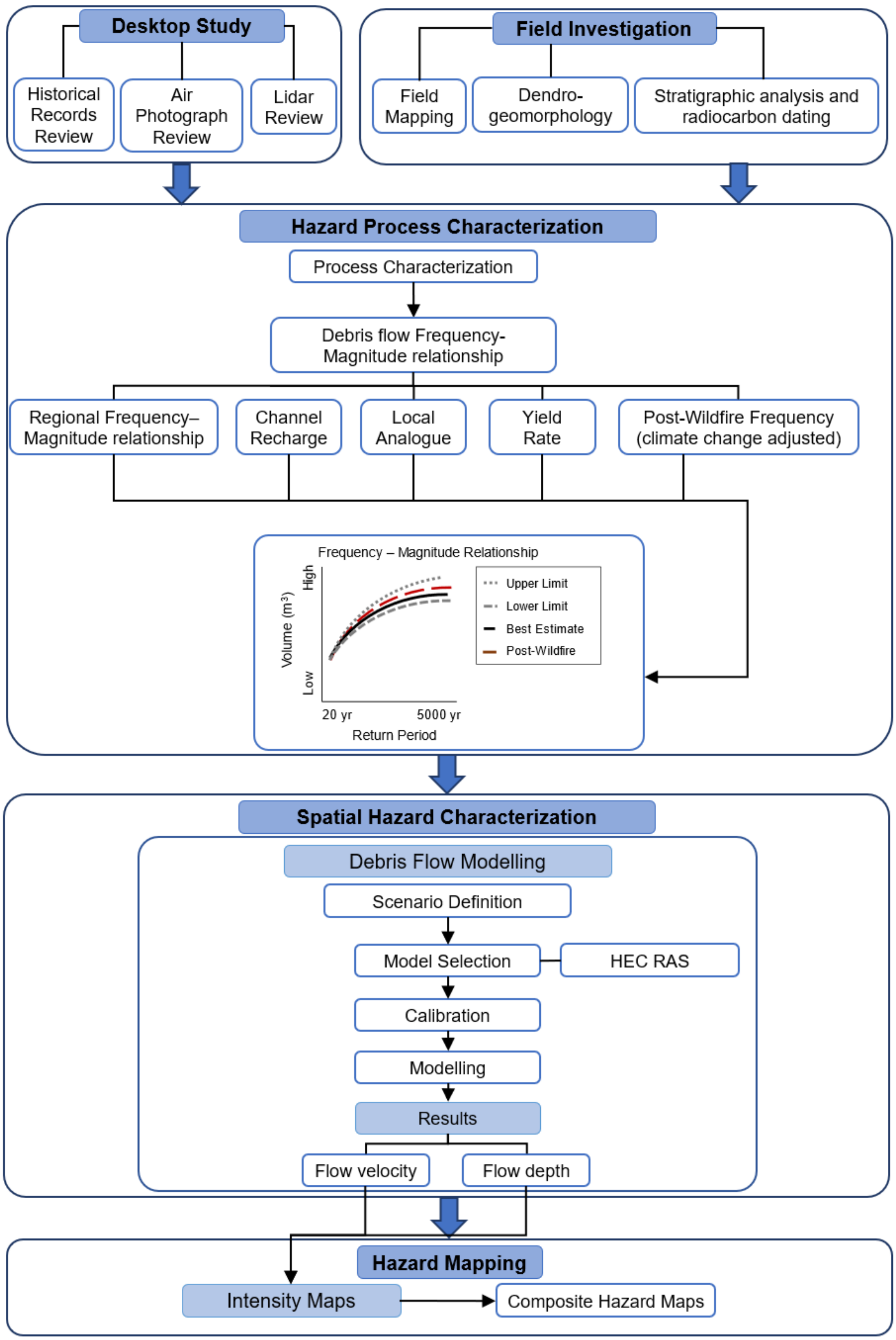


**Figure 4-2. Debris-flow prone steep creek assessment workflow. BGC applied this workflow to Daisy Creek.**

## 4.2. Steep Creek Process Classification

A desktop-level process classification of the study creeks based on watershed- and fan characteristics is provided in Figure 3-2. This classification is supplemented by BGC's field observations and previous assessments on the creeks as summarized in Table 4-1. Based on the watershed characteristics and site visits, BGC's interpreted classification of dominant process types(s) are shown in the highlighted row.

**Table 4-1. Process type classification for Daisy, Thistle, and Gravel creeks. The dominant process type relied upon in this analysis is highlighted in blue.**

| Dominant Process Type Classification | Daisy Creek | Thistle Creek | Gravel Creek |
|---|---|---|---|
| Morphometric classification (Figure 3-2) | Mixed debris floods and debris flows | Debris flows | Mixed debris floods and debris flows |
| Previous assessments | Debris flow<br>(Thurber, October 21, 1996; February 15, 2012; June 13, 2016) | Debris flood and debris flow<br>(Thurber, October 21, 1996) | Debris flow<br>(Thurber, October 21, 1996) |
| BGC field observations | Evidence of boulder lobes, levees, scarred trees in upper watershed, debris flow deposits in exposed channel bank. | No debris-flow features observed[1]. Bedrock-controlled channel. | No debris-flow features observed[1]. Bedrock-controlled channel. |
| BGC air photo observations (Drawing 04) | Historic debris avalanche scars in upper watershed. | Single debris avalanche scar identified in air photo record.[2] | No historic debris avalanche scars in watershed. |
| BGC classification[3] | Debris flows and debris floods | Floods and debris floods | Floods and debris floods |

Notes:
1. Characteristic evidence of debris flows includes the presence of boulder lobes and levees, high water marks, scarred trees, inverse grading of deposits, and matrix-supported deposits.
2. The debris avalanche scar was identified in 1932. It is in low-angle terrain that is not characteristic of slope instability in this environment. BGC suspects it may have been related to surface water drainage and possible pipe failure of water pipelines for historic mining at Britannia Mine. Remnants of water pipelines (metal casings and rotted wooden pipes) were observed in the area.
3. BGC classified the dominant process type(s) based on morphometric analysis, review of aerial imagery, and field observations.

The watersheds of each study creek are forested and there is potential for woody debris to enter the channels and form log jams. Log jams can impound material that may become dislodged during periods of high flow. They can also serve as natural check dams that form step-pools that stabilize creek channels. Based on review of field observations and lidar, BGC assessed that log jams formed on Gravel and Thistle creeks would not be sufficiently large to result in debris flows that could result loss of life within the proposed developed area. Instead, logs and debris transported during periods of high flows may become suspended in debris floods as evaluated by BGC.

## 4.3. Frequency-Magnitude Analysis

This section summarizes the F-M analysis of steep creek hazards in the study area and answers the following questions:

- How frequently have/will steep creek hazards occur(red) in the past and future?
- When they occur, how much sediment and water volume will be transported and what will be the likely peak discharge (volume and peak discharge are referred to collectively as "magnitude")?
- How will the answers to the two questions above change with continued climate change?

We present the answers to these questions in the form of an F-M relationship for specific return periods on each creek. Estimating the most realistic F-M relationships is important, as it influences the outcome of numerical modelling, informs risk assessments, and is a fundamental design input for potential mitigation measures.

### 4.3.1. Historical Events

Historical geohazard events can be assessed through historical records, air photo and satellite imagery interpretation, and field observations, namely dendrogeomorphology and radiocarbon dating. These methods are described in Appendix D. Table 4-2 summarizes the records of geohazard features at Daisy, Thistle, and Gravel creeks.

BGC did not find any records of damaging historical steep creek events on Thistle or Gravel creek. In January 2016, Daisy Creek overflowed onto Highway 99 and some sedimentation was reported downstream of the highway (Turje, May 31, 2020b). MoTI has no records of events or sediment clean out in the Daisy Creek basin since construction in 2009.

For all three study creeks, BGC reviewed air photographs between 1932 to 2003 provided by the UBC Geographic Information Centre (UBC GIS) and the National Air Photo Library (NAPL), satellite imagery from 2009 to 2022 available through Google Earth and ESRI World Imagery, and lidar from June 2019. Over the period with aerial imagery, BGC did not identify any debris flows or debris floods that reached the proposed development on the fan areas. BGC notes that the level of modification of the fan areas may obscure evidence of past events, if such events occurred during this period. Representative air photographs with annotations to show hazard features are provided in Drawing 04.

On Daisy Creek, BGC collected dendrogeomorphological samples on two trees in the upper watershed on the northern channel (Photos 6, 7; elevation 480 m) and three samples from paleosols overlying debris-flow deposits in an exposed channel bank downstream of the existing roadway culvert in the proposed development area (elevation 14 m). Most trees along the channel were either too young or too high above a potential debris-flow trim line to be suitable for dendrochronological investigation. A stratigraphic section and radiocarbon dating results from the paleosol samples are included in Appendix D.

In summary, we can make the following observations about the occurrence and types of steep creek processes at Daisy, Thistle, and Gravel creeks:

- No reported debris flows or debris floods on any of the study creeks that reached the proposed development area in the historical air photo record (1932 to 2020). The emphasis is on “reported” as clearly Type 1 debris floods (Church and Jakob, 2020) did occur.
- Evidence of debris flows or debris floods within the historical air photo record, if they occurred, was likely obscured by anthropogenic modification or not visible due to the resolution of the air photographs.
- The most recent evidence of debris flows on Daisy Creek was observed from trees with impact scars interpreted to be from past debris flows in the mid watershed. The age of impact was 104 and 135 years ago, respectively.
- Evidence was identified of multiple, historical debris flows on Daisy Creek large enough to deposit sediment downstream of the fan apex approximately 900 to 3,000 years ago.

**Table 4-2. Summary of observed steep creek events at Daisy- and Thistle creeks in reverse chronological age. No historical events were observed on Gravel Creek.**

| Creek | Event Date | Type of Event | Source of Event | Notes |
|---|---|---|---|---|
| Daisy Creek | 821 – 768 BC (2843 – 2790 years before present) | Unknown | Radiocarbon date from BGC-D-03 (Appendix D) | A prehistoric debris flow reached the Daisy Creek fan. The deposit was approximately 2 m thick. |
| | 41 BC – 820 AD (2063 – 1898 years before present) | Unknown | Radiocarbon date from BGC-D-02 (Appendix D) | A prehistoric debris flow reached the Daisy Creek fan. The deposit was approximately 0.5 m thick. |
| | 1032 – 1202 AD (990 – 820 years before present) | Unknown | Radiocarbon date from BGC-D-01 (Appendix D) | A prehistoric debris flow reached the Daisy Creek fan. The deposit was approximately 1.6 m thick. |
| | 1889 ± 5 years | Debris flow | Dendrochronology (Photo 7) | Dating of tree rings on stump suggests a debris-flow occurred on the Daisy Creek north channel 135 +/- 5 years before 2022. |
| | 1918 | Debris flow | Dendrochronology (Photo 6) | Dating of tree rings on a Douglas fir with an impact scar suggests a debris flow occurred on the Daisy Creek north channel in 1912. |
| | 1932- 1940 | Debris Avalanche | Air Photo Record: UBC GIC | Possible debris avalanche scars visible in the Daisy Creek watershed on the 1940 air photos. |
| | 1940-1969 | Debris Avalanche | Air Photo Record: UBC GIC | Possible debris avalanche scars visible in the Daisy Creek watershed on the 1969 air photos. |
| | 1969-1994 | Debris Avalanche | Air Photo Record: UBC GIC | Possible debris avalanche scars visible in the Daisy Creek watershed on the 1994 air photos. |
| Thistle Creek | Prior to 1932 | Debris Avalanche | Air Photo Record: National Air Photo Library | Possible debris avalanche scar visible in the lower portion of Thistle Creek on the 1932 air photos. |

Notes:

1. Sediment volume, peak discharge, and damages associated with the events listed in this table are unknown. Flow depth would likely have been some 50% larger than the deposit thickness
2. Before present is reported in relation to 1950 for radiocarbon dating results.

#### 4.3.2. Climate Change Considerations

Climate change is increasingly affecting most geophysical phenomena, including many landslide types and integrating climate change effects in landslide hazard assessments, while still in its infancy, is becoming standard practice.

Jakob and Owen (2021) found that the North Shore Mountains (which share similar topography, morphometry and climate to the present study area) are expected to experience a four-fold (300% increase) increase in shallow landslide frequency associated with climate change assuming the Relative Concentration Path (RCP) of 8.5. Shallow landslides, when they occur on slopes upstream of creeks, can directly trigger debris flows or impound the creek leading to debris flows when the water breaches the landslide deposit. The authors predicted this increase in frequency would be accompanied by an increase of 50% in average expected landslide volume.

Jakob and Owen's (2021) work examined regional debris-flow frequency and magnitude and those findings cannot be directly translated to individual creeks as they do not account for sediment supply limitations. What can be said, however, is that debris-flow frequency will increase in conjunction with higher rainfall intensities and higher antecedent conditions. For Daisy Creek, this implies more debris flows, but at a lesser magnitude because Daisy Creek is sediment supply-limited which means that the recharge time between subsequent events will be shorter, thus leading to a decrease in sediment volume per event (Jakob et al., 2005, Jakob, 2021). Effects of past and future logging have and will likely exacerbate these trends due to transient loss in root strength and potential drainage alterations along logging roads. The consequences of those anticipated shifts at Daisy Creek will be that existing mitigation and future upgrades will need more frequent clean-outs, but at lesser sediment volumes compared to a stationary climate.

The predicted trends outlined in Jakob and Owen (2021) are informed by historical climate data. It should also be acknowledged that climate conditions have entered a stage where events outside of human memory or records are becoming increasingly likely. This implies that storms like that witnessed in November 14/15, 2021 on the South Coast of BC will become more frequent and will at some point in the future affect Howe Sound. Impact by such storms could trigger multiple quasi-simultaneous debris avalanches in the watershed with all tributaries producing debris flows. This possibility has been acknowledged in the higher return period estimates in the F-M analysis (see Section 4.3.4).

Finally, with continued summer heating and drying, the chance of wildfires increases, especially with proposed urbanization as this increases the possibility of human-caused fires (cigarette butts, camp fires, barbeque fires, arson). Wildfires in the Daisy Creek watershed could be followed by post-wildfire debris flows in the few years immediately following the fire. This potential impact is quantified in Section 4.3.4.1.

Given the findings in Section 3.5, the following adjustments were made to the F-M considering climate change effects:

- Debris flows on Daisy Creek are possible for the 30 to 100-year return period given the projected increase in the frequency and magnitude of high intensity rainfall.

- Assuming a 50% climate change adjustment for rainfall total estimates relating to debris floods for all study creeks (Appendix D).
- Assuming an increasing likelihood for wildfires and tree mortality, given the marked increases in air temperature will enhance drying and increase the chance of beetle infestation-related mortality. Tree mortality may affect post-fire debris flows on Daisy Creek due to root strength loss.

The relative effects of these factors are captured in Table 4-3.

**Table 4-3. Summary of climate change effects on debris flood and debris flow F-M relationships.**

| Effect | F-M impact | Confidence |
|---|---|---|
| Increases in extreme rainfall frequency | Moves the F-M curve to the left (more frequent events of the same or higher magnitude) | Very High |
| Increases in extreme rainfall intensity | Moves the F-M curve upwards (larger events at the same return period) | Very High |
| Increase in wildfire burn severity | Addition of post-fire F-M | High |

### 4.3.3. Return Periods for Frequency-Magnitude Relationship

Debris flows and debris floods do not occur at regular intervals. As a result, the frequency of these events is better approximated using a range of years that cover the approximate recurrence of events of a certain size. For simplicity, within this report, BGC uses a representative return period from within the range that can also be expressed using an annual exceedance probability (AEP). Table 4-4 outlines the return periods / AEPs chosen by BGC for this hazard assessment that represent the spectrum of observed event magnitudes. The selected return periods are in accordance with the EGBC Guidelines for Legislated Flood Assessments in a Changing Climate (2018) and Guidelines for Landslide Assessments in BC (EGBC, 2022). Consistent with these guidelines, BGC only considered the upper return period range of 3,000- to 10,000-years (5,000-year representative return period) for Daisy Creek.

**Table 4-4. Range of return periods considered for the hazard assessment on Daisy, Thistle, and Gravel creeks.**

| Return Period Range (years) | Representative Return Period (years) | AEP (%) | Study Creeks |
|---|---|---|---|
| 10 to 30 | 20 | 5 | Daisy, Thistle, Gravel |
| 30 to 100 | 50 | 2 | |
| 100 to 300 | 200 | 0.5 | |
| 300 to 1,000 | 500 | 0.2 | |
| 1,000 to 3,000 | 2,500 | 0.04 | |
| 3,000 to 10,000 | 5,000 | 0.02 | Daisy |

Note:
The 50-, 500-, 2,500-, and 5,000-year events do not precisely fall at the mean of the return period ranges but were chosen as round figures due to uncertainties and because some of these return periods have a long tradition of use in BC.

### 4.3.4. Frequency-Magnitude Relationship

BGC used a suite of techniques to assess the F-M relationships for Daisy, Thistle, and Gravel creeks. By doing so, BGC increased the overall confidence in the results as individual techniques have considerable uncertainty and limitations. The use of model ensembles is done routinely for weather forecasts, hurricane prediction, El Niño Southern Oscillation (ENSO) forecasts, and climate change models. A summary of the resulting best estimates of peak discharge and sediment volume for each study creek at representative return periods (Table 4-4) is presented in Table 4-5. These estimates include consideration of climate change impacts to the end of the century (2100). The following subsections provide more detailed summaries for each creek.

Descriptions of the methods BGC used to develop the F-M relationships are outlined in Appendix D.

**Table 4-5. Summary of best estimate F-M relationships for each study creek. Sediment volumes are reported as those arriving at the fan apex. For each return period the highest magnitude event is reported.**

| Representative Return Period (years) | Daisy Creek | | Thistle Creek | | Gravel Creek | |
|---|---|---|---|---|---|---|
| | Sediment Volume ($m^3$) | Peak Discharge ($m^3/s$) | Sediment Volume ($m^3$) | Peak Discharge ($m^3/s$) | Sediment Volume ($m^3$) | Peak Discharge ($m^3/s$) |
| 20 | 1,600 | 28 | 1,300 | 16 | - | 8 |
| 50 | 1,900 | 31 | 1,800 | 18 | - | 9 |
| 200 | 8,000 | 170 | 3,000 | 20 | 1,000 | 10 |
| 500 | 13,000 | 250 | 4,000 | 22 | 1,400 | 11 |
| 2,500 | 20,000 | 350 | 5,000 | 26 | 2,000 | 12 |
| 5,000 | 24,000 | 410 | - | - | - | - |

Notes:

1. Sediment volume estimates are weighted averages of the constituent techniques employed within the model ensemble (Appendix D).
2. Sediment volumes are rounded to the nearest 100 for volumes less than 2,000 $m^3$ and to the nearest 1,000 $m^3$ for greater volumes.
3. Peak discharges in excess of 100 $m^3/s$ are rounded to the nearest 10.
4. Sediment volumes and peak discharges estimates for 5,000-year return period are included for Daisy Creek which is susceptible to debris flows (EGBC, 2022) but not for Thistle and Gravel creeks which are susceptible to floods and debris floods consistent with EGBC (2018) guidelines.
5. The Daisy Creek sediment volumes and peak discharges are based on the best estimate for debris floods and debris flows at the fan apex (i.e., they account for storage in the watershed) for conditions projected to the end of the century without the presence of a wildfire. Post-fire estimates are included in Section 4.3.4.1.

#### 4.3.4.1. Daisy Creek

BGC assessed Daisy Creek to be susceptible to debris floods and debris flows (Table 4-1). For smaller, more frequent events (less than 100-year return period), long duration rainfall will likely initiate Type 1 or Type 2 debris floods. Higher intensity rainfall or debris slides(s) could initiate debris flows for return periods in excess of the 30 to 100-year return period range (50-year representative return period). BGC expects that the higher rainfall associated with less frequent storm events (greater than 100-year return period) would trigger debris flows, thereby replacing debris floods as the hydro-geomorphologically significant process. The influence of wildfires on watersheds (Section 3.4) suggests that post-wildfire debris flows could be expected at return periods lower than 30 years if a sufficiently large storm occurred in the first two years following a fire in the Daisy Creek watershed.

The best estimates of sediment volume and peak discharge associated with the representative return periods considered in this study (Table 4-4) are summarized in Table 4-6 for Daisy Creek and shown graphically in Figure 4-3.

**Table 4-6. Daisy Creek F-M relationship including climate change impacts to end of century (2100).**

| Representative Return Period (years) | Process | Baseline | | Post-Wildfire | |
|---|---|---|---|---|---|
| | | Sediment Volume ($m^3$) | Peak Discharge ($m^3/s$) | Sediment Volume ($m^3$) | Peak Discharge ($m^3/s$) |
| 20 | Debris Flood (Post-Wildfire: Debris Flow) | 1,600 | 28 | 2,000 | 80 |
| 50 | Debris Flood (Post-Wildfire: Debris Flow) | 1,900 | 31 | 3,000 | 100 |
| 200 | Debris Flow | 8,000 | 170 | 8,000 | 170 |
| 500 | Debris Flow | 13,000 | 250 | 12,000 | 230 |
| 2,500 | Debris Flow | 20,000 | 350 | 25,000 | 420 |
| 5,000 | Debris Flow | 24,000 | 410 | 35,000 | 550 |

Notes:

1. Baseline conditions represent those where the watershed has not experienced a wildfire. Post-wildfire conditions are estimated in the first two years following a wildfire that burns 40% of the watershed at moderate to high intensity.
2. Sediment volume estimates for baseline conditions are weighted averages of the constituent techniques employed within the model ensemble and for post-wildfire conditions are derived from Gartner et al. (2014) model (Appendix D). At the 500-year return period, the best estimate sediment volume from the model ensemble predicted higher volume than the post-fire model.
3. Sediment volumes are rounded to the nearest 100 for volumes less than 2,000 $m^3$ and to the nearest 1,000 $m^3$ for greater volumes.
4. Peak discharges for debris floods (20-, 50-year return period) are based on rainfall-runoff modelling and peak discharges for debris flows (>50-year return period in baseline conditions, all return periods for post-wildfire conditions) as based on empirical relationships between sediment volume and peak discharge as described in Appendix D.
5. Peak discharges in excess of 100 $m^3/s$ are rounded to the nearest 10.

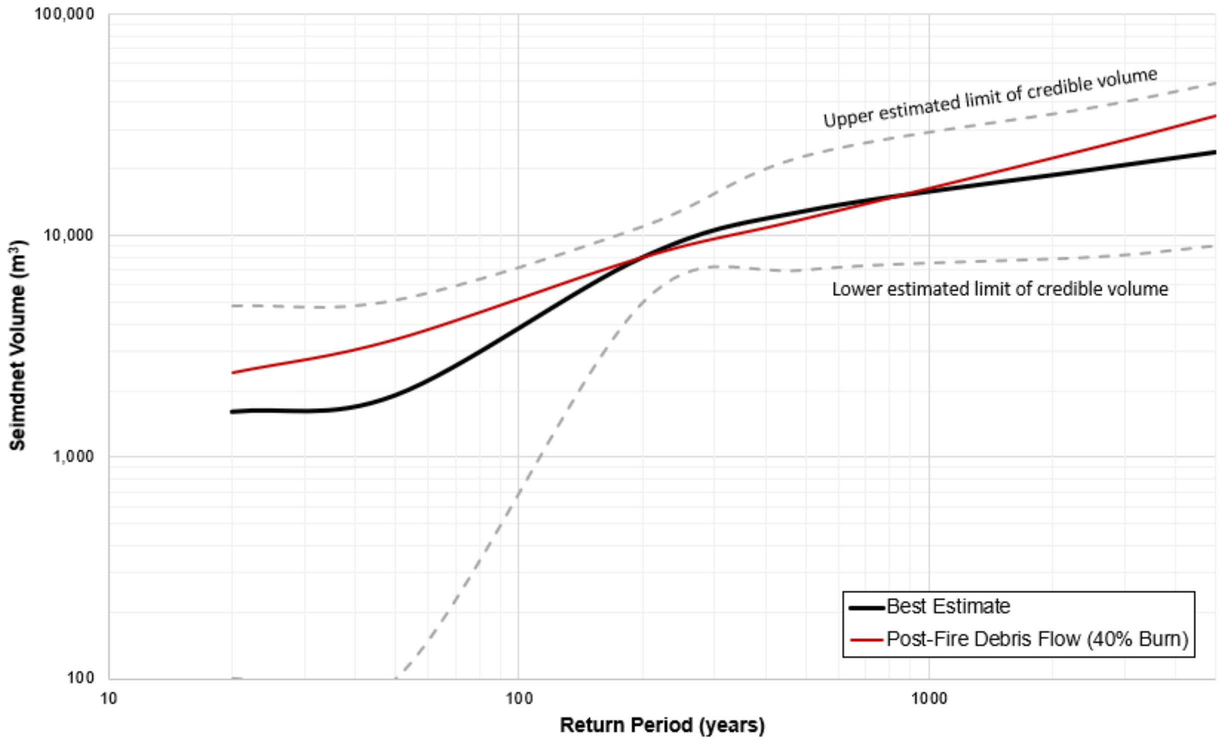


**Figure 4-3. Frequency-magnitude curves (baseline and post-wildfire conditions) derived from Daisy Creek F-M model ensemble. Upper and lower limits of credible volume are based on baseline conditions.**

### 4.3.4.2. Thistle Creek

BGC assessed Thistle Creek to be susceptible to floods and debris floods, but not debris flows (Table 4-1). The rainfall associated with storm events with return periods in excess of 30-years are expected to produce peak flows in the creek of sufficient intensity to initiate Type 1 debris floods upstream of the fan apex on Thistle Creek. The best estimates of peak discharge and sediment volume associated with the representative return periods considered in this study (Table 4-4) are summarized in Table 4-7 and shown graphically in Figure 4-4.

**Table 4-7. Thistle Creek F-M relationship including climate change impacts to end of century (2100).**

| Representative Return Period (years) | Peak Instantaneous Discharge ($m^3/s$) | Debris Flood Type | Bulking Factor | Bulked Peak Discharge ($m^3/s$) | Sediment Volume ($m^3$) |
|---|---|---|---|---|---|
| 20 | 15.9 | - | 1.00 | 16 | 1,300 |
| 50 | 17.5 | 1 | 1.02 | 18 | 1,800 |
| 200 | 19.5 | 1 | 1.05 | 20 | 3,000 |
| 500 | 20.4 | 1 | 1.10 | 22 | 4,000 |
| 2,500 | 21.7 | 1 | 1.20 | 26 | 5,000 |

Notes:
1. Peak discharges are based on rainfall-runoff modelling (floods and debris floods) and sediment bulking for debris floods as described in Appendix D.
2. Sediment volume estimates are weighted averages of the constituent techniques employed within the model ensemble as described in Appendix D.
3. Sediment volumes are rounded to the nearest 100 for volumes less than 2,000 $m^3$ and to the nearest 1,000 $m^3$ for greater volumes.

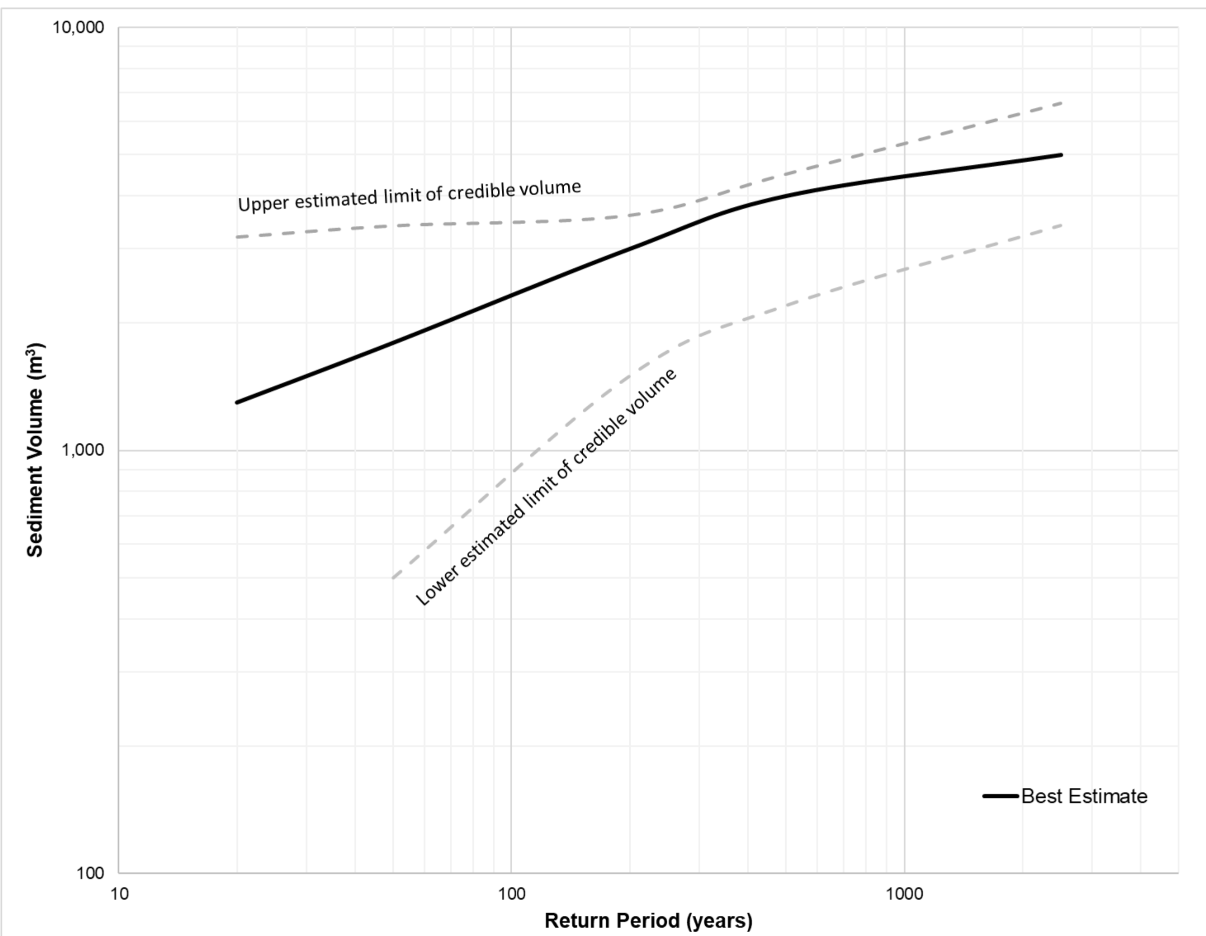


**Figure 4-4. Thistle Creek best estimate debris flood F-M curve derived from F-M model ensemble.**

#### 4.3.4.3. Gravel Creek

BGC assessed Gravel Creek to be susceptible to floods and debris floods (Table 4-1). The rainfall associated with storm events with return periods in excess of 100-years are expected to produce peak flows in the creek of sufficient intensity to initiate Type 1 debris floods on Gravel Creek. The best estimates of peak discharge and sediment volume associated with the representative return periods considered in this study (Table 4-4) are summarized in Table 4-8 and shown graphically in Figure 4-5.

**Table 4-8. Gravel Creek F-M relationship including climate change impacts to end of century (2100).**

| Representative Return Period (years) | Peak Instantaneous Discharge ($m^3/s$) | Debris Flood Type | Bulking Factor | Bulked Peak Discharge ($m^3/s$) | Sediment Volume ($m^3$) |
|---|---|---|---|---|---|
| 20 | 8.1 | - | 1.00 | 8 | - |
| 50 | 9.0 | - | 1.00 | 9 | - |
| 200 | 10.0 | 1 | 1.02 | 10 | 1,000 |
| 500 | 10.5 | 1 | 1.02 | 11 | 1,400 |
| 2,500 | 11.1 | 1 | 1.10 | 12 | 2,000 |

Notes:

1. Peak discharges are based on rainfall-runoff modelling (floods and debris floods) and sediment bulking for debris floods as described in Appendix D.
2. Sediment volume estimates are weighted averages of the constituent techniques employed within the model ensemble as described in Appendix D.
3. Sediment volumes are rounded to the nearest 100 for volumes less than 2,000 $m^3$ and to the nearest 1,000 $m^3$ for greater volumes.

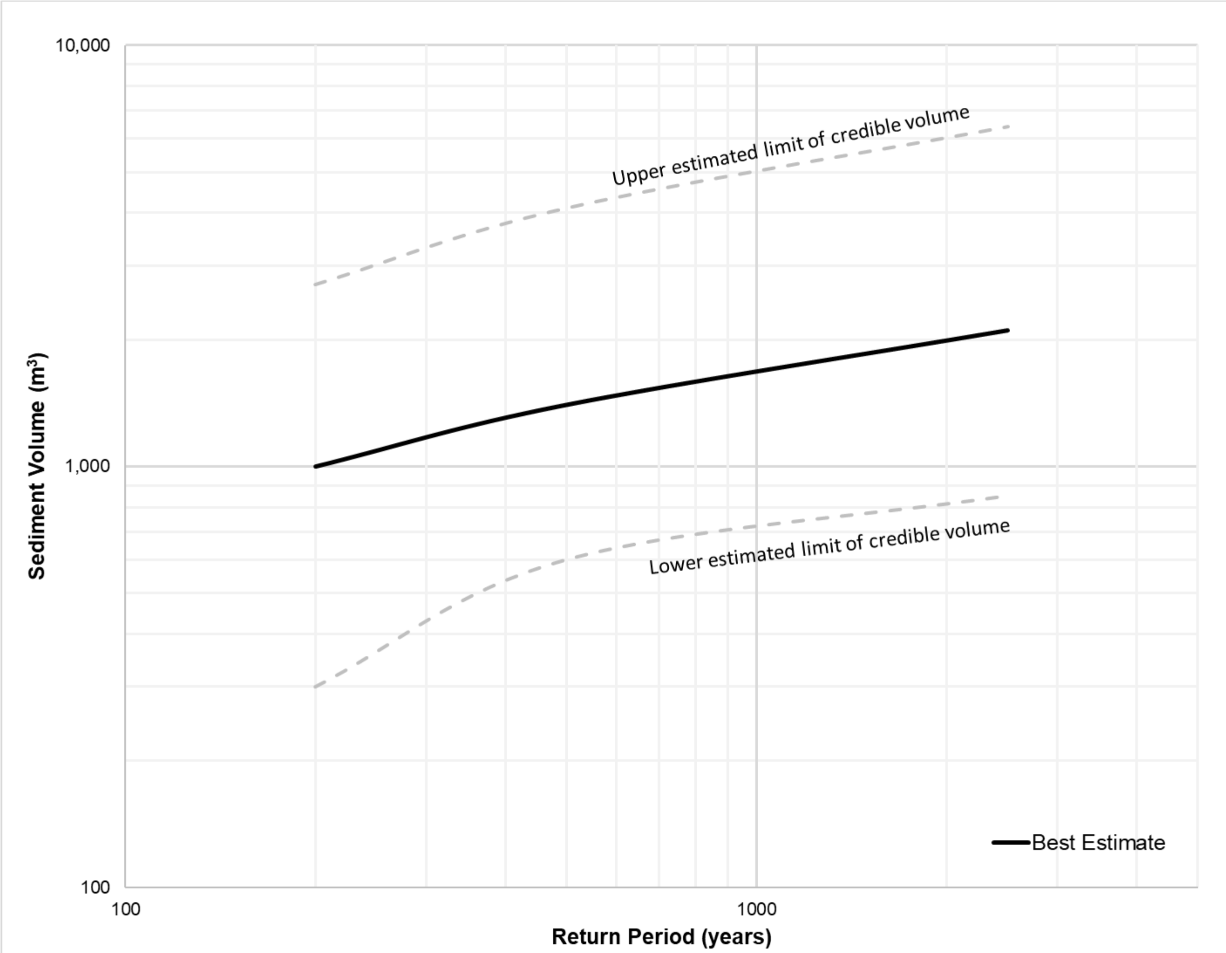


**Figure 4-5. Gravel Creek best estimate F-M curve derived from F-M model ensemble.**

#### 4.3.4.4. Uncertainties and Limitations of Frequency-Magnitude Relationships

The F-M relationships for the three study creeks includes floods, debris floods and debris flows (Daisy Creek). This section summarizes the limitations associated with the techniques applied by BGC to develop the F-M relationships.

BGC used rainfall-runoff modelling to estimate peak flows (flood quantiles) on all study creeks (Appendix D). Limitations with this method include:

- A model is only as reliable as the data that is used to support it. There is inherent measurement error in the recording of rainfall, especially for the larger (and rarer) storm events.
- The meteorology of storms can be highly variable: a strong double-fronted (warm- and cold-front) storm may lead to two distinct rainfall intensity peaks, while a single front storm would lead to a single peak, perhaps amplified, or lagged by snowmelt contribution. The shape of the hydrograph similarly influences the threshold at which debris begins to mobilize and the amount of sediment moved. In this analysis, BGC used a single hydrograph which introduces some uncertainty.

- The impacts of climate change, land use change, wildfires, or insect infestations on the hydrology of a watershed are not easily quantified. Trends associated with these changes are often not identifiable at a statistically significant level.

BGC used bulking factors to account for the increased sediment concentration associated with debris floods (Appendix D). Limitations of this method include:

- While based on scientific literature and best practice guidance, selection of appropriate bulking factors requires informed judgement on the part of the practitioner. Additional research and case studies on debris-flood sediment concentration are required to continue to refine these estimates.

BGC used a suite of techniques to estimate the sediment volumes associated with debris foods and debris flows (Appendix D). No individual method can produce precise results, and each have limitations and uncertainties. This situation is analogous to weather forecasting where a single meteorological model only produces one possible outcome. Weather forecasts often compile, compare, and evaluate several models (named a model ensemble) to increase confidence and credibility. Given the uncertainty associated with climate change effects on flood volumes and forestry operations in the watersheds potentially initiating debris avalanches and debris flows, selecting reasonably conservative estimates was warranted due to the potential for life loss and major infrastructure damage. BGC employed five independent semi-empirical models to develop the Daisy Creek F-M relationship and three independent semi-empirical models to develop the Thistle Creek and Gravel Creek F-M relationships. BGC complemented the analyses with professional judgment based on dozens of previous similar studies to estimate the most credible F-M relationships thereby gaining confidence in the best estimate.

BGC was only able to obtain three samples for radiocarbon dating from test pits and soil exposures across the fan. The reason is that the fan surface has been heavily disturbed over the years making radiocarbon sampling unreliable and because much of the original fans of the study creeks have been artificially removed for aggregate use. This lack of data challenged the debris-flow hazard assessment and required a higher reliance on empirical methods to decipher F-M relationships.

BGC used empirical relationships that relate sediment volume to peak discharge derived from past debris flows in British Columbia and Japan to estimate peak discharges associated with the debris flows on Daisy Creek (Appendix D). The limitations of this method include:

- Empirical relationships are developed from limited data sets and further reduced to select appropriate analogues to the study watershed.
- Uncertainty in the sediment volumes impacts the resultant peak discharge estimates.

### 4.4. Numerical Modelling

This section summarizes the results of flood-, debris-flood, and debris-flow numerical modelling of steep creek hazards at Daisy, Thistle, and Gravel creeks. The numerical models are based on the F-M relationships developed for each creek (Section 4.3.4). These models answer the following questions:

- When steep creek hazards occur, how far do they spread across the fan?
- How deep and fast is the flow during a steep creek event?
- What impact forces (the product of the flow depth, velocity, and density) are produced during these events?

BGC completed all numerical modelling using HEC-RAS 2D (version 6.2), a public domain hydraulic modelling program developed and supported by the United States Army Corps of Engineers. Appendix E describes the numerical modelling methodology.

### 4.4.1. Hazard Scenarios

Hazard scenarios represent specific events of a particular frequency and magnitude that may impact a site. Hazard scenarios are organized by representative return period (Table 4-4). BGC developed hazard scenarios to include the potential for bridge, culvert, and / or channel blockages, as appropriate given the anticipated flows and sediment volumes. At this stage, BGC modelled the road crossings associated with the proposed development as open channels as design of the crossings are not yet available and will be informed by the outcomes of this assessment. As part of the design process for these crossings, BGC recommends that numerical modelling with the proposed designs in place be undertaken to evaluate the residual hazard and risk[10]. In total, BGC modelled 19 hazard scenarios on the study creeks (Appendix E).

BGC modelled Thistle and Gravel creeks together, as they are adjacent and flows on these creeks have the potential to interact within the proposed development area. Moreover, both creeks are classified as flood- and debris-flood-prone by BGC (Table 4-1). BGC modelled Daisy Creek independently as it is classified as debris-flood- and debris-flow-prone (Table 4-1). BGC modelled Daisy Creek debris flows as two-phased flow with a coarse front and muddy afterflow to better approximate the surge-type behaviour of debris flows. This flow behaviour is described in Appendix C and the modelling approach is summarized in Appendix E.

For all scenarios, BGC used a lidar-derived DEM dated 2019 that does not include the grading and topographic modifications associated with the proposed development excepting where BGC modified the DEM to remove bridge decks within the proposed development that are anticipated to be redesigned. As such, the numerical model results establish a baseline for hazards at the site that can inform grading and infrastructure design in future phases of project planning.

### 4.4.2. Modelling Results

On Thistle and Gravel creeks, results from the models indicate that significant inundation (up to 3 m) will occur in all modelled return periods. Most overbank flow stems from Gravel Creek which has a poorly defined channel within the proposed development area. The inundation area is expected to extend approximately from the Gravel Creek fan apex west to Highway 99, where it extends north and south along the highway. To the south, flow joins Thistle Creek and ponds before outletting to Howe Sound through the Thistle Creek culvert below Highway 99. To the north, flow parallels the east edge and overtops Highway 99 for approximately 800 m. Maximum

[10] Residual hazard and risk refer to the hazard and risk that exist once a mitigation is in place.

inundation depths range from 2.8 m in the 20-year return period event to 3.2 m in the 2,500-year return period event. Should the Thistle Creek railway culvert become blocked during the 2,500-year event, inundation depths are expected to increase to a maximum of 3.7 m. These model results illustrate the importance of channel design to minimize overbank flooding and avulsion.

The results of the Daisy Creek modelling are summarized in Table 4-9.

**Table 4-9. Daisy Creek – summary of modelling results.**

| Process and Representative Return Period Range (years) | Key Observations |
|---|---|
| Debris flood<br>(20- and 50-year return periods) | • The Highway 99 culvert has insufficient capacity to convey the peak discharge (flow). Flow is expected to overtop Highway 99 and pond in and around the northeast shoulder of the highway.<br>• Downstream of the Highway 99 crossing, flow is expected to exit the channel over both banks.<br>• Overbank flow and ponding is also expected in topographic lows on the southwest side of Daisy Creek upstream of the existing road crossing (approximately 200 m downstream of the Highway 99 crossing).<br>• Overtopping of the CN Rail bridge rail tracks is expected due to bridge conveyance exceedance.<br>• Inundation depths are expected to range from a maximum of 1.7 m in the 20-year return period event to a maximum of 1.8 m for the 50-year return period. |
| Debris flow<br>(50-year return period.) | • The coarse front of the debris flow deposits in the debris basin. All downstream flow associated with the muddy afterflow is expected to remain channelized, and the majority of sediment deposition is expected to occur within the channel, upstream of the debris basin. |
| Debris flow<br>(200- and 500- year return periods) | • Flow is expected to remain channelized upstream of the Highway 99 crossing, with the majority of sediment deposition occurring in the debris basin and in the channel upstream of the debris basin.<br>• The debris basin culverts are expected to be of insufficient capacity to convey the entire discharge, and flow is expected to travel over the debris basin spillway before entering the Highway 99 culvert. The Highway 99 culvert has insufficient capacity to convey the peak discharge associated with the muddy afterflow of 500-year and may not have sufficient capacity to convey the 200-year debris flow muddy afterflow.<br>• Approximately 200 m downstream of the Highway 99 crossing, flow is expected to exit the channel, inundating the left bank of Daisy Creek before returning to the channel.<br>• Flow is expected to overtop the rail tracks due to bridge conveyance exceedance.<br>• Should additional culverts become blocked, inundation extents are expected to increase. |
| Debris flow<br>(2,500- and 5,000- year return periods) | • Flow is expected to exit the channel upstream of Highway 99 from the debris basin spillway and upstream of the Highway 99 culvert. This flow is expected to overtop Highway 99, and both continue downstream and travel northwest down Highway 99, and in the Highway 99 ditches.<br>• Approximately 200 m downstream Highway 99, flow is expected to exit the channel, inundating the left bank of Daisy Creek before returning to the channel. In the 5,000-year event, more flow is expected to travel down and alongside Highway 99, reducing inundation depths and extents along the left bank of Daisy Creek.<br>• Flow is expected to overtop the rail tracks. |

Drawing 06 shows the flow depth associated with modelled 200-year return period scenarios on all the study creeks. The depth shown is the maximum of any modelled scenario (Appendix E) at this return period. Within the proposed development area, flow depths outside of the creek channels are highest in topographic lows north of Thistle Creek. Drawing 07 shows the buildings within the proposed development that are intersected by flow depths in excess of 0.5 m and colour coded by the return period when flow depths are expected to exceed this threshold. This map provides an indication of the locations where economic losses associated with floods, debris floods, and debris flows on the study creeks may be highest and where mitigation is merited to limit inundation and associated impacts. Model results shown on Drawings 06 and 07 assume that the debris basin on Daisy Creek works as intended during debris floods and debris flows. However, as noted, a debris flow reportedly occurred in the January 2016 storm that blocked the lower culvert in the debris basin resulting in water and sediment spilling through the upper culvert and clearwater flowing down Highway 99 and into lands to the north (Thurber, June 13, 2016). This scenario did not occur during BGC's modelled scenarios, largely because the model does not incorporate erosion and is identified as an auxiliary hazard (Section 4.4.3).

### 4.4.3. Auxiliary Hazard Scenarios

It is not possible to model all potential hazard scenarios at a given site given the stochastic nature of natural processes and uncertainties associated with flow behaviour. As a result, auxiliary hazards not identified in the numerical results are possible on the study creeks. The probability and estimated frequency of such events is not easily assigned and therefore BGC did not assign return periods for them. Auxiliary hazards on the study creeks include:

- Thistle and Gravel creeks
  - Uncontrolled flow through the deltaic sediments from upstream surface water management on logging and access roads could lead to significant erosion and channel avulsion.
- Daisy Creek
  - Uncontrolled flow on the north side of Highway 99 in the highway ditch, could erode the highway shoulder and lead to partial asphalt undermining and eventual collapse unless all water crosses the highway and flows on the south side of the north-bound lanes. The degree of asphalt loss and channelization cannot be predicted with any confidence. Should the former occur, the eroded channel could eventually discharge towards the south into the proposed developed area where it could erode a substantial gully in loose glaciofluvial sediment. In this case, a small alluvial fan would form a the bottom of the gully.
  - The main crossing of Daisy Creek within the proposed development, in the current condition, or if the replacement planned as part of the proposed development is insufficiently designed, could be outflanked by erosion. Should the bridge collapse it could become a significant flow obstruction, possibly leading to upstream aggradation and unpredictable bank erosion.

- In the event that the railway bridge is overwhelmed, the abutments could be eroded and outflanked and flow discharge towards the ocean following grade. Given the somewhat chaotic nature of such events, exact predictions are not possible.
- In the unlikely event that the west embankment of the Daisy Creek debris basin would fail through overtopping or otherwise, debris would spill onto Highway 99. Such an event was not modelled nor quantified in terms of its probability by BGC and the assumption was that the berm functions as intended for all modelled scenarios.

#### 4.4.4. Uncertainties and Limitations of Numerical Modelling

The numerical modelling for the three study creeks includes floods, debris floods and debris flows (Daisy Creek). This section summarizes the uncertainties and limitations associated with the modelling approach applied by BGC to assess potential impacts of these hazards. The uncertainties and limitations can be categorized according to the stochastic nature of natural processes, model inputs, and model limitations as follows:

- Natural Processes
  - Steep creek hazards are natural processes with complex behavioural feedback mechanisms associated with meteorological, orographic, and topographic factors. Such interactions are complicated by future change associated with a changing climate and natural or man-made modifications to the landscape. Given this, there is a stochastic or unpredictable nature to these process types that lead to inherent uncertainty and limitations to the accuracy of numerical models.
- Model Inputs
  - The lidar-derived topography from 2019 is a ‘snapshot in time’. Future modification of the landscape will influence the flow behaviour.
  - The topography is ‘bare-earth’ meaning it does not include three-dimensional natural (e.g., trees) and man-made (e.g., buildings) structures that influence flow behaviour through flow restriction, concentration, and redirection.
- Model limitations
  - HEC-RAS does not compute channel aggradation, bank erosion, or highway erosion. As such there is uncertainty in the precise flow behavior of each modelled scenario, as each of these factors can influence the flow path(s) and associated impact forces.

The influence of future modifications in the study creek watersheds and fan areas should be reviewed to determine if there is a resultant change in the hazard and risk within the proposed development.

### 4.5. Composite Hazard Map

BGC presents the results of the hazard assessment in the form of a composite hazard map which combines the impact force and frequency of steep creek processes. In other words, for any location in the study area, it describes how often and how intense a flood, debris flood, or debris flow could be. By combining both hazard frequency and intensity for multiple hazard scenarios, such maps exemplify true hazard. The warmer the colours, the higher the hazard (i.e., dark reds signify a higher hazard than, for example, yellow). The results were generated from the methods outlined in Appendix F. The composite hazard map does not provide information on the frequency of debris floods or debris flows at specific locations, nor does it allow interpretation of site-specific impact forces. This information, if required, can be determined from the numerical modelling results for individual hazard scenarios (Section 4.4.1). The composite hazard map for the study area is shown in Drawing 08.

The composite hazard map is based on baseline (pre-mitigation) conditions and does not account for any future mitigation measures designed to deflect or stop debris or provide additional bank armouring. Similarly, the composite hazard map does not account for any major fan surface alterations by smaller debris flows, bank erosion, or by construction. It also does not account for the presence of structures and their effects on steep creek processes. The hazard zones are not and cannot be precise and should not be interpreted as such. Debris flows and debris floods are to some extent chaotic processes and their exact behaviour cannot be predicted with precision. Any future global (i.e., for the entire fans) mitigation measures will, depending on their scale, location and effectiveness, reduce the hazard. Future mitigation measures will require re-modelling of floods, debris floods, and debris flows to estimate the effect of hazard reduction cartographically.

# 5. RISK ASSESSMENT

## 5.1. Introduction

Risk is a measure of the probability and severity of an adverse effect to health, property, or the environment, and is estimated by the product of hazard probability (or likelihood) and consequences (Australian Geomechanics Society (AGS), 2007).

At the proposed development, BGC assessed baseline (pre-mitigation) life safety risk[11] associated with steep creek processes on Daisy, Thistle, and Gravel Creeks. This assessment was completed for individuals in buildings. It does not include economic risk or risk to people outside of buildings[12]. The composite hazard map (Drawing 08) provides an indication of the hazard levels outside of buildings can be used to inform mitigation and land-use selection

## 5.2. Risk Assessment Framework

BGC assessed life safety risk for individuals and groups.

### 5.2.1. Individual Risk

Individual risk, quantified as the annual Probability of Death of an Individual (PDI), evaluates the chance that a specific person will be killed by the hazard. This typically focuses on the person judged to be most at risk, corresponding to a person spending the greatest proportion of time at home, such as a young child, stay-at-home person, or an elderly person. For this assessment, individual risk is calculated as follows:

$$PDI_j = \sum_{i=1}^{n} P(H)_i P(S{:}H)_{i,j} P(T{:}S)_{i,j} V_{i,j} \qquad \text{[Eq. 5-1]}$$

Where:

- $PDI_j$ is the PDI at a given building $(j)$
- $P(H)_i$ is the annual probability of geohazard scenario $(i)$
- $P(S{:}H)_{i,j}$ is the spatial probability of impact of geohazard scenario $(i)$ at a given building $(j)$
- $P(T{:}S)_{i,j}$ is the temporal probability of a person occupying building $(j)$
- $V_{i,j}$ is the probability of fatality (vulnerability) of a person occupying building $(j)$ given impact by the estimated hazard intensity[13] of geohazard scenario $(i)$
- $n$ are the total number of geohazard scenarios considered.

[11] Life safety risk considers the potential for a hazard event to result in loss of life for one or more individuals.

[12] Risk to individuals outside of buildings is subject to significant uncertainties associated with estimating the location and number of people outside of buildings and within an area impacted by a hazard at the time it occurs. For this reason, it is standard practice to not evaluate the risk to individuals outside of buildings.

[13] Intensity refers to the destructive potential of an event (see Section 5.3.1)

### 5.2.2. Group Risk

Group risk, also known as societal risk, evaluates the number of people that could be killed by a debris-flood or debris-flow related hazard, considering all people located within the proposed development area.

Group risk is derived from f-N pairs where the annual probability of a given geohazard scenario, $f_i$, corresponds with an estimated number of fatalities, $N_i$ defined as follows:

$$f_i = P(H)_i \qquad \text{[Eq. 5-2]}$$

$$N_i = \sum_{j=1}^{m} P(S:H)_{i,j} P(T:S)_{i,j} V_{i,j} E_j \qquad \text{[Eq. 5-3]}$$

Where:

- $P(H)_i$, $P(S:H)_{i,j}$, $P(T:S)_{i,j}$, and $V_{i,j}$ are the same as defined in [Eq. 5-1; and
- $E_j$ is the number of people exposed to the hazard in building ($j$)
- $m$ are the total exposed buildings.

## 5.3. Risk Assessment Methods

The variables in Equations 5-1 to 5-3 can be estimated based on:

- numerical model results ($P(H)_i$, $P(S:H)_{i,j}$),
- duration a building is occupied in a given day based on primary building use ($P(T:S)_{i,j}$)
- vulnerability criteria developed for debris floods and debris flows ($V_{i,j}$)
- anticipated building occupancy rates ($E_j$).

If any of these variables are zero at a location of interest, then the calculated life safety risk for that location is zero. Based on BGC's numerical modelling, buildings within the proposed development are anticipated to be impacted by one or a combination of flood, debris flood, or debris flow hazards originating on the study creeks (Section 4.4). BGC reviewed whether the modelled flows were of sufficient intensity to result in a fatality at any of the proposed buildings ($V_{i,j}$) as described in the following section.

### 5.3.1. Vulnerability

Vulnerability is defined as the probability that a fatality occurs if a given a building is impacted in the hazard scenario. BGC estimated vulnerability of persons within buildings to debris-flood and debris-flow impact as an indirect consequence of building damage based on the criteria outlined in Table 5-1. These criteria are based on the debris-flow intensity index (Jakob, Stein, & Ulmi, 2012), which describes the severity of the debris-flow impact at any location in the model domain. It is calculated as:

$$\mathrm{I_{DF}} = \mathrm{d} \times \mathrm{v}^2 \qquad \text{[Eq. 5-4]}$$

where $\mathrm{d}$ is flow depth (m) and $\mathrm{v}$ is flow velocity (m/s).

The debris-flow intensity index, or intensity, is an output of the HEC-RAS model results. For each hazard scenario, BGC assigned the maximum intensity intersecting a building footprint and associated a vulnerability to that building using the best estimate criteria in Table 5-1. Lower and upper bound estimates represent the range of uncertainty in this parameter, as it depends on factors that cannot be accounted for at the scale of assessment, such as the location of persons within buildings or the building construction materials.

**Table 5-1. Vulnerability criteria for persons within buildings.**

| Intensity ($m^3/s^2$) | Building Damage | Description | Life-loss Vulnerability | | |
|---|---|---|---|---|---|
| | | | Lower Bound | Best Estimate | Upper Bound |
| ≤ 1 | Minor | Slow flowing shallow and deep water with little or no debris. High likelihood of water damage, but structural damage is unlikely. | ~0 | ~0 | ~0 |
| 1 to 3 | Moderate | Mostly slow flow with minor debris. High likelihood of sedimentation and water damage. Potentially dangerous to people in buildings, or in areas with higher water depths. | 0.01 | 0.02 | 0.04 |
| 3 to 10 | Major | Potentially fast flowing but mostly shallow water with debris. Moderate likelihood of building damage and high likelihood of major sediment and/or water damage. Potentially dangerous to people on the first floor or in the basement of buildings without elevated concrete footings | 0.05 | 0.2 | 0.4 |
| 10 to 30 | Extensive | Fast flowing water and debris. High likelihood of structural building damage and severe sediment and water damage. Dangerous to people on the first floor or in the basement of buildings. | 0.2 | 0.4 | 0.6 |
| 30 to 100 | Severe | Fast flowing debris. High likelihood of severe structural building damage and severe sediment damage. Very dangerous to people in buildings irrespective of floor. | 0.4 | 0.6 | 0.8 |
| > 100 | Complete Destruction | Very fast flowing debris. Very high likelihood of complete building destruction for unreinforced and reinforced buildings, and extreme sediment damage. A person in the building will almost certainly be killed. | 0.8 | 0.9 | 1 |

Note: These vulnerability criteria were selected based on expert judgement and experience, as no systematic analysis of debris-flood or debris-flow vulnerability is available in literature. These criteria are consistent with other risk assessments completed within the SLRD (for example, BGC, December 4, 2020).

## 5.4. Risk Assessment Results

At the proposed development, all modelled flows from Daisy, Thistle, and Gravel Creeks resulted in intensities less than 1 $m^3/s^2$ at the proposed building locations provided by Tigerbay (Drawing 02). The resultant life-loss vulnerability for all proposed buildings to date is effectively zero based on the vulnerability criteria outlined in Table 5-1. Individual and group risk are negligible (effectively zero). Therefore, there are no proposed buildings where there is credible life safety risk from steep creek hazards originating on the study creeks and group risk from the assessed hazards is negligible. As described in Table 5-1 and shown on Drawings 06 and 07, water damage is expected at multiple buildings where flow depths are sufficient to ingress buildings and result in economic losses. This assessment does not include risk to motorists on Highway 99. However, BGC acknowledges that impacts to motor vehicles in the event of a debris flood or debris flow overtopping the Daisy Creek crossing is a credible hazard given the channel configuration through this reach and the existing culvert capacity below Highway 99.

# 6. CONCLUSIONS

BGC completed a detailed assessment of steep creek hazards on Daisy, Thistle, and Gravel creeks through the proposed development south of Britannia Beach, BC. The creeks are susceptible to a range of process types as summarized in Table 6-1.

**Table 6-1. Dominant process types on study creeks.**

| Dominant Process Type Classification | Daisy Creek | Thistle Creek | Gravel Creek |
|---|---|---|---|
| BGC classification | Debris flows and debris floods | Floods and debris floods | Floods and debris floods |

Using a combination of aerial imagery, desktop analysis, and field observations, BGC developed an F-M relationship for each of the study creeks for a range of representative return periods informed by best practice guidelines for flood and landslide hazards in BC (EGBC, 2018; 2022). The resultant sediment volumes are summarized in Table 6-2.

**Table 6-2. Summary of best estimate F-M relationships for each study creek. Sediment volumes are reported as those arriving at the fan apex. For each return period the highest magnitude event is reported.**

| Representative Return Period (years) | Daisy Creek | | Thistle Creek | | Gravel Creek | |
|---|---|---|---|---|---|---|
| | Sediment Volume ($m^3$) | Peak Discharge ($m^3/s$) | Sediment Volume ($m^3$) | Peak Discharge ($m^3/s$) | Sediment Volume ($m^3$) | Peak Discharge ($m^3/s$) |
| 20 | 1,600 | 28 | 1,300 | 16 | - | 8 |
| 50 | 1,900 | 31 | 1,800 | 18 | - | 9 |
| 200 | 8,000 | 170 | 3,000 | 20 | 1,000 | 10 |
| 500 | 13,000 | 250 | 4,000 | 22 | 1,400 | 11 |
| 2,500 | 20,000 | 350 | 5,000 | 26 | 2,000 | 12 |
| 5,000 | 24,000 | 410 | - | - | - | - |

At Daisy Creek, BGC coordinated radiocarbon dating of samples collected from the channel bank within the proposed development area to determine the dates of past debris flows. The resultant dates are outside of the historical record and BGC did not identify evidence of more recent debris flows reaching the proposed development from air photos. This suggests that debris flows pose a credible hazard to the proposed development; however, the historic frequency of such events is very low.

The F-M relationships were the foundational input for numerical modelling of the steep creek hazards. BGC used the numerical modelling program HEC-RAS to model floods, debris floods and debris flows on the creeks. The results illustrate that:

- Daisy Creek

  - The debris basin is effective at retaining debris-flow sediment volumes up to 2,500-year return period flows.
  - The Highway 99 culvert is undersized to convey debris floods and debris flows for all return periods considered and overflow along Highway 99 is expected.
  - The CN Rail bridge has insufficient capacity and is expected to experience additional sedimentation which will further reduce the capacity.
- Thistle and Gravel creeks
  - Significant inundation (up to 3 m) will occur in all modelled return periods.
  - Most overbank flow stems from Gravel Creek which has a poorly defined channel within the proposed development area.
  - Water flow and ponding is expected on the upstream (east) side of Highway 99.

BGC created a composite hazard map to illustrate the hazard level associated with steep creek processes within the proposed development area under baseline (pre-mitigation) conditions (Drawing 08). The areas of highest hazard are within the creek channels. Moderate to low hazard was identified for areas along Daisy Creek where flow leaves the channel at the Highway 99, CN Rail, and downstream culvert crossings. Gravel Creek is poorly confined and overland flow contributes to low to moderate hazard in areas north of the main channel.

BGC assessed baseline individual and group life safety risk to individuals in buildings within the proposed development area. For the hazard scenarios considered in this assessment, modelled flows associated with floods, debris floods, and debris flows on the study creeks did not result in sufficient intensities that life loss is expected at any of the proposed building locations. However, flow depths are sufficient to result in economic damages within the proposed development (Drawings 06, 07). The amount of potential economic damages has not been assessed in the current study. Moreover, risk to motor vehicles on Highway 99 has not been assessed.

Hazard and risk management at the proposed development site should include:

- Grading of the proposed development site to minimize potential inundation.
- Establishment of creek channels with sufficient capacity and erosion protection to convey debris flood / debris flow peak discharge.
- Design of water conveyance structures (culverts, bridges) with sufficient capacity to convey debris flood / debris flow peak discharge and development of regular maintenance programs for such structures to preserve the required capacity and integrity of the structures. This includes consideration of upgrades to existing crossings (e.g., Highway 99 and CN Rail crossings on Daisy Creek), addition of new crossings (e.g., below Highway 99 for Gravel Creek), and design of crossings within the proposed development area.

The design return period for creek channels, erosion protection, and water conveyance structures should consider relevant design standards, best practice guidelines, and the numerical modelling results presented herein. Any future changes to the site topography, layout, creek channels, and infrastructure or addition of mitigation measures should be remodelled to evaluate the residual hazard and risk in the proposed development area.

# 7. CLOSURE

We trust the above satisfies your requirements at this time. Should you have any questions or comments, please do not hesitate to contact us.

Yours sincerely,

**BGC ENGINEERING INC.**
**per:**

PROFESSIONAL
PROVINCE OF
L. HUTCHINSON
# 44726
BRITISH COLUMBIA
ENGINEER

December 12, 2022

Lauren Hutchinson, M.Sc., P.Eng.
Geotechnical Engineer

Coauthored by:

Matthias Jakob, Ph.D., P.Geo., P.L.Eng.
Principal Geoscientist

Reviewed by:

Hamish Weatherly, M.Sc., P.Geo.
Principal Hydrologist

LCH/HW/sf/syt

# REFERENCES

American Geosciences Institute. (2011). *Glossary of Geology* (5th ed.). Virginia: Author.

American Geological Institute. (1972). *Glossary of Geology*. Washington, DC.: Author.

Australian Geomechanics Society (AGS). (2007). Guideline for Landslide Susceptibility, Hazard and Risk Zoning for Land Use Planning. *Australian Geomechanics,* Vol 42.

Bartels, S., Chen, H., Wulder, M., & White, J. (2016) Trends in post-disturbance recovery rates of Canada's forests following wildfire and harvest. *Forest Ecology and Management, 361*(1), 194-207. https://doi.org/10.1016/j.foreco.2015.11.015

Bates, R.L. & Jackson, J.A. (1995). *Glossary of Geology* (2nd ed.). Virginia: American Geological Institute.

BC Wildfire Service (BCWS). (2022). *Fire Perimeters – Historical* [dataset]. Retrieved from: https://open.canada.ca/data/en/dataset/22c7cb44-1463-48f7-8e47-88857f207702.

Bellefontaine, K., Alldrick, D., & Desjardins, P.J. (1994). Mid Coast. British Columbia Ministry of Energy, Mines, and Petroleum Resources. British Columbia Geological Survey Open File 1994-17.

BGC Engineering Inc. (BGC) (2014, October 31). *Three Sisters Creek debris-flood hazard assessment* [Report]. Prepared for the Town of Canmore.

BGC Engineering Inc. (2020, November 13). *Gravel Creek Hazard Assessment* [Report]. Prepared for Tigerbay Development Corp.

BGC Engineering Inc. (2020, December 4). *Baseline Risk Assessment - Rev. 2B* [Report]. Prepared for Sqomish Sea to Sky Developments LP.

BGC Engineering Inc. (2022, January 24). *Steep Creek Hazard and Risk Assessment of Daisy and Thistle Creeks* [Proposal]. Prepared for Tigerbay Development Corp.

Blais-Stevens, A. (2008). *Surficial geology and landslide inventory of the lower Sea to Sky corridor, British Columbia.* Geological Survey of Canada, Open File 5322, scale 1:50,000.

Bovis, M. & Jakob, M. (1999). The role of debris supply conditions in predicting debris flow activity. *Earth Surface Processes and Landforms*, 24, 1039-1054.

Bovis, M., & Jakob, M. (2000). The July 29, 1998 debris-flow and landslide dam at Capricorn Creek, Mount Meager Volcanic Complex, southern Coast Mountains, British Columbia. *Canadian Journal of Earth Sciences, 37*, 1321-1334.

Bunte, K., Abt, S., Swingle, K., Cenderelli, D.A., & Schneider, J.M. (2013). Critical Shields values in coarse-bedded steep streams. *Water Resources Research*, 49, 7427–7447. https://doi.org/10.1002/2012wr012672

Canadian Avalanche Association (CAA). (2016). Technical Aspects of Snow Avalanche Risk Management – Resources and Guidelines for Avalanche Practitioners in Canada (C. Campbell, S. Conger, B. Gould, P. Haegeli, B. Jamieson, & G. Statham Eds.). Revelstoke, BC, Canada: Canadian Avalanche Association.

Canadian Standards Association (CSA). (1997). *CAN/CSA – Q859-97 Risk Management: Guideline for Decision Makers*. CSA Group, Toronto, ON, pp. 55.

Cannon, S.H. & Gartner, J.E. (2005). Wildfire-related debris flow from a hazards perspective. In M. Jakob, & O. Hungr (Eds.), *Debris flow hazards and related phenomena* (pp. 363-385). Springer, Berlin, Heidelberg. https://doi.org/10.1007/3-540-27129-5_15

Cannon, S.H., Gartner, J.E. Rupert, M.G., Michael, J.A., Rea, A.H., & Parrett, C. (2010). Predicting the probability and volume of post wildfire debris flows in the intermountain western United States. *Geological Society of America Bulletin, 122*(1-2), 127-144. https://doi.org/.10.1130/B26459.1

Church, M. & Jakob, M. (2020). What is a debris flood? Water Resources Research, 56(8). https://doi.org/10.1029/2020WR027144

Church, M., & Zimmermann, A. (2007). Form and stability of step-pool channels: Research progress. *Water Resources Research, 43*(3). https://doi.org/10.1029/2006WR005037

Cui, Y., Miller, D., Schiarizza, P., & Diakow, L.J. (2017). British Columbia digital geology. British Columbia Ministry of Energy, Mines and Petroleum Resources, British Columbia Geological Survey Open File 2017-8, 9 p. Data version 2019-12-19.

D'Agostino, V., Cerato, M., & Coali, R. (1996). Il trasporto solido di eventi estremi nei torrenti del Trentino Orientale. Schutz des Lebensraumes vor Hochwasser, Muren, Massenbewegungen und Lawinen, vol. 1, Interpraevent 1996, Tagungsband, Garmisch-Partenkirchen: Germany; 377–386 (in Italian).

De Graff, J., Cannon, S. & Gartner, J. (2015). The Timing of Susceptibility to Post-Fire Debris Flows in the Western United States. *Environmental & Engineering Geoscience, 21*, 277-292. https://doi.org/10.2113/gseegeosci.21.4.277.

Ekistics. (2021). Schedule B13 CONTEXT PLAN, South Britannia, Britannia Beach, BC.

Engineers and Geoscientists BC (EGBC). (2017). *Professional Practice Guidelines - Flood Mapping in BC.* Version 1.0.

Engineers and Geoscientists BC (EGBC). (2018). *Professional Practice Guidelines - Legislated Flood Assessments in a Changing Climate in BC*. Version 2.1.

Engineers and Geoscientists BC (EGBC). (2022). *Professional Practice Guidelines - Landslide Assessments in BC*.

Fell, R., Ho., K.K.S., LaCasse, S., & Leroi, E. (2005). A framework for landslide risk assessment and management. In Hungr, O., Fell, R., Couture, R. (Eds.) *Landslide Risk Management:* Proceedings *of the International Conference on Landslide Risk Management.* Vancouver, BC.

Forest Practices Board. (2017). Resource Road Construction in Steep Terrain. Special Investigation.

Gartner, J.E., Cannon, S.H., & Santi, P.M. (2014). Empirical models for predicting volumes of sediment deposited by debris flows and sediment-laden floods in the transverse ranges of southern California. *Engineering Geology, 176*(24), 45-56, https://doi.org/10.1016/j.enggeo.2014.04.008.

GHD. (2018, August 3). *Study of the Impacts of Climate Change on Precipitation and Stormwater Management* [Report]. Prepared for Greater Vancouver Sewerage and Drainage District.

Gomi, T. & Sidle, R. (2003). Bed load transport in managed steep-gradient headwater streams of southeastern Alaska. *Water Resources Research, 39*(12). https://doi.org/10.1029/2003WR002440

Grant, G. (1997). Critical flow constrains flow hydraulics in mobile-bed streams: a new hypothesis. *Water Resources Research, 33*(2), 349-358. 10.1029/96WR03134

Guthrie, R.H., Friele, P., Allstadt, K., Roberts, N., Evans, S.G., Delaney, K.B., Roche, D., Clague, J.J., & Jakob, M. (2012). The 6 August 2010 Mount Meager rock slide-debris flow, Coast Mountains, British Columbia: characteristics, dynamics, and implications for hazard and risk assessment. *Natural Hazards and Earth System Sciences, 12*, 1277-1294.

Hassan, M., Church, M., Lisle, T., Brardinoni, F., Benda, L., & Grant, G. (2005). Sediment transport and channel morphology of small, forested streams. *Journal of the American Water Resources Association, 41*(4), 853-876. https://doi.org/10.1111/j.1752-1688.2005.tb03774.x

Hatch Mott Macdonald (2009, September 28). As built drawings of HWY 99 from Horseshoe Bay to Whistler [Drawing]

Hungr, O., Morgan, G.C., & Krllerhals, R. (1984). Quantitative Analysis of Debris Torrent Hazard for Design of Remedial Measures. *Canadian Geotechnical Journal, 21*, 663-667. https://doi.org/10.1139/t84-073

Hungr, O., Leroueil, S., & Picarelli, L. (2014). Varnes classification of landslide types, an update. *Landslides*, 11, 167-194. https://doi.org/10.1007/s10346-013-0436-y

Hunziker, R.P., and Jäggi, M. (2002). Grain sorting processes. *Journal of Hydraulic Engineering, 128*, 1060- 1068. https://doi.org/10.1061/(ASCE)0733-9429(2002)128:12(1060)

International Organization for Standardization (ISO). (2018). *ISO 31000:2018 Risk Management – Guidelines*. Retrieved from https://www.iso.org/standard/65694.html

Iverson, R.M. (2014). Debris flows: behaviour and hazard assessment. *Geology Today, 30(1)*, 15-20. https://doi.org/10.1111/gto.12037

Jäggi, M. (2007). The flood of August 22-23, 2005, in Switzerland: some facts and challenges. *Developments in Earth Surface Processes, 11*, 587-603. https://doi.org/10.1016/S0928-2025(07)11144-5

Jakob, M. (1996). *Morphometric and geotechnical controls of debris-flow frequency and magnitude in Southwestern British Columbia* (Doctoral dissertation). University of British Columbia, Vancouver, BC. https://open.library.ubc.ca/soa/cIRcle/collections/ubctheses/831/items/1.0087740

Jakob, M. (2000). The impacts of logging on landslide activity at Clayoquot Sound, British Columbia. *Catena, 38,* 279-300. https://doi.org/10.1016/S0341-8162(99)00078-8

Jakob, M. (2012). The fallacy of frequency: statistical techniques for debris-flow frequency-magnitude analysis. In Eberhardt E, Froese C, Turner AK, Leroueil S (Eds.), *Landslides and Engineered Slopes: Protecting Society through Improved Understanding: Proceedings of the 11th International Symposium on Landslides and 2nd North American Symposium on Landslides, 2–8 June 2012* (pp. 741–750). Banff, AB: Taylor &Francis.

Jakob, M. (2021). Landslides in a changing climate. In J. Shroder, T. Davies, & N. Rosser (Eds.), *Landslide hazards, risks, and disasters* (2nd ed., pp. 505-579). Amsterdam, Netherlands: Elsevier.

Jakob, M., & Bovis, M.J. (1996). Morphometrical and geotechnical controls of debris flow activity, southern Coast Mountains, British Columbia, Canada. *Zeitschrift für Geomorphologie Supplementband*, *104*, 13-26.

Jakob, M. & Jordan, P. (2001). Design flood estimates in mountain streams – the need for a geomorphic approach. *Canadian Journal of Civil Engineering, 28*, 425-239. https://doi.org/10.1139/l01-010.

Jakob, M. & Owen, T. (2021). Projected effects of climate change on shallow landslides, North Shore Mountains, Vancouver, Canada. *Geomorphology, 393.* https://doi.org/10.1016/j.geomorph.2021.107921

Jakob, M., Bovis, M., & Oden, M. (2005). The significance of channel recharge rates for estimating debris-flow magnitude and frequency. *Earth Surface Processes and Landforms, 30*(6), 755-766. https://doi.org/10.1002/esp.1188

Jakob, M., Stein, D., and Ulmi, M. (2012). Vulnerability of buildings to debris-flow impact. *Natural Hazards, 60*(2), 241-261.

Jakob, M., Bale, S., McDougall, S., & Friele, P. (2016). Regional debris-flow and debris-flood frequency-magnitude curves. In *Proceedings of the 69th Canadian Geotechnical Society Conference: history and innovation, GeoVancouver 2016, Vancouver, BC, 2-5 October 2016* (pp. 1-8). Richmond, BC: Canadian Geotechnical Society.

Jakob, M., Mark, E., McDougall, S., Friele, P., Lau, C-A, & Bale, S. (2020). Regional debris-flow and debris-flood frequency–magnitude relationships. *Earth Surface Processes and Landforms, 45*(12), 2954-2964. https://doi.org/10.1002/esp.4942

Jakob, M., Davidson, S., Bullard, G., Busslinger, M., Collier-Pandya, B., Grover, P., & Lau, C-A. (2022). Debris-Flood Hazard Assessments in Steep Streams. *Water Resources Research, 58.* https://doi.org/10.1029/2021WR030907

Jakob, M. & Nolde, N. (2022). Statistical methods for debris-flow frequency-magnitude assessments. In: Jakob, M., McDougall, S. and Santi, P. (Eds.), *Advances in Debris-Flow Science and Practice*. Springer. Heidelberg. In preparation.

Jarrett, R. (1984). Hydraulics of high-gradient streams. *Journal of Hydraulic Engineering, 110*(11). https://doi.org/10.1061/(ASCE)0733-9429(1984)110:11(1519)

Jordan, P. (2001). Regional incidence of landslides. In D.A.A. Toews and S. Chatwin (Eds.) *Watershed Assessment in the Southern Interior of British Columbia,* Proceedings of a Workshop, March 9-10, 2000, Penticton, B.C. British Columbia, Ministry of Forests. Victoria, B.C.

Jordan, P. (2015) Post-wildfire debris flows in southern British Columbia, Canada. *International Journal of Wildland Fire, 25*(3), 322-336. http://dx.doi.org/10.1071/WF14070.

Klock, G.O., & Helvey, J.D. (1976). Debris flows following wildfire in North Central Washington. *In* Proceedings of the 3rd Federal Inter-Agency Sedimentation Conference, March 22-25, Denver, Colorado. Water Resources Council, Denver, CO. pp. 91-98.

Kwan, J. (2012). Supplementary Technical Guidance on Design of Rigid Debris-resisting Barriers. Geotechnical Engineering Office, Civil Engineering and Development Department, The Government of the Hong Kong Special Administrative Region. GEO Report No. 270.

Loukas, A. (1994). *Mountain precipitation analysis for the estimation of flood runoff in Coastal British Columbia* (Ph.D. Thesis). Department of Civil Engineering, University of British Columbia.

Mackenzie, L., Eaton, B.C., & Church, M. (2018). Breaking from the average: Why large grains matter in gravel-bed streams. *Earth Surface Processes and Landforms*, *43*, 3190–3196. https://doi.org/10.1002/esp.4465

Magirl, C.S., Hilldale, R.C., Curran, C.A., Duda, J.J., Straub, T.D., Domanski, M., ... Foreman, J.R. (2015). Large-scale dam removal on the Elwha River, Washington, USA: Fluvial sediment load. *Geomorphology, 246*, 669-686. https://doi.org/10.1016/j.geomorph.2014.12.032

Ministry of Transportation and Infrastructure (MoTI). (2015, February). *Subdivision Preliminary Layout Review – Natural Hazard Risk.*

Ministry of Water, Land and Air Protection. (MWLAP) (2004). *Flood Hazard Area Land Use Management Guidelines*.

Mizuyama, T., Kobashi, S., & Ou, G. (1992). Prediction of debris flow peak discharge. Interpraevent, International Symposium, Bern, Switzerland, Tagespublikation, 4, 99±108.

Moody, J. & Martin, D. (2001). Initial hydrologic and geomorphic response following a wildfire in the Colorado Front Range. *Earth Surface Processes and Landforms, 26*, 1049-1070. https://doi.org/10.1002/esp.253.

Mosbrucker, A.R., & Major, J.J. (2019). North Fork Toutle River debris flows initiated by atmospheric rivers. Paper Presented at the joint Federal Interagency Sedimentation Conference and Federal Interagency Hydrologic Modelling Conference, Reno, NV.

National Oceanic and Atmospheric Administration. (n.d.) What is LIDAR? [Web page]. Retrieved from https://oceanservice.noaa.gov/facts/lidar.html

No Author (2006, June 5). *Design Certification: DB6 South* [Design Certificate].

Northwest Hydraulic Consultants Ltd. (2009a, August 21). *Daisy Creek Culvert Hydrotechnical Design Brief* [Design Brief].

Northwest Hydraulic Consultants Ltd. (2009b, August 21). *Daisy Creek Debris Flow Mitigation Measures (Debris Berm) Hydrotechnical Design Brief* [Design Brief].

Northwest Hydraulic Consultants (NHC). (2016, July 13). *Drainage System Model Development and Assessment Peak Flow Estimates in the District of North Vancouver: Regional Analysis and Hydrologic Modelling* [Report]. Prepared for District of North Vancouver.

Oxford University Press. (2008). *A dictionary of Earth Sciences* (3rd ed.). Oxford, England: Author.

Parise, M. & Cannon, S. H. (2012). Wildfire impacts on the processes that generate debris flows in burned watersheds. *Natural Hazards*, *61*, 217-227. https://doi.org/10.1007/s11069-011-9769-9

Parisien, M., Kafka, V., Hirsch, K., Todd, B., Lavoie, S., & Maczek, P. (2005). Mapping fire susceptibility with the Burn-P3 simulation model. Natural Resources Canada, Canadian Forest Service, Northern Forestry Centre, Edmonton, Alberta. Information Report NOR-X-405.

Park, J. (2018). Dendro-geomorphology. Directed studies report. The University of British Columbia.

Pacific Climate Impacts Consortium (PCIC). (2012). Plan2Adapt. https://www.pacificclimate.org/analysis-tools/plan2adapt. [Accessed August 17, 2018]

Piton, G., & Recking, A. (2019). Steep bedload-laden flows: near critical?. *Journal of Geophysical Research: Earth Surface, 124*. https://doi.org/10.1029/2019JF005021

Porter, M., Jakob, M., & Holm, K. (2009, September). Proposed Landslide Risk Tolerance Criteria. *GeoHalifax 2009*. Paper presented at the meeting of the Canadian Geotechnical Society, Halifax, Canada.

Prein, A.F., Rasmussen, R.M., Ikeda, K., Liu, C., Clark, M.P, and Holland, G.J. (2017). The future intensification of hourly precipitation extremes. *Nature Climate Change, 7*, 48-52. https://doi.org/10.1038/nclimate3168

Recking, A., Frey, P., Paquier, A., Belleudy, P., & Champagne, J.Y. (2008). Feedback between bed load transport and flow resistance in gravel and cobble bed rivers. *Water Resource Research, 44*(5). https://doi.org/10.1029/2007WR006219

Recking, A., Piton, G., Vazquez-Tarrio, D., & Parker, G. (2015). Quantifying the morphological print of bedload transport. *Earth Surface Processes and Landforms, 41*(6), 809-822. https://doi.org/10.1002/esp.3869

Rengers, F., McGuire, L.A., Oakley, N.S., Kean, J.W., Staley, D.M., & Tang, H. (2020). Landslides after wildfire: initiation, magnitude, and mobility. *Landslides, 17*, 2631-2641. https://doi.org/10.1007/s10346-020-01506-3

Richply. (2022, June 9). Logging Plans for Richmond Operating Area, 1:20,000. [Map]

Rickenmann, D. (2001). Comparison of bed load transport in torrents and gravel bed streams. *Water Resources Research, 37*(2), 3295-3305. https://doi.org/10.1029/2001WR000319

Rickenmann, D. (2005). Runout prediction methods. In M. Jakob & O. Hungr (Eds.), *Debris-flow hazards and related phenomena* (pp. 305-324). New York: Springer.

Rickenmann, D., & Koschni, A. (2010). Sediment loads due to fluvial transport and debris flows during the 2005 flood events in Switzerland. *Hydrological Processes, 24*(8), 993-1007. https://doi.org/10.1002/hyp.7536

SFA Geotechnical Engineering. (2019, April 15). *Preliminary Geotechnical Recommendations and Summary Report, Proposed Comprehensive Development, South Britannia Beach, BC* [Report]. Prepared for Tigerbay Development Corporation.

Shakesby, R. & Doerr, S. (2006). Wildfire as a hydrological and geomorphological agent. *Earth-Science Reviews, 74*(3-4), 269-307. https://doi.org/10.1016/j.earscirev.2005.10.006.

Sidle, R.C. (1991). A conceptual model of changes in root cohesion in response to vegetation management. *Journal of Environmental Quality, 20,* 43-52. https://doi.org/10.2134/jeq1991.00472425002000010009x

Sidle, R.C. (2005). Influence of forest harvesting activities on debris avalanches and flows. In M. Jakob & O. Hungr (Eds.), *Debris-flow hazards and related phenomena* (pp. 387-409). Springer, Berlin, Heidelberg. https://doi.org/10.1007/3-540-27129-5_15

Simonovic, S.P., Schardong, A., Srivastav, R., & Sandink, D. (2015). IDF_CC Web-based Tool for Updating Intensity-Duration-Frequency Curves to Changing Climate – ver 6.0, Western University Facility for Intelligent Decision Support and Institute for Catastrophic Loss Reduction, open access https://www.idf-cc-uwo.ca.

Soil Conservation Service (SCS). (1972). *National Engineering Handbook, Section 4*. U.S. Department of Agriculture, Washington, D.C.

Staley, D., Kean, J., & Rengers, F. (2020). The recurrence interval of post-fire debris-flow generating rainfall in the southwestern United States. *Geomorphology, 370*(1). https://doi.org/10.1016/j.geomorph.2020.107392.

Strouth, A., & McDougall, S. (2022). Individual risk evaluation for landslides: key details. *Landslides, 19*, 977-991. https://doi.org/10.1007/s10346-021-01838-8

Takahashi, T. (1991). *Debris flows*. Rotterdam, Balkema.

Thurber Environmental Consultants Ltd. (1996, October 21). *Makin Property, Britannia Beach, B.C., Environmental and Geotechnical Assessment* [Report]. Prepared for Campbell Saunders Ltd.

Thurber Engineering. (2006, May 4). *Daisy Creek Debris Flow Hazard Mitigation Measures DOCUMENT NO: 40-R-06-002-0* [Report]. Prepared for Hatch Mott MacDonald.

Thurber Engineering Ltd. (2006, March 4). *Daisy Creek Debris Flow Hazard Mitigation Measures As-Built Record* [Memorandum]. Prepared for Hatch Mott Macdonald.

Thurber Engineering. (2012, February 15). *South Britannia Beach B.C. Geotechnical Assessment* [Report]. Prepared for Taicheng Development Corporation.

Thurber Engineering Ltd. (2006, March 16). *DB6 South Highway Design – Geotechnical Recommendations* [Memorandum]. Prepared for InterCAD Services Ltd.

Thurber Engineering (2016, June 13). *Detailed Debris Flow Hazard Assessment and Preliminary Evaluation of Mitigation Options* [Report]. Prepared for Taicheng Development Corporation.

Turje & Associates, P.S. (2020, May 22). Site Plan – Final [Drawing].

Turje, P.S. (2020a, May 31). *Britannia South Development Master Plan, Vol. 1 of 5 - Summary* [Report]. Prepared for Tigerbay Development Corp.

Turje, P.S. (2020b, May 31). *Britannia South Development Master Plan, Vol. 3 of 5 - Engineering* [Report]. Prepared for Tigerbay Development Corp.

United States Army Corps. of Engineers (USACE). (2020). HEC-HMS Technical Reference Manual, CN Tables [Web page]. Retrieved from https://www.hec.usace.army.mil/confluence/hmsdocs/hmstrm/cn-tables

United States Army Corps of Engineers. HEC HMS (Version 4.9) [Computer software]. Retrieved from https://www.hec.usace.army.mil/software/hec-hms/downloads.aspx

US Army Corps of Engineers. HEC RAS (Version 6.2) [Computer software]. Retrieved from https://www.hec.usace.army.mil/confluence/rasdocs/rasrn

United States Geological Survey (2020). How Wildfires threaten U.S. Water Supplies [website]. Accessed at https://labs.waterdata.usgs.gov/visualizations/fire-hydro/index.html#/.

VanDine, D.F. (1985) Debris flow and debris torrents in the Southern Canadian Cordillera. *Canadian Geotechnical Journal*, 22, 44–68. https://doi.org/10.1139/t85-006

Watt, E.W. (Ed.). (1989). *Hydrology of Floods in Canada – A Guide to Planning and Design.* National Research Council of Canada, Associate Committee on Hydrology.

Whitfield, P.H., Cannon, A.J., & Reynolds, C.J. (2002). Modelling Streamflow in Present and Future Climates: Examples from the Georgia Basin, British Columbia. *Canadian Water Resources Journal, 27(*4), 427 – 456. https://doi.org/10.4296/cwrj2704427

Wilford, D., Sakals, M., Innes, J., Sidle, R., & Bergerud, W.A. (2004). Recognition of debris flow, debris flood and flood hazard through watershed morphometrics. *Landslides, 1*(1), 61-66. https://doi.org/10.1007/s10346-003-0002-0

Zimmermann, A. (2010). Flow resistance in steep streams: An experimental study. *Water Resources Research, 46*. https://doi.org/10.1029/2009WR007913

# APPENDIX A
# TERMINOLOGY

Table A-1 defines terms that are commonly used in geohazard assessments. BGC notes that the definitions provided are commonly used, but international consensus on geohazard terminology does not fully exist. Bolded terms within a definition are defined in other rows of Table A-1.

**Table A-1. Geohazard terminology.**

| Term | Definition | Source |
|---|---|---|
| Active Alluvial Fan | The portion of the fan surface which may be exposed to contemporary hydrogeomorphic or avulsion hazards. | BGC |
| Aggradation | Deposition of sediment by a (river or stream). | BGC |
| Alluvial fan | A low, outspread, relatively flat to gently sloping mass of loose rock material, shaped like an open fan or a segment of a cone, deposited by a stream at the place where it issues from a narrow mountain valley upon a plain or broad valley, or where a tributary stream is near or at its junction with the main stream, or wherever a constriction in a valley abruptly ceases or the gradient of stream suddenly decreases | Bates and Jackson (1995) |
| Annual Exceedance Probability ($P_H$) (AEP) | The Annual Exceedance Probability (AEP) is the estimated **probability** that an event will occur exceeding a specified magnitude in any year. For example, a flood with a 0.5% AEP has a one in two hundred chance of being reached or exceeded in any year. AEP is increasingly replacing the use of the term **'return period'** to describe flood recurrence intervals. | Fell et al. (2005) |
| Avulsion | Lateral displacement of a stream from its main channel into a new course across its fan or floodplain. An "avulsion channel" is a channel that is being activated during channel avulsions. An avulsion channel is not the same as a paleochannel. | Oxford University Press (2008) |
| Bank Erosion | Erosion and removal of material along the banks of a river resulting in either a shift in the river position, or an increase in the river width. | BGC |
| Clear–water flood | Riverine and lake flooding resulting from inundation due to an excess of clear-water discharge in a watercourse or body of water such that land outside the natural or artificial banks which is not normally under water is submerged. | BGC |
| Climate normal | Long term (typically 30 years) averages used to summarize average climate conditions at a particular location. | BGC |
| Consequence (C) | In relation to risk analysis, the outcome or result of a **geohazard** being realised. Consequence is a product of **vulnerability** (V) and a measure of the **elements at risk** (E) | Fell et al. (2005); Fell et al. (2007), BGC |

| Term | Definition | Source |
|---|---|---|
| Consultation Zone | The Consultation Zone (CZ) includes all proposed and existing development in a geographic zone defined by the approving authority that contains the largest credible area affected by specified **geohazards**, and where damage or loss arising from one or more simultaneously occurring specific **geohazards** would be viewed as a single catastrophic loss. | Adapted from Porter et al. (2009) |
| Debris Flow | Very rapid to extremely rapid surging flow of saturated, non-plastic debris in a steep channel (Hungr, Leroueil & Picarelli, 2014). Debris generally consists of a mixture of poorly sorted sediments, organic material and water (see Appendix B of this report for detailed definition). | BGC |
| Debris Flood | A very rapid flow of water with a sediment concentration of 3-10% in a steep channel. It can be pictured as a flood that also transports a large volume of sediment that rapidly fills in the channel during an event (see Appendix B of this report for detailed definition). | BGC |
| Dendrogeomorphology | Study of geomorphic processes through analysis of tree-rings and its correlation to local, site-specific geomorphological processes. By identifying certain patterns and features on the tree-rings, reconstruction of past events is possible. | Park, 2018 |
| Elements at Risk (E) | This term is used in two ways:<br>a) To describe things of value (e.g., people, infrastructure, environment) that could potentially suffer damage or loss due to a **geohazard**.<br>b) For risk analysis, as a measure of the value of the elements that could potentially suffer damage or loss (e.g., number of persons, value of infrastructure, value of loss of function, or level of environmental loss). | BGC |
| Encounter Probability | This term is used in two ways:<br>a) **Probability** that an event will occur and impact an element at risk when the element at risk is present in the **geohazard** zone. It is sometimes termed **"partial risk"**<br>b) For quantitative analyses, the **probability** of facilities or vehicles being hit at least once when exposed for a finite time period L, with events having a **return period** T at a location. In this usage, it is assumed that the events are rare, independent, and discrete, with arrival according to a statistical distribution (e.g., binomial or Bernoulli distribution or a Poisson process). | BGC |

| Term | Definition | Source |
|---|---|---|
| Erosion | The part of the overall process of denudation that includes the physical breaking down, chemical solution and transportation of material. | Oxford University Press (2008) |
| Flood | A rising body of water that overtops its confines and covers land not normally under water. | American Geosciences Institute (2011) |
| Flood Construction Level (FCL) | A designated flood level plus freeboard, or where a designated flood level cannot be determined, a specified height above a natural boundary, natural ground elevation, or any obstruction that could cause flooding. | BGC |
| Flood mapping | Delineation of flood lines and elevations on a base map, typically taking the form of flood lines on a map that show the area that will be covered by water, or the elevation that water would reach during a flood event. The data shown on the maps, for more complex scenarios, may also include flow velocities, depth, or other hazard parameters. | BGC |
| Floodplain | The part of the river valley that is made of unconsolidated river-borne sediment, and periodically flooded. | Oxford University Press (2008) |
| Flood setback | The required minimum distance from the natural boundary of a watercourse or waterbody to maintain a floodway and allow for potential bank erosion. | BGC |
| Freeboard | Freeboard is a depth allowance that is commonly applied on top of modelled flood depths. There is no consistent definition, either within Canada or around the world, for freeboard. Overall, freeboard is used to account for uncertainties in the calculation of a base flood elevation, and to compensate for quantifiable physical effects (e.g., local wave conditions or dike settlement). Freeboard in BC is commonly applied as defined in the BC Dike Design and Construction manual (BC Ministry of Water, Land and Air Protection [BC MWLAP], 2004): a fixed amount of 0.6 m (2 feet) where mean daily flow records are used to develop the design discharge or 0.3 m (1 foot) for instantaneous flow records. | BC Ministry of Water, Land and Air Protection [BC MWLAP] (2004) |

| Term | Definition | Source |
|---|---|---|
| Frequency (f) | Estimate of the number of events per time interval (e.g., a year) or in a given number of trials. Inverse of the **recurrence interval** (**return period**) of the **geohazard** per unit time. Recurring **geohazards** typically follow a **frequency**-magnitude (F-M) relationship, which describes a spectrum of possible **geohazard magnitudes** where larger (more severe) events are less likely. For example, annual **frequency** is an estimate of the number of events per year, for a given **geohazard event magnitude**.<br>In contrast, annual **probability** of exceedance is an estimate of the **likelihood** of one or more events in a specified time interval (e.g., a year). When the expected **frequency** of an event is much lower than the interval used to measure **probability** (e.g., **frequency** much less than annual), **frequency** and **probability** take on similar numerical values and can be used interchangeably. When **frequency** approaches or exceeds 1, defining a relationship between **probability** and **frequency** is needed to convert between the two. The main document provides a longer discussion on **frequency** versus **probability**. | Adapted from Fell et al. (2005) |
| Hazard | Process with the potential to result in some type of undesirable outcome. Hazards are described in terms of scenarios, which are specific events of a particular frequency and magnitude. | BGC |
| Hazardous flood | A flood that is a source of potential harm. | BGC |
| Geohazard | Geophysical process that is the source of potential harm, or that represents a situation with a potential for causing harm.<br>Note that this definition is equivalent to Fell et al. (2005)'s definition of Danger (threat), defined as an existing or potential natural phenomenon that could lead to damage, described in terms of its geometry, mechanical and other characteristics. Fell et al. (2005)'s definition of danger or threat does not include forecasting, and they differentiate Danger from Hazard. The latter is defined as the **probability** that a particular danger (threat) occurs within a given period of time. | Adapted from CSA (1997), Fell et al. (2005). |

| Term | Definition | Source |
|---|---|---|
| Geohazard Assessment | Combination of **geohazard analysis** and evaluation of results against a **hazard tolerance standard** (if existing). Geohazard assessment includes the following steps:<br>a. **Geohazard analysis**: identify the **geohazard** process, characterize the geohazard in terms of factors such as mechanism, causal factors, and trigger factors; estimate **frequency** and magnitude; develop **geohazard scenarios**; and estimate extent and intensity of **geohazard scenarios**.<br>b. Comparison of estimated hazards with a hazard tolerance standard (if existing) | Adapted from Fell et al. (2007) |
| Geohazard Event | Occurrence of a **geohazard**. May also be defined in reverse as a non- occurrence of a **geohazard** (when something doesn't happen that could have happened). | Adapted from ISO (2018) |
| Geohazard Intensity | A set of parameters related to the destructive power of a **geohazard** (e.g. depth, velocity, discharge, impact pressure, etc.) | BGC |
| Geohazard Inventory | Recognition of existing **geohazards.** These may be identified in geospatial (GIS) format, in a list or table of attributes, and/or listed in a **risk register**. | Adapted from CSA (1997) |
| Geohazard Magnitude | Size-related characteristics of a **geohazard**. May be described quantitatively or qualitatively. Parameters may include volume, discharge, distance (e.g., displacement, encroachment, scour depth), or acceleration. In general, it is recommended to use specific terms describing various size-related characteristics rather than the general term magnitude. Snow avalanche magnitude is defined differently, in classes that define destructive potential. | Adapted from CAA (2016) |
| Geohazard Risk | Measure of the **probability** and severity of an adverse effect to health, property the environment, or other things of value, resulting from a geophysical process. Estimated by the product of **geohazard probability** and **consequence**. | Adapted from CSA (1997) |
| Geohazard Scenario | Defined sequences of events describing a **geohazard** occurrence. Geohazard scenarios characterize parameters required to estimate risk such **geohazard extent** or **runout exceedance probability,** and **intensity.** Geohazard scenarios (as opposed to **geohazard risk scenarios**) typically consider the chain of events up to the point of impact with an element at risk, but do not include the chain of events following impact (the **consequences**). | Adapted from Fell et al. (2005) |

| Term | Definition | Source |
|---|---|---|
| Hazard | Process with the potential to result in some type of undesirable outcome. Hazards are described in terms of scenarios, which are specific events of a particular frequency and magnitude. | BGC |
| Inactive Alluvial Fan | Portions of the fan that are removed from active hydrogeomorphic or avulsion processes by severe fan erosion, also termed fan entrenchment. | BGC |
| LiDAR | Stands for Light Detection and Ranging, is a remote sensing method that uses light in the form of a pulsed laser to measure ranges (variable distances) to the Earth. These light pulses - combined with other data recorded by the airborne system - generate precise, three-dimensional information about the shape of the Earth and its surface characteristics. | National Oceanic and Atmospheric Administration, (n.d.). |
| Likelihood | Conditional **probability** of an outcome given a set of data, assumptions and information. Also used as a qualitative description of **probability** and **frequency**. | Fell et al. (2005) |
| Melton Ratio | Watershed relief divided by square root of watershed area. A parameter to assist in the determination of whether a creek is susceptible to flood, debris flood, or debris flow processes. | BGC |
| Nival | Hydrologic regime driven by melting snow. | Whitfield, Cannon and Reynolds (2002) |
| Orphaned | Without a party that is legally responsible for the maintenance and integrity of the structure. | BGC |
| Paleofan | Portion of a fan that developed during a different climate, base level or sediment transport regime and which will not be affected by contemporary geomorphic processes (debris flows, debris floods, floods) affecting the active fan surface | BGC |
| Paleochannel | An inactive channel that has partially been infilled with sediment. It was presumably formed at a time with different climate, base level or sediment transport regime. | BGC |
| Pluvial – hybrid | Hydrologic regime driven by rain in combination with something else. | BGC |

| Term | Definition | Source |
|---|---|---|
| Probability | A measure of the degree of certainty. This measure has a value between zero (impossibility) and 1.0 (certainty) and must refer to a set like occurrence of an event in a certain period of time, or the outcome of a specific event. It is an estimate of the **likelihood** of the magnitude of the uncertain quantity, or the **likelihood** of the occurrence of the uncertain future event.<br>There are two main interpretations:<br>i) Statistical – **frequency** or fraction – The outcome of a repetitive experiment of some kind like flipping coins. It includes also the idea of population variability. Such a number is called an “objective” or relative frequentist probability because it exists in the real world and is in principle measurable by doing the experiment.<br>ii) Subjective (or Bayesian) probability (degree of belief) – Quantified measure of belief, judgement, or confidence in the **likelihood** of an outcome, obtained by considering all available information honestly, fairly, and with a minimum of bias. Subjective probability is affected by the state of understanding of a process, judgement regarding an evaluation, or the quality and quantity of information. It may change over time as the state of knowledge changes. | Fell et al. (2005) |
| Return Period (Recurrence Interval) | Estimated time interval between events of a similar size or **intensity**. Return period and **recurrence interval** are equivalent terms. Inverse of **frequency**. | BGC |
| Risk | Likelihood of a geohazard scenario occurring and resulting in a particular severity of consequence. In this report, risk is defined in terms of safety or damage level. | BGC |
| Rock (and debris) Slides | Sliding of a mass of rock (and debris). | BGC |
| Rock Fall | Detachment, fall, rolling, and bouncing of rock fragments. | BGC |
| Scour | The powerful and concentrated clearing and digging action of flowing air or water, especially the downward erosion by stream water in sweeping away mud and silt on the outside curve of a bend, or during a time of flood. | American Geological Institute (1972) |
| Steep-creek flood | Rapid flow of water and debris in a steep channel, often associated with avulsions and bank erosion and referred to as debris floods and debris flows. | BGC |

| Term | Definition | Source |
|---|---|---|
| Steep Creek Hazard | Earth-surface process involving water and varying concentrations of sediment or large woody debris. (see Appendix B of this report for detailed definition). | BGC |
| Uncertainty | Indeterminacy of possible outcomes. Two types of uncertainty are commonly defined:<br>a) Aleatory uncertainty includes natural variability and is the result of the variability observed in known populations. It can be measured by statistical methods, and reflects uncertainties in the data resulting from factors such as random nature in space and time, small sample size, inconsistency, low representativeness (in samples), or poor data management.<br>b) Epistemic uncertainty is model or parameter uncertainty reflecting a lack of knowledge or a subjective or internal uncertainty. It includes uncertainty regarding the veracity of a used scientific theory, or a belief about the occurrence of an event. It is subjective and may vary from one person to another. | BGC |
| Waterbody | Ponds, lakes and reservoirs | BGC |
| Watercourse | Creeks, streams and rivers | BGC |

# APPENDIX B
# DATA COMPILATION

The following data sources, organized by date of publication, were reviewed by BGC for the Daisy, Thistle, and Gravel creeks hazard and risk assessments:

- Bedrock geological mapping completed by the BC Geological Survey (Bellefontaine et al., 1994; Cui et al., 2017)
- As-built design drawings of bridges and culverts along the Britannia Creek Forest Service Road (FSR) for structures (DSQ-3148 and DSQ-3149, March 1995) and inspection reports for structures (DSQ-3148, DSQ-3149, DSQ-3150, DSQ-3151, and DSQ-3152, September 16, 2019).
- Daisy Creek Debris Flow Hazard Mitigation Measures As-Built Record (Thurber Engineering Ltd., March 4, 2006).
- DB6 South Highway Design - Geotechnical Recommendations (Thurber Engineering Ltd., March 16, 2006).
- Design Certification: DB6 South (June 5, 2006).
- Surficial geology and landslide inventory of the lower Sea to Sky corridor (Blais-Stevens, 2008)
- Daisy Creek Culvert Hydrotechnical Design Brief (Northwest Hydraulic Consultants, August 21, 2009).
- Daisy Creek Debris Flow Mitigation Measures (Debris Berm) Hydrotechnical Design Brief (Northwest Hydraulic Consultants, August 21, 2009).
- As built drawings of HWY 99 from Horseshoe Bay to Whistler, including the Daisy Creek Debris Flow Berm ( Hatch Mott Macdonald, September 28, 2009).
- Drawing of Final Site Plan (P.S. Turje & Associates, May 22, 2020).
- Britannia Beach South Site Development Master Development Master Plan – Volumes 1-5/5 (P.S. Turje & Associates Ltd., May 31, 2020).
- Logging plans for Britannia Operating Area at 1:15,000 scale from RichPly (November 8, 2021)
- Historical wildfire burn perimeters provided by the BC Wildfire Service (2022)

BGC also reviewed aerial imagery (air photos and satellite imagery) of the study area between 1932 and 2020 (Table B-1).

**Table B-1. Air photo imagery used in hazard assessment.**

| Roll | Photo Numbers | Imagery Date | Scale | Notes |
|---|---|---|---|---|
| A4425 | 036-037 | 4/29/1932 | 1:15,000 | Fan only |
| BC 201 | 24-25 | 1940 | 1: 31,680 | |
| BC 1634 | 52, 56 | 1952 | 1: 31,680 | |
| BC 2349 | 6, 8 | 1957 | 1: 15,840 | |
| BC7202 | 59, 138 | 1969 | 1: 16,000 | |
| BC82 060 | 132 | 1982 | 1: 20,000 | |
| 30BCB90020 | 26 | 1990 | 1:15,000 | |
| 30BCC94122 | 195 | 1994 | 1:15,000 | |
| 30BCC03040 | 087 | 2003 | 1:15,000 | |
| ESRI World Imagery | | 4/9/2020 | - | |

# APPENDIX C
# STEEP CREEK PROCESSES

## C.1. INTRODUCTION

Steep creeks (here-in defined as having channel gradients steeper than 5%, or 3°) may be subject to a spectrum of sediment transport processes ranging with increasing sediment concentration from clearwater floods to debris floods, hyperconcentrated flows (in fine-rich sediment), to debris flows. These events can be referred to collectively as hydrogeomorphic processes because water and sediment (in suspension and bedload) are being transported. Depending on process and severity, hydrogeomorphic processes can alter landscapes (Figure C-1).

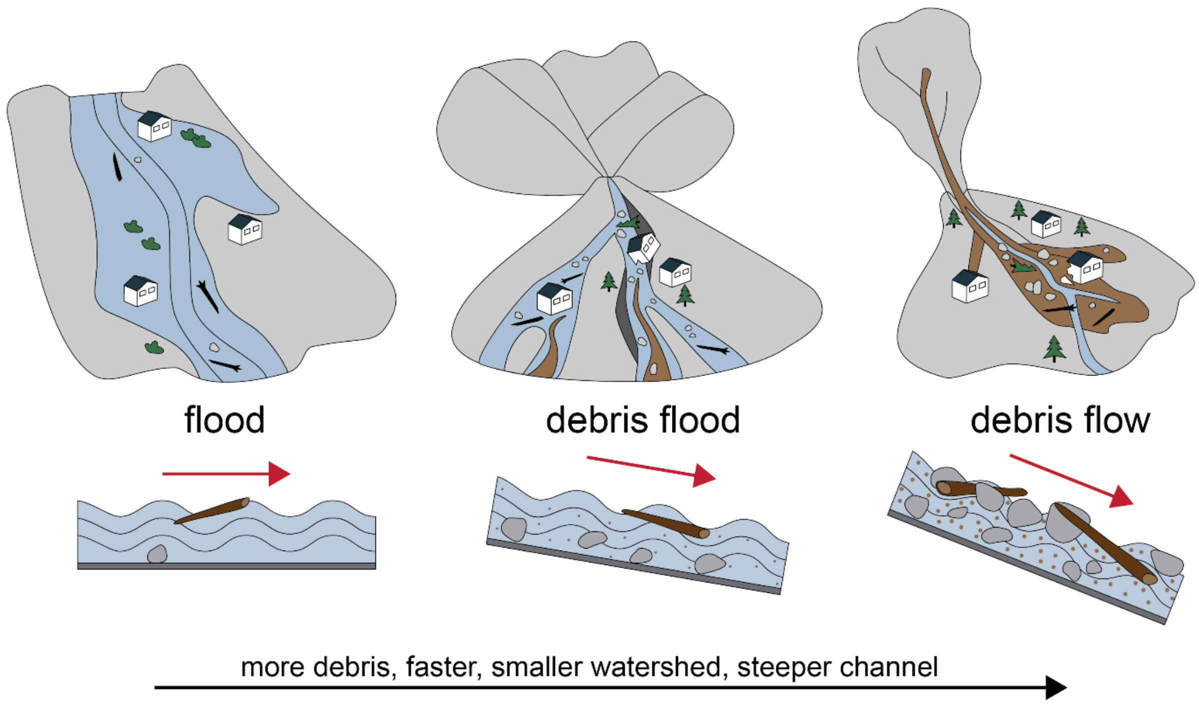


**Figure C-1. Simplified illustration summarizing the hazards associated with each hydrogeomorphic process. BGC-created figure.**

Clearwater floods do transport bedload and other sediments; they are not completely clear. The transition of a flood into a debris flood occurs when most of the channel bed is mobilized except possibly the largest clasts (Church and Jakob, 2020). As more and more fines (clays, silts and fine sands) are incorporated into the flow, hyperconcentrated flows may develop (not of relevance to Daisy, Thistle, or Gravel Creeks). Debris flows are typically triggered by side slope landslides or progressive bulking with erodible sediment in particularly steep (>15°) channels. Debris flows are more prevalent following wildfires of moderate to high burn severity when there is ample surface sediment exposed without the sheltering vegetative cover. Dilution of a debris flow through partial sediment deposition on lower gradients (approximately less than <15°) channels, and tributary injection of water can lead to a transition towards hyperconcentrated flows or debris floods and eventually floods. Most steep creeks can be classified as hybrids, implying variable hydrogeomorphic processes at different return periods.

Figure C-2 summarizes the different hydrogeomorphic processes by their appearance in plan form, velocity, and sediment concentration

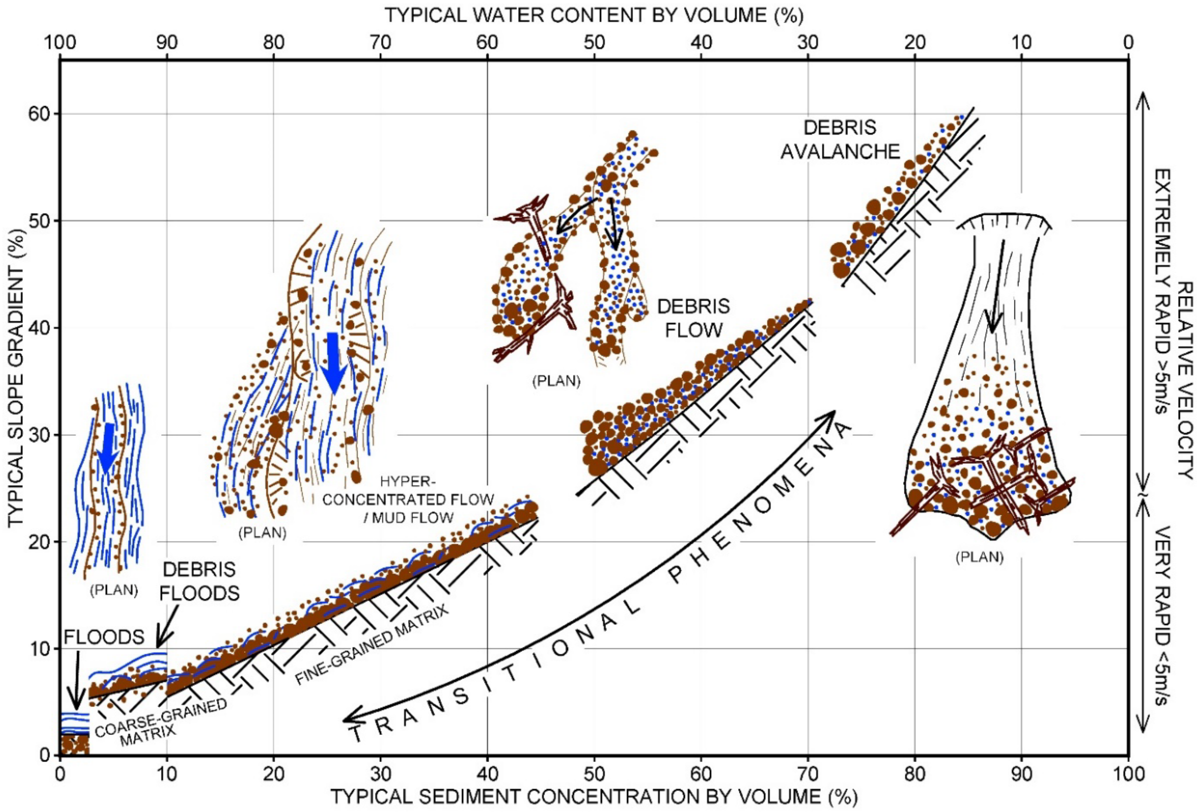


**Figure C-2. Hydrogeomorphic process classification by sediment concentration, slope velocity and planform appearance. BGC-created figure.**

### C.1.1. Debris Floods

Debris floods typically occur on creeks with channel gradients between 5 and 30% (3-17$^{o}$), but in contrast to common belief, can also occur on lower gradient gravel bed rivers. Debris floods occur when large volumes of water in a creek or river entrain the gravel, cobbles and boulders on the channel bed; this is known as “full bed mobilization”. The peak discharges are often very similar to those of clearwater floods, but the flow is more heavily charged with debris and sediment. Debris floods are known for their ability to cause extensive and rapid bank erosion (Church and Jakob, 2020; Jakob et al. 2022), scour, and aggrade channel beds increasing the risk of channel avulsion (Hungr et al., 2014). Cycles of scour and aggradation can occur in different phases throughout a debris flood.

Church and Jakob (2020) developed a three-fold typolgy for debris floods, which had previously not been defined well. This typology is summarized in Table C-1. Identifying the correct debris-flood type is important in understanding the sediment concentration the debris flood may carry and the changes to peak discharge, both which feed into the frequency-magnitude relationship discussed in Appendix D. Type 1 debris floods are initiated from rainfall or snowmelt generated streamflow that is sufficiently powerful to fully mobilize the channel bed. Type 2 debris floods are generated from diluted debris flows. Type 3 are generated by natural or man-made dam breaches. Type 1 debris floods are of relevance to Daisy, Thistle and Gravel creeks.

**Table C-1. Debris-flood classification based on Church and Jakob (2020).**

<table>
<tr><th>Term</th><th>Definition</th><th>Typical sediment concentration by volume (%)</th><th>Typical factor applied to clearwater peak discharge</th><th>Typical impacts</th></tr>
<tr><td>Type 1<br>(Meteorologically generated debris flood)</td><td>Rainfall/snowmelt generated through exceedance of critical shear stress threshold when most of the surface bed grains are being mobilized.</td><td>< 5</td><td>1.02 to 1.2 (depending on the proximity of major debris sources to the fan apex as well as organic debris loading)</td><td rowspan="2">Widespread bank erosion, avulsions, alternating reaches of bed aggradation and degradation, blocked culverts, scoured bridge abutments, damaged buried infrastructure particularly in channel reaches u/s of fans.</td></tr>
<tr><td>Type 2<br>(Debris flow to debris flood dilution)</td><td>Substantially higher sediment concentration compared to a Type 1 debris flood and can transport larger volumes of sediment. All grain sizes are mobilized, except those from lag deposits (big glacial or rock fall boulders)</td><td>< 50</td><td>Up to 1.5 depending on the distance of the debris-flow transition to the area of interest. If the debris flow tributary is immediately upstream of the fan apex, the bulking factor may be higher.</td></tr>
<tr><td>Type 3<br>(Outbreak floods)</td><td>Outbreak flood in channels that are not steep enough for debris-flow generation. The critical shear stress for debris-flood initiation is exceeded abruptly due to sharp hydrograph associated with the outbreak flood. All grains are mobilized in the channel bed and non-cohesive banks.</td><td>< 10<br>(except immediately downstream of the outbreak)</td><td>Up to 100 depending on size of dam and distance to dam failure. Peak discharges should be calculated through dam breach analyses and flood routing</td><td>Vast bank erosion, avulsions, substantial bed degradation along channels and aggradation on fans, destroyed culverts, outflanked or overwhelmed bridges, damaged buried infrastructure on channels and fans.</td></tr>
</table>

### C.1.2. Debris Flows

Debris flows originate from a single or distributed source area(s) of sediment mobilized by the influx of ground or surface water. Liquefaction occurs shortly after the onset of landsliding due to turbulent mixing of water and sediment, and the slurry begins to flow downstream, ‘bulking’ by entraining additional water and channel debris as the flow moves down a confined gully or channel. Post-wildfire debris flows are a special case where the lack of vegetation and root strength can lead to abundant rilling and gullying that deliver sediment to the main channel where mixing leads to the formation of debris flows. In those cases, no single source or sudden liquefaction is required to initiate or maintain a debris flow.

Coarse granular debris flows require a channel gradient of at least 27% ($15^{\circ}$) for transport over significant distances (Takahashi, 1991) and have volumetric sediment concentrations greater than 50% (i.e., there is more debris and sediment than there is water). Transport is possible at gradients as low as 20% (11°), although some momentum transfer from side-slope landslides is needed to sustain flow on those slopes. Debris flows may continue to run out onto lower gradients even as they lose momentum and drain.

Flow velocities typically range from 1 to 10 m/s leading to peak discharges during debris flows that are at least an order of magnitude larger than those of clearwater floods of comparable return period floods and can be 50 times larger or more (Jakob & Jordan, 2001; Jakob et al., 2016).

Debris flows are more than 50% sediment by volume and typically transport large boulders and woody debris meaning the flow is quite dense. The dense flow travels at high speeds meaning it can have very high impact forces and can cause extensive damage to structures, infrastructure, and cause life loss.

Channel banks can be severely eroded during debris flows, although lateral erosion is often associated with the trailing hyperconcentrated flow phase that is characterized by lower volumetric sediment concentrations. The most severe damage results from direct impact of large clasts or coarse woody debris against structures that are not designed for the impact forces. Even where the supporting walls of buildings may be able to withstand the loads associated with debris flows, building windows and doors can be crushed and debris may enter the building, leading to extensive damage to the interior of the structure (Jakob et al., 2012). Similarly, linear infrastructure such as roads and railways can be subject to complete destruction. On the medial and distal fan (the lower 1/3 to 2/3), debris flows tend to deposit their sediment rather than scour. Therefore, exposure or rupture of buried infrastructure such as telecommunication lines or pipelines is rare. However, if a linear infrastructure is buried in the proximal fan portions that undergo cycles of incision and infill, or in a recent debris deposit, it is likely that over time or during a significant runoff event, the tractive forces of water will erode through the debris until an equilibrium slope is achieved, and the infrastructure thereby becomes exposed or may rupture due to boulder impact or abrasion. This necessitates understanding the geomorphic state of the fans being traversed by a buried linear infrastructure.

Channel avulsions are likely in poorly confined channel sections (particularly on the outside of channel bends where debris flows tend to super-elevate). Sudden loss of confinement and decrease in channel slope cause debris flows to decelerate, drain their inter-granular water, and increase shearing resistance, which slow the advancing bouldery flow front and block the channel. The more fluid afterflow (hyperconcentrated flow) is then often deflected by the slowing front, leading to secondary avulsions and the creation of distributary channels on the fan. Because debris flows often display surging behaviour, in which bouldery fronts alternate with hyperconcentrated afterflows, the cycle of coarse bouldery lobe and levee formation and afterflow deflection can be repeated several times during a single event. These flow aberrations and varying rheological characteristics pose a challenge to numerical modelers seeking to create an equivalent fluid (Iverson, 2014).

### C.1.3. Peak Discharge Estimation

Clear-water flood, debris-flood, and debris-flow processes can differ widely in terms of peak discharge. The peak discharge of a debris flood is typically 1 to 1.2 times that of a clear-water flood in the same creek but could be much greater for Type 2 and 3 debris floods. If the creek is subject to debris flows, the peak flow may be much higher (as much as 50 times) than the flood peak discharge (Jakob & Jordan, 2001). Figure C-3 shows a hypothetical cross-section of a steep creeks, including:

- Peak flow for the 2-year return period ($Q_2$)
- Peak flow for the 200-year return period flood ($Q_{200}$)
- Peak flow for Type 1 debris flood ($Q_{max}$ full bed mobilization)
- Peak flow for Type 3 debris flood ($Q_{max}$ outburst flood)
- Peak flow for debris flow ($Q_{max}$ debris flow).

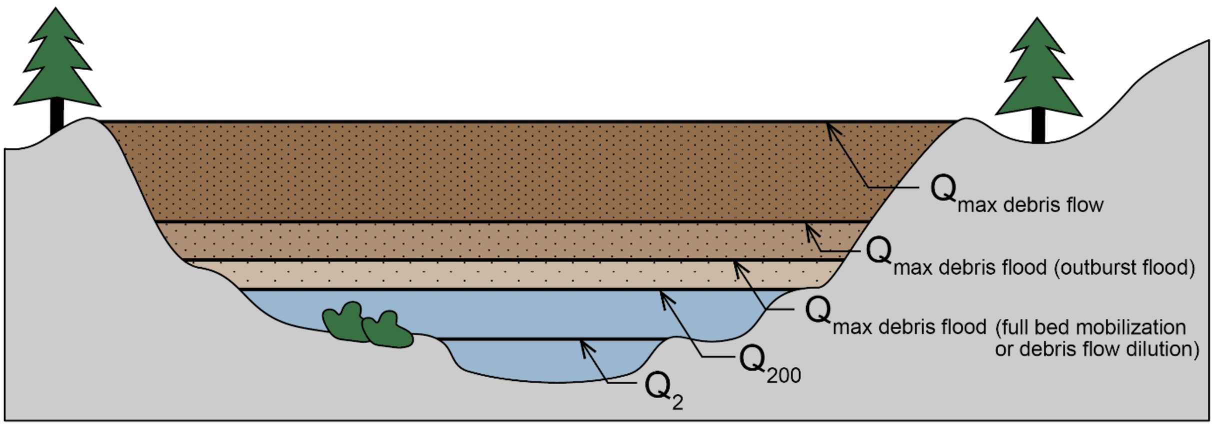


**Figure C-3. Steep creek flood profile showing schematically peak flow levels for different events.**

### C.1.4. Avulsions

An avulsion occurs when a watercourse jumps out of its main channel into a new course across its fan or floodplain. This can happen because the main channel cannot convey the flood discharge and simply overflows, or because the momentum of a flow allows overtopping on the outside of a channel bend. Finally, an avulsion can occur because a log jam or blocked bridge redirects flow away from the present channel. The channel an avulsion flow travels down is referred to as an avulsion channel. An avulsion channel can be a new flow path that forms during a flooding event or a channel that was previously occupied.

In Figure C-4, a schematic of a steep creek and fan is shown where the creek avulses on either side of the main channel. The avulsion channels are shown as dashed blue lines as avulsions only occur during severe floods (i.e., rarely). On high resolution topographic maps generated from Lidar, avulsion channels are generally visible and are tell-tale signs of past and potential future avulsions.

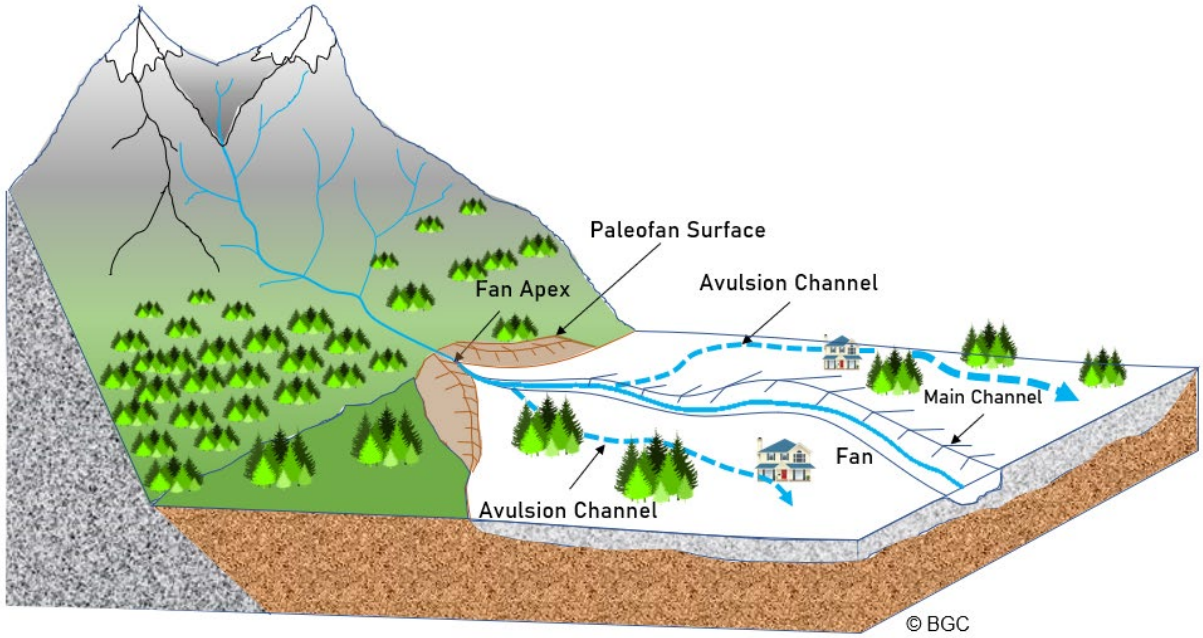


**Figure C-4. Schematic of a steep creek channel with avulsions downstream of the fan apex. Artwork by BGC.**

### C.1.5. Bank Erosion

Floods and debris floods exert high shear stresses on channel banks which can lead to bank erosion. Alluvial fans may be particularly susceptible to bank erosion as channel bed armouring limits the erodibility of the bed relative to the channel banks, which are often composed of non-cohesive materials such as sands and gravels. In contrast, rivers that typically experience overbank flooding and deposition of fine sediment during clearwater floods are likely to have cohesive banks composed of silt and clay, which are relatively strong compared to the channel bed.

Bank erosion along steep creeks is not considered in standard hydraulic models, and therefore needs to be assessed separately. Bank erosion is a self-limiting process as channel widening lowers the flow depth and shear stress associated with a given flood magnitude (Figure C-5).

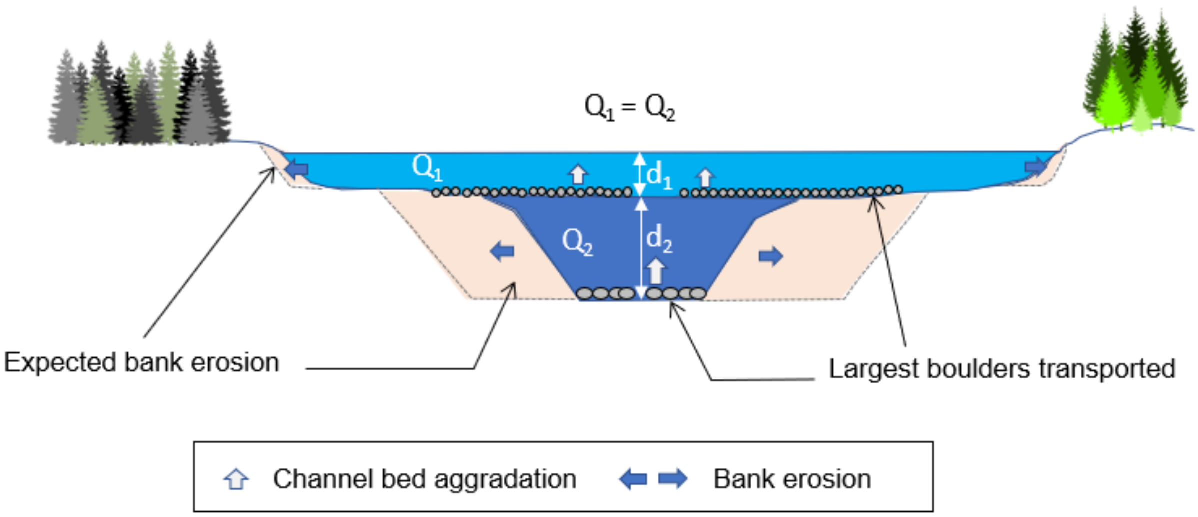


| Channel configuration | Flow characteristics and bank erosion potential |
|---|---|
| Wide channel and floodplain (light blue) | • Low flow depth ($d_1$) and velocity lead to low shear stresses exerted on channel banks.<br>• Lower bank erosion potential and smaller grain sizes transported.<br>• Lesser erosion protection and channel maintenance requirements. |
| Narrow channel (dark blue) | • High flow depth ($d_2$) and velocity lead to high shear stresses exerted on channel banks.<br>• Higher bank erosion potential and larger grain sizes transported.<br>• Greater erosion protection and channel maintenance requirements. |

**Figure C-5. Schematic of channel configuration and associated bank erosion potential.**

## C.2. CLIMATE CHANGE

Climate change is expected to impact steep creek geohazards both directly and indirectly through complex feedback mechanisms. Given that hydrological and mass movement processes are higher order effects of air temperature increases, their prediction is highly complex and often site-specific.

Regional climate change projections indicate that there will be an increase in winter rainfall (PCIC, 2012), an increase in the hourly intensity of extreme rainfall and increase in frequency of events (Prein et al., 2017). Changes to short duration (one hour and less) rainfall intensities are particularly relevant for post-fire situations in debris-flow generating watersheds. Within the year to a few years after a wildfire affecting large portions of a given watershed, short duration and high intensity rainfall events are much more likely to trigger debris flows or debris floods, than prior to a wildfire event.

Steep creek basins can be generally categorized as being either:

- Supply-limited: meaning that debris available for transport is a limiting factor on the magnitude and frequency of steep creek events. In other words, once debris in the source zone and transport zone has been depleted by a debris flow or debris flood, another event even with the same hydro-climatic trigger will be of lesser magnitude; or,

- Supply-unlimited: meaning that debris available for transport is not a limiting factor on the magnitude and frequency of steep creek events, and another factor (such as precipitation frequency/magnitude) is the limiting factor. In other words, there is always an abundance of debris along a channel and in source areas so that whenever a critical hydro-climatic threshold is exceeded, an event will occur. The more severe the hydro-climatic event, the higher the resulting magnitude of the debris flow or debris flood.

Further subdivisions into channel supply-limited and unlimited and basin supply-limited and unlimited are possible but not considered herein.

The sensitivity of the two basic types of basins to increases in rainfall (intensity and frequency increases) differ (Figure C-6):

- Supply-limited basins would likely see a decrease in individual geohazard event magnitude, but an increase in their frequency as smaller amounts of debris that remain in the channel are easily mobilized (i.e., more, but smaller events).
- Supply-unlimited basins would likely see an increase in hazard magnitude and a greater increase in frequency (i.e., significantly more, and larger events).

Supply-limited basins can transition into supply-unlimited due to landscape changes. For example, sediment supply could be increased by wildfires, landslide occurrence, or human activity (e.g., related to road building or resource extraction). In the case of wildfires, the impact on debris supply is greatest immediately after the wildfire, with its impact diminishing over time as vegetation regrows (see Section C.2.1). Wildfires are known to both increase the sediment supply and lower the precipitation threshold for steep creek events to occur.

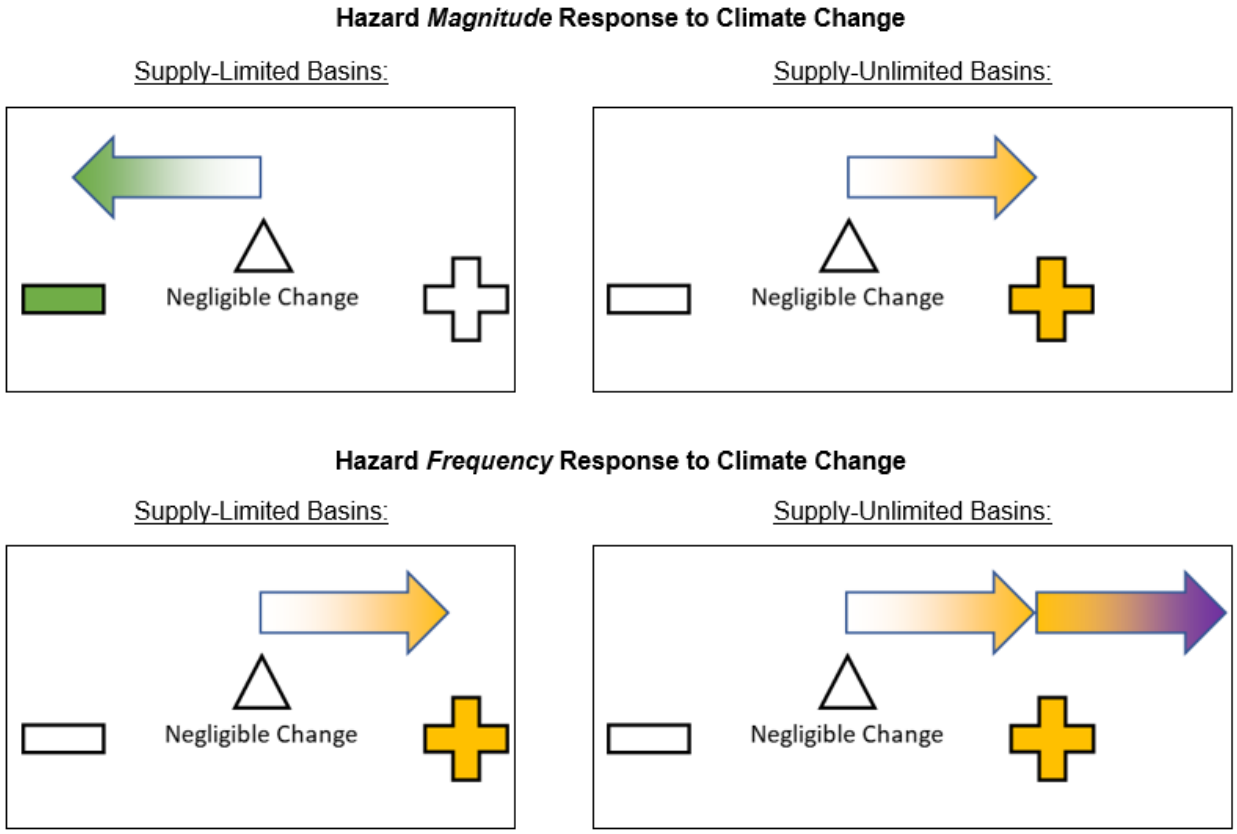


**Figure C-6. Steep creek hazard sensitivity to climate change – supply-limited and supply unlimited basins.**

### C.2.1. Wildfires

Wildfires in steep mountainous terrain are often followed by a temporary period of increased geohazard activity. This period is most pronounced within the first three to five years after the fire (Cannon & Gartner, 2005; DeGraff et al., 2015). After about three to five years, vegetation can reestablish on hillslopes and loose, unconsolidated sediment mantling hillslopes and channels may have been eroded and deposited downstream. A second period of post-fire debris-flow activity is possible about ten years following a fire, when long duration storms with high rainfall totals or rain-on-snow events cause landslides that more easily mobilize due to a loss of cohesion caused by tree root decay (DeGraff et al., 2015; Klock & Helvey, 1976; Sidle, 1991; 2005). This second period of heightened debris-flow activity is rare.

### C.2.2. Landslide Dam Outbreak Flood Potential

Some steep creek watersheds are prone to LDOFs, which could trigger flooding, debris floods, or debris flows with larger magnitudes than "typical" hazards. An example of this hazard in the Squamish Lillooet Regional District is landslides in the Mount Meager volcanic complex, which have generated several landslide dams along Meager Creek and Lillooet River (Figure C-7; Bovis & Jakob, 2000; Guthrie et al., 2012). LDOFs are not expected to occur on Daisy, Thistle, or Gravel creeks and have not been included in the present assessment.

**Figure C-7. Landslide dam on Meager Creek from the August 6, 2010 rockslide-debris flow from Capricorn Creek. The dam impounded Meager Creek for some time. Photo by D. Steers.**

# APPENDIX D
# FREQUENCY-MAGNITUDE ANALYSIS

## D.1. INTRODUCTION

A frequency-magnitude (F-M) relationship answers the question "how often (frequency) and how big (magnitude) can steep creek hazards events become?". The objective of an F-M analysis is to develop a relationship between the frequency of the hazard and its magnitude. For this assessment, frequency is expressed using return periods[1]. Both peak discharge (for clearwater flows, debris floods and debris flows) and volume (for debris floods and debris flows) are used as measures of magnitude.

BGC assessed that Thistle and Gravel creeks are subject to floods and debris floods for the entire assessed return period spectrum, and Daisy Creek is subject to debris floods (lower return periods) and debris flows (greater than approximately 50-year representative return period). The following sub-sections describe the methods employed by BGC to develop F-M relationships for debris floods and debris flows on Daisy, Thistle, and Gravel creeks. The representative return periods assessed in this study are summarized in Table D-1.

**Table D-1. Range of return periods for the hazard assessment on Daisy, Thistle, and Gravel creeks.**

| Return Period Range (years) | Representative Return Period (years) | Annual Exceedance Probability (%) | Study Creeks |
|---|---|---|---|
| 10 to 30 | 20 | 5 | Daisy, Thistle, Gravel |
| 30 to 100 | 50 | 2 | |
| 100 to 300 | 200 | 0.5 | |
| 300 to 1,000 | 500 | 0.2 | |
| 1,000 to 3,000 | 2,500 | 0.04 | |
| 3,000 to 10,000 | 5,000 | 0.02 | Daisy |

Note: The 50-, 500-, 2,500-, and 5,000-year events do not precisely fall at the mean of the return period ranges but were chosen as round figures due to uncertainties and because these return periods have a long tradition of use in BC.

## D.2. HISTORICAL OBSERVATIONS

Historical evidence of geohazard events can be observed via historical records, field assessments and aerial imagery interpretations. There is a reported debris flow on Daisy Creek in 2016 with an estimated volume of 2,000 to 3,000 $m^3$ (Thurber, June 13, 2016). BGC did not identify records of any historical events on Thistle or Gravel creeks. Methods specific to the hazard types present in the study area are described the corresponding sections in this appendix.

[1] Except for periods of T<1, the return period (T) is the inverse number of frequency F (i.e., T=1/F). A return period of 100 years is equivalent to a frequency of 0.01 events/year, or a 1% probability that an event may occur in any given year. In a changing climate or because of adverse human interference with watershed processes, the return period of a given magnitude event may decrease over time. For example, a 100-year return period debris flood based on historical data, may become a 20-year return period debris flood by the end of the century.

### D.2.1. Fieldwork

BGC completed field assessments on the Thistle and Daisy creek channels, watersheds, and fan areas on May 11 and June 7, 2022. Fieldwork was completed by Lauren Hutchinson, M.Sc., P.Eng., Dr. Matthias Jakob, P.Geo., P.L.Eng., and Hilary Shirra, B.A.Sc., EIT. Fieldwork for Gravel Creek was completed by Lauren Hutchinson and Matthias Jakob on June 16, 2020 ,as part of the Gravel Creek hazard assessment (BGC, November 13, 2020).

Field observations were recorded in field notebooks and iPad-assisted mapping applications that are integrated with web-based servers. Photos were captured with location data (georeferencing) using the iPad or cell phones. BGC collected representative dimensions of channel characteristics (width, gradient, channel bank conditions, presence of bedrock), grain sizes, and estimated channel yield rates (Daisy Creek). BGC also measured the dimensions of culvert and bridge crossings in the watersheds and within the proposed development. A representative selection of photos collected as part of the field work are presented in the Photo Appendix.

On Daisy Creek, two dendrochronology measurements were collected in the upper watershed on the north channel (Section D.6.1.2) and samples for radiocarbon dating were collected on the fan area (Section D.6.1.3).

### D.2.2. Aerial Imagery Interpretation

#### D.2.2.1. Air Photo Interpretation

BGC examined air photos dated between 1932 and 2003 for evidence of past major transport events at the study creeks (Appendix B). Events can be identified from the appearance of bright areas and disturbed vegetation relative to previous air photos that is indicative of debris-flood- and debris-flow deposits. Smaller events that did not deposit sediment outside the channel or significantly change the course of the channel are not captured in this analysis. Similarly, events that occurred during large gaps between air photos or successive events that overlap may also not be identified by this approach.

A summary of observations from the air photo interpretation is included in Table D-2. A selection of air photos are annotated with observations on Drawing 04.

**Table D-2. Summary of observations from air photo interpretation.**

| Imagery Date | Summary of Observations |
|---|---|
| 1932 | Debris avalanche scar visible in the lower portion of Thistle Creek in the 1932 air photos. |
| 1940 | Debris avalanche scars visible in the Daisy Creek watershed in the 1940 air photos. Anthropomorphic modification including earthworks within the Daisy, Thistle and Gravel creek fans are visible. |
| 1952 | A road has been constructed through the lower portion of the Daisy, Thistle and Gravel creek watersheds, presumably for logging. |
| 1957 | Railway and Highway 99 constructed through the Daisy, Thistle and Gravel creek fans. Earthworks within the fan to the north and south of Highway 99 are visible. |
| 1969 | Debris avalanche scars visible along Daisy Creek. Logging or burn area identified. Further earthworks visible within the Thistle and Gravel Creek fans, north and south of Highway 99. |
| 1982 | Powerline constructed through the Daisy, Thistle and Gravel creek fans, north of Highway 99. Further earthworks visible within the Daisy, Thistle and Gravel creek fans south of the new powerline and north of Highway 99. Further logging visible in the upper Daisy and Thistle creek watersheds. |
| 1990 | Further earthworks visible within the Daisy, Thistle and Gravel creek fans, south of the powerline. |
| 1994 | Debris avalanche scar visible in the Daisy Creek watershed. |
| 2003 | Extensive clear-cuts visible throughout the watersheds. Logging roads extended. |

BGC delineated the study creek fan areas using the 1932 air photos, which was prior to most of the fan areas being removed by mining activities.

#### D.2.2.2. Satellite Imagery and Remote-Sensing Data

BGC also reviewed satellite imagery from 2004 to 2022 and lidar data from 2019. Satellite imagery is available through Google Earth and ESRI World Imagery. BGC noted the presence of the Daisy Creek debris basin after 2009 but did not note any additional evidence of debris floods or debris flows that reached the fan areas. The 2019 lidar, supplemented with the observations from aerial imagery interpretation and publicly available geological mapping, informed the geomorphic mapping of the study watersheds as shown on Drawing 03.

## D.3. CLIMATE AND CLIMATE CHANGE

The nearest Environment and Climate Change Canada (ECCC) weather observation location is Squamish Auto climate station (ID 10476F0), approximately 19 km north of the study creeks. The station has rainfall data records from 1982-2021.

### D.3.1. Rainfall

Maximum annual daily rainfall totals were abstracted from the Squamish Auto Climate record and converted to 24-hour values by a factor of 1.13 which accounts for the average 13% increase in maximum rainfall amounts observed in 24-hour periods as compared with the maximum rainfall amounts observed in a fixed calendar day from approximately 500 climate stations across Canada (Watt, 1989). Updated 24-hour totals are provided in Table D-3 and Figure D-1 based on four probability distributions: Pearson Type III (PIII), log Pearson Type III (LPIII), Generalized Extreme Value (GEV, linear moments (lm)), and GEV (maximum likelihood estimate (mle)).

**Table D-3. Historical 24-hour rainfall quantile estimates for the Squamish climate station (ID 10476F0) based on data from the period 1982-2021.**

| Return Period (years) | 24-hour Rainfall (mm) | | | |
|---|---|---|---|---|
| | 1982-2021 Dataset | | | IDF (1982-1991) Dataset |
| | GEV_lm | LPIII | PIII | |
| 2 | 112 | 112 | 112 | 114 |
| 5 | 137 | 137 | 136 | 146 |
| 10 | 150 | 149 | 149 | 168 |
| 20 | 161 | 159 | 160 | - |
| 25 | 164 | 162 | 164 | 195 |
| 50 | 172 | 170 | 173 | 214 |
| 100 | 179 | 177 | 182 | 234 |
| 200 | 185 | 183 | 190 | - |
| 500 | 192 | 190 | 200 | - |
| 2500 | 201 | 199 | 216 | - |

- value not available in publicly available IDF data.

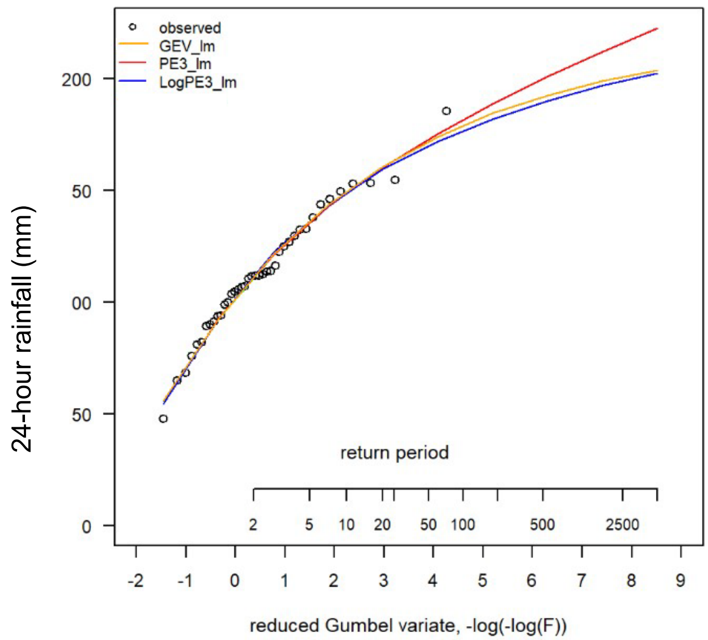


**Figure D-1. R-generated 24-hour rainfall frequency analysis of the Squamish Auto climate station from using data from 1982 to 2021 with multiple probability distributions.**

Table D-3 and Figure D-1 suggest good conformance in the 24-hour rainfall amounts derived from the four different probability distributions with small differences between the distributions at higher return periods. This is due to the increased uncertainty in the rainfall estimates for return periods exceeding the 39-year record length (i.e., >50-year return period estimates). BGC used the Generalized Extreme Value (GEV) values in this assessment. Note that as a rule of thumb, frequency analysis become highly uncertain beyond two times the record length. In other words, estimates exceeding 100-year return periods are much less reliable than those of lesser return periods.

Sub-daily rainfall records are also available at the Squamish climate station for the period 1982-1991. Based on these records, ECCC have published rainfall intensity-duration-frequency (IDF) data for durations of 5 minutes to 24 hours. Table  includes 24-hour rainfall estimates for various return periods from the ECCC IDF analysis. The IDF values are generally higher than the BGC estimates, which is not surprising in that the IDF dataset is only 10 years (resulting in less confidence at higher return periods) compared to the 39-year dataset used by BGC.

### D.3.2. Climate Change

Climate change is expected to impact flood hazards directly and indirectly through complex feedback mechanisms. This challenges reliable future flood hazard estimates. To estimate the impacts of climate change on future rainfall amounts in the study creek watersheds, BGC reviewed Northwest Hydraulic Consultants' (NHC, July 13, 2016) analysis of the potential impacts of climate change in the District of North Vancouver (DNV), and the GHD study of the impacts of climate change on precipitation and storm water management for Greater Vancouver (GHD, August 3, 2018) both using RCP 8.5. The results of the two studies are as follows:

- NHC projected increases to mid-century (2040-2070) in the 200-year 5-minute to 24-hour duration rainfall amounts from approximately 30% to 23%, respectively. For end of century (2070-2100), NHC projected increases in the 200-year 5-minute to 24-hour duration rainfall amounts from approximately 50% to 38%, respectively. NHC recommended adoption of the higher of each range based on the timeline considered (mid-century or end of century).
- GHD projected increases in rainfall intensities for the 2050s time horizon between 21% and 44% for moderate to high climate change scenarios, respectively; and increases in rainfall intensities for the 2100 time horizon between 41% and 75% for moderate to high climate change scenarios, respectively).
- More specifically, the GHD study area includes Zone 6, which encompasses the DNV. In this zone, the GHD results indicate increases in rainfall intensities for the 2050s time horizon between 20% and 37% for moderate to high climate change scenarios, respectively; and increases in rainfall intensities for the 2100 time horizon between 35% and 62% for moderate to high climate change scenarios, respectively.

The DNV is believed to be a reasonable proxy for the study creek watersheds. For this reason, BGC adopted an increase in the 24-hour rainfall depths of 50% as it aligns with the NHC recommendation (NHC, July 13, 2016) and is within the range presented for the DNV by GHD (August 3, 2018). The 50% increase was applied to all return periods. This increase is also consistent with the value BGC adopted for the Gravel Creek assessment (BGC, November 13, 2020).

## D.4. CLEARWATER PEAK FLOW ESTIMATION

BGC estimated peak flows for clearwater floods by modeling rainfall-runoff. This allows development of hydrographs for each of the representative return periods considered in this study (Table D-1) which were used as inputs to the numerical modelling. The Soil Conservation Service (SCS) unit hydrograph method (SCS, 1972) was implemented using the HEC-HMS (Version 4.9) program developed by the United States Army Corps of Engineers (USACE). This method is widely used to derive synthetic unit hydrographs and applies a design storm event and physical watershed characteristics to predict peak flows.

Required inputs to the model include:

- The storm event hyetograph (rainfall intensity over time).
- The time of concentration (Tc) defined as the time taken for the storm runoff event to travel from the most remote point of a basin to the point of interest.
- A curve number (CN), an empirically derived relationship between soil type, land use, antecedent conditions and runoff used to establish initial soil moisture conditions and infiltration response. CN values for various hydrologic soil groups are provided in USACE (2000).

### D.4.1. Hyetograph

A SCS Type 1A storm event hyetograph was used for the rainfall-runoff simulation. This storm type has been shown to accurately generate flood runoff from watersheds within the region

(Loukas, 1994). Table D summarizes the 24-hour rainfall estimates adopted by BGC for HEC-HMS modelling, including climate change-adjusted values.

**Table D-4. Summary of 24-hour rainfall estimates for the Squamish Auto (10476F0) climate station using data from 1982 to 2021 and GEV mle distribution and +50% climate change adjustment.**

| Representative Return Period (years) | Existing Conditions (mm) | Climate Change (2100) (mm) |
|---:|---:|---:|
| 20 | 160 | 240 |
| 50 | 170 | 260 |
| 200 | 185 | 280 |
| 500 | 190 | 290 |
| 2,500 | 200 | 300 |

### D.4.2. Watershed Characteristics

BGC delineated the study watersheds and creeks using lidar available through the BC Public Lidar Portal and dated 2019. The required parameters for hydrological analysis using the SCS method are summarized in Table D-4.

**Table D-4. Hydrological parameters of the Gravel Creek watershed.**

| Parameters | Daisy Creek | Thistle Creek | Gravel Creek |
|---|---:|---:|---:|
| Watershed Area ($km^2$) | 1.81 | 2.86 | 0.73 |
| Average Gradient (m/m) | 0.4 | 0.35 | 0.52 |
| SCS Curve Number (CN II)[1] | 75 | 75 | 75 |
| Initial Abstraction (mm) | 16.9 | 16.9 | 16.9 |
| Lag time (min)[2] | 29 | 23 | 10 |

Notes:
1. Based on Soil Type C, for poor to fair quality woods.
2. SCS Lag Formula.

### D.4.3. Peak Flow Results

The resulting peak discharge values are summarized in Table D for 2100 conditions.

**Table D-5. Estimated peak instantaneous discharge for Daisy, Thistle and Gravel creeks for end-of century including climate change impacts.**

| Return Period (years) | Peak Instantaneous Discharge ($m^3/s$) | | |
|---|---|---|---|
| | Daisy Creek | Thistle Creek | Gravel Creek |
| 20 | 27.0 | 15.9 | 8.1 |
| 50 | 29.8 | 17.5 | 9.0 |
| 200 | -[1.] | 19.5 | 10.0 |
| 500 | -[1.] | 20.4 | 10.5 |
| 2,500 | -[1.] | 21.7 | 11.1 |

Notes:

1. BGC's analysis determined that Daisy Creek is not prone to debris floods at return period events higher than 1 in 50 years but that higher return period rainfall events will results in debris flows. For the same reason, peak instantaneous discharge is not presented for Daisy Creek for higher return periods as it was not used in the corresponding frequency magnitude calculations.

## D.5. DEBRIS-FLOOD ASSESSMENT

Clearwater floods and debris floods as defined by Church and Jakob (2020) are related processes as both are classified as Newtonian processes, which implies no yield strength resisting motion. However, debris floods have been characterized by their higher sediment concentrations and propensity to erode banks, scour and avulse (Hungr et al., 2014). While some measurements of sediment concentration exist from steep creeks, especially near volcanic centres and downstream of recently deactivated dams (Magirl et al., 2015; Mosbrucker & Major, 2019), systematic bedload and suspended sediment measurements in steep channels during extreme flows are rare. This section outlines methods to estimate debris flood F-M relationships.

### D.5.1. Debris-Flood Initiation Threshold

BGC determined the threshold for initiation of debris floods based on the flow exceeding a critical threshold as outlined in Jakob et al. (2022).

### D.5.2. Discharge Bulking Method

Sediment concentration influences debris-flood behaviour. Higher suspended sediment concentration can transport larger stones. The mobilization of large particles implies full bed mobilization (MacKenzie et al. , 2018; Church & Jakob, 2020; Jakob et al. 2022), the characteristics of a Type 1 debris flood (Appendix C).

BGC selected bulking factors to approximate sediment concentration on the study creeks based on geomorphological indicators in the watersheds and after the method shown graphically in Figure D-2. The three types of debris floods are described in Appendix C. BGC only considered Type 1 debris floods on the study creeks as there was no evidence of debris flows or slope instability likely to generate landslide dams on Thistle or Gravel creeks. On Daisy Creek, at return periods in excess of 50-years, debris flows are expected to be the dominant hazard. The bulking factors selected are not precise as they are based on geomorphological indicators instead of direct observations of sediment concentration.

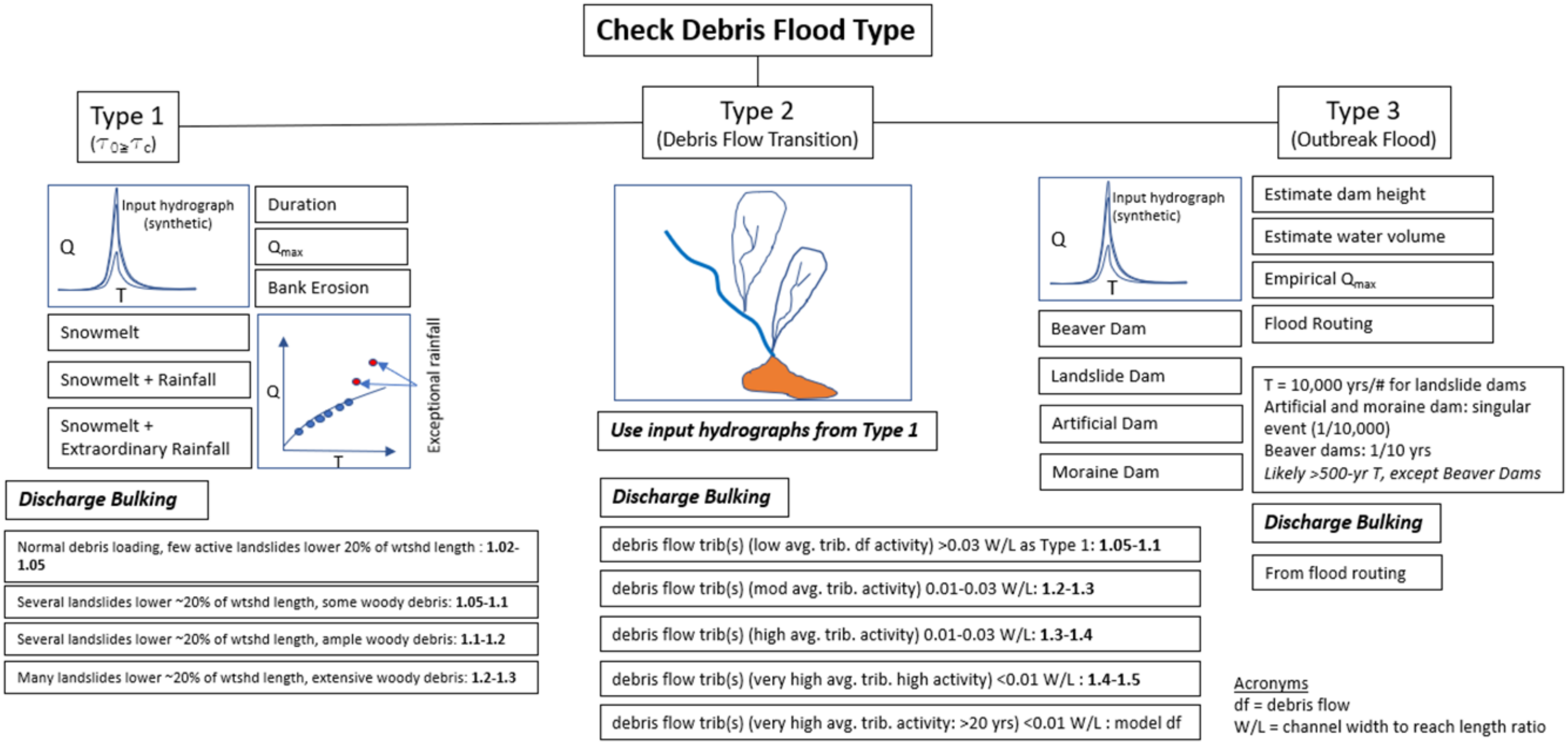


**Figure D-2. Debris flood bulking method logic chart for Daisy, Thistle, and Gravel creeks. Only Type 1 debris floods were considered for the study creeks.**

The bulking factors and bulked peak discharges for each of the study creeks are summarized in Table D-6, Table D-7, and Table D-8. As shown, only those return periods where BGC assessed a credible potential for debris floods are included. On Daisy Creek, only debris flows are anticipated at higher return periods while on Thistle- and Gravel creeks floods are anticipated at lower return periods (bulking factor of 1).

**Table D-6. Daisy Creek bulked peak discharge for representative return periods.**

| Representative Return Period (years) | Peak Instantaneous Discharge ($m^3/s$) | Debris Flood Type | Bulking Factor | Bulked Peak Discharge ($m^3/s$) |
|---:|---:|---:|---:|---:|
| 20 | 27 | 1 | 1.05 | 28 |
| 50 | 30 | 1 | 1.05 | 31 |
| 200 | - | - | - | - |
| 500 | - | - | - | - |
| 2,500 | - | - | - | - |

**Table D-7. Thistle Creek bulked peak discharge for representative return periods.**

| Representative Return Period (years) | Peak Instantaneous Discharge ($m^3/s$) | Debris Flood Type | Bulking Factor | Bulked Peak Discharge ($m^3/s$) |
|---:|---:|---:|---:|---:|
| 20 | 15.9 | - | 1.00 | 16 |
| 50 | 17.5 | 1 | 1.02 | 18 |
| 200 | 19.5 | 1 | 1.05 | 20 |
| 500 | 20.4 | 1 | 1.10 | 22 |
| 2,500 | 21.7 | 1 | 1.20 | 26 |

**Table D-8. Gravel Creek bulked peak discharge for representative return periods.**

| Representative Return Period (years) | Peak Instantaneous Discharge ($m^3/s$) | Debris Flood Type | Bulking Factor | Bulked Peak Discharge ($m^3/s$) |
|---:|---:|---:|---:|---:|
| 20 | 8.1 | - | 1.00 | 8 |
| 50 | 9.0 | - | 1.00 | 9 |
| 200 | 10.0 | 1 | 1.02 | 10 |
| 500 | 10.5 | 1 | 1.02 | 11 |
| 2,500 | 11.1 | 1 | 1.10 | 12 |

### D.5.3. Debris-Flood Sediment Volume Estimation

BGC used three independent semi-empirical methods to estimate sediment volumes associated with debris floods on the study creeks. An expert judgement-based weighted average informed by dozens of previous studies was employed to develop a best estimate of sediment volume. The results for each of the study creeks are summarized in Table D-9, Table D-10, Table D-11, Figure D-3, and Figure D-4. The frequency-magnitude curve for Daisy Creek is presented in Figure D-9. The following subsections outline the process employed for each of the methods.

**Table D-9. Daisy Creek sediment volume estimates from constituent techniques and best estimate.**

| Representative Return Period (years) | Sediment Volume ($m^3$) | | | |
|---|---|---|---|---|
| | Regional Fan F-M Analysis | Empirical Rainfall-Sediment | Empirical Bedload Transport | Best Estimate |
| Confidence | Low | Medium | Medium | Weighted Average |
| Weighting Factor | 1 | 2 | 2 | |
| 20 | 0 | 4,800 | - | 2,000 |
| 50 | 500 | 5,100 | - | 2,000 |
| 200 | - | - | - | - |
| 500 | - | - | - | - |
| 2,500 | - | - | - | - |

Notes:

1. At return periods higher than 50-years, BGC assessed that Daisy Creek is only susceptible to debris flows.
2. BGC did not apply the empirical bedload method to Daisy as it is appropriate mostly to lower gradient (<20%) creeks.
3. Sediment volumes for each method rounded to nearest 100 $m^3$, best estimate rounded to nearest 1,000 $m^3$.

**Table D-10. Thistle Creek sediment volume estimates from constituent techniques and best estimate.**

| Representative Return Period (years) | Sediment Volume ($m^3$) | | | |
|---|---|---|---|---|
| | Regional Fan F-M Analysis | Empirical Rainfall-Sediment | Empirical Bedload Transport | Best Estimate |
| Confidence | Low | Medium | Medium | Weighted Average |
| Weighting Factor | 1 | 2 | 2 | |
| 20 | 0 | 3,200 | 0 | 1,000 |
| 50 | 500 | 3,400 | 800 | 2,000 |
| 200 | 1,500 | 3,600 | 3,100 | 3,000 |
| 500 | 2,200 | 3,700 | 4,500 | 4,000 |
| 2,500 | 3,400 | 3,900 | 6,600 | 5,000 |

Notes:

1. Sediment volumes for each method rounded to nearest 100 $m^3$, best estimate rounded to nearest 1,000 $m^3$.

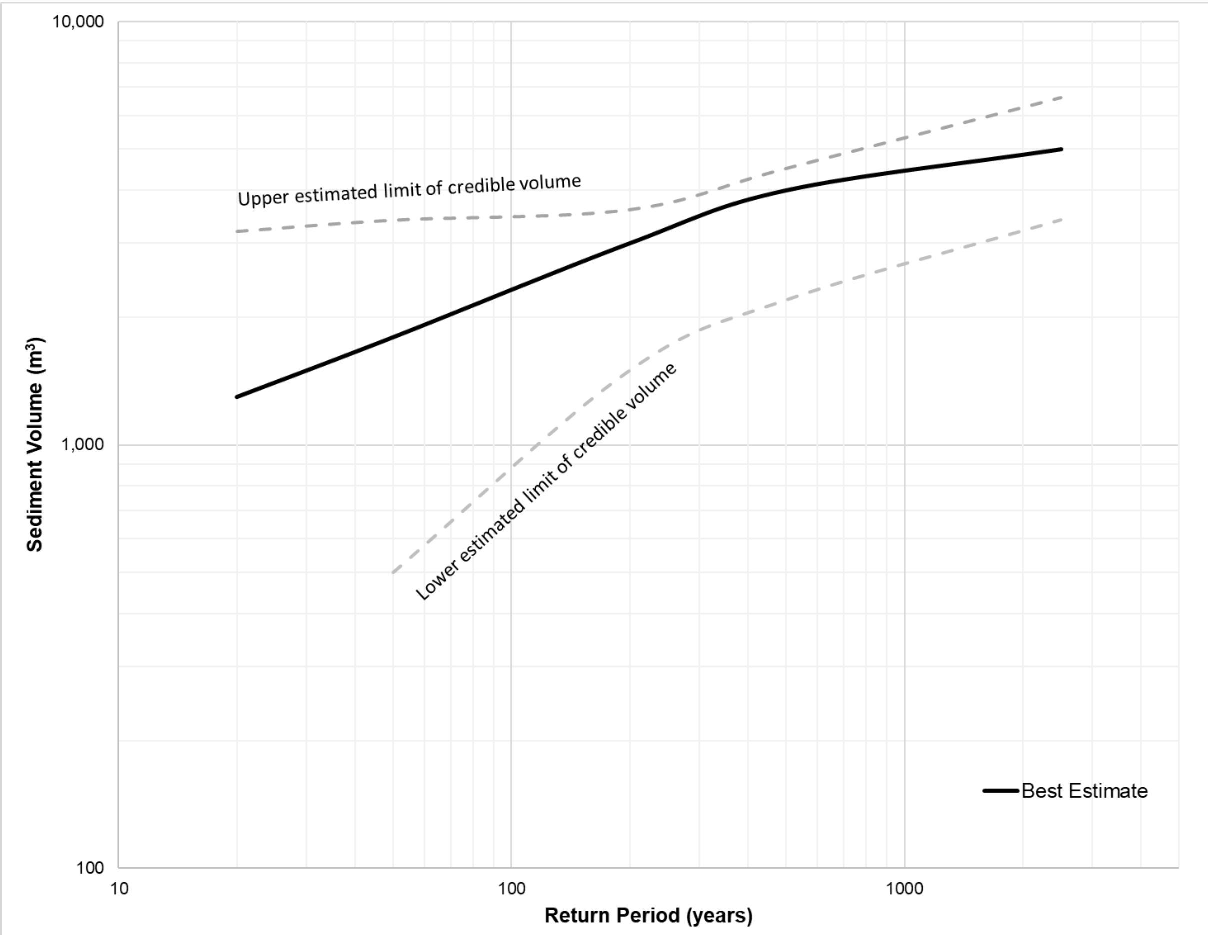


**Figure D-3. Thistle Creek best estimate debris flood F-M curve derived from F-M model ensemble.**

### Table D-11. Gravel Creek sediment volume estimates from constituent techniques and best estimate.

| Representative Return Period (years) | Sediment Volume ($m^3$) | | | |
|---|---|---|---|---|
| | Regional Fan F-M Analysis | Empirical Rainfall-Sediment | Empirical Bedload Transport | Best Estimate |
| Confidence | Low | Medium | Medium | Weighted Average |
| Weighting Factor | 1 | 2 | 2 | |
| 20 | 0 | 700 | 0 | - |
| 50 | 700 | 750 | 0 | - |
| 200 | 2,700 | 800 | 300 | 1,000 |
| 500 | 4,100 | 850 | 600 | 1,500 |
| 2,500 | 6,400 | 850 | 1,100 | 2,000 |

Notes:
1. At return periods less than 200-years, BGC assessed that Gravel Creek is only susceptible to floods and BGC has not included sediment volumes for these return periods.
2. Sediment volumes for each method rounded to nearest 100 $m^3$, best estimate rounded to nearest 500 $m^3$.

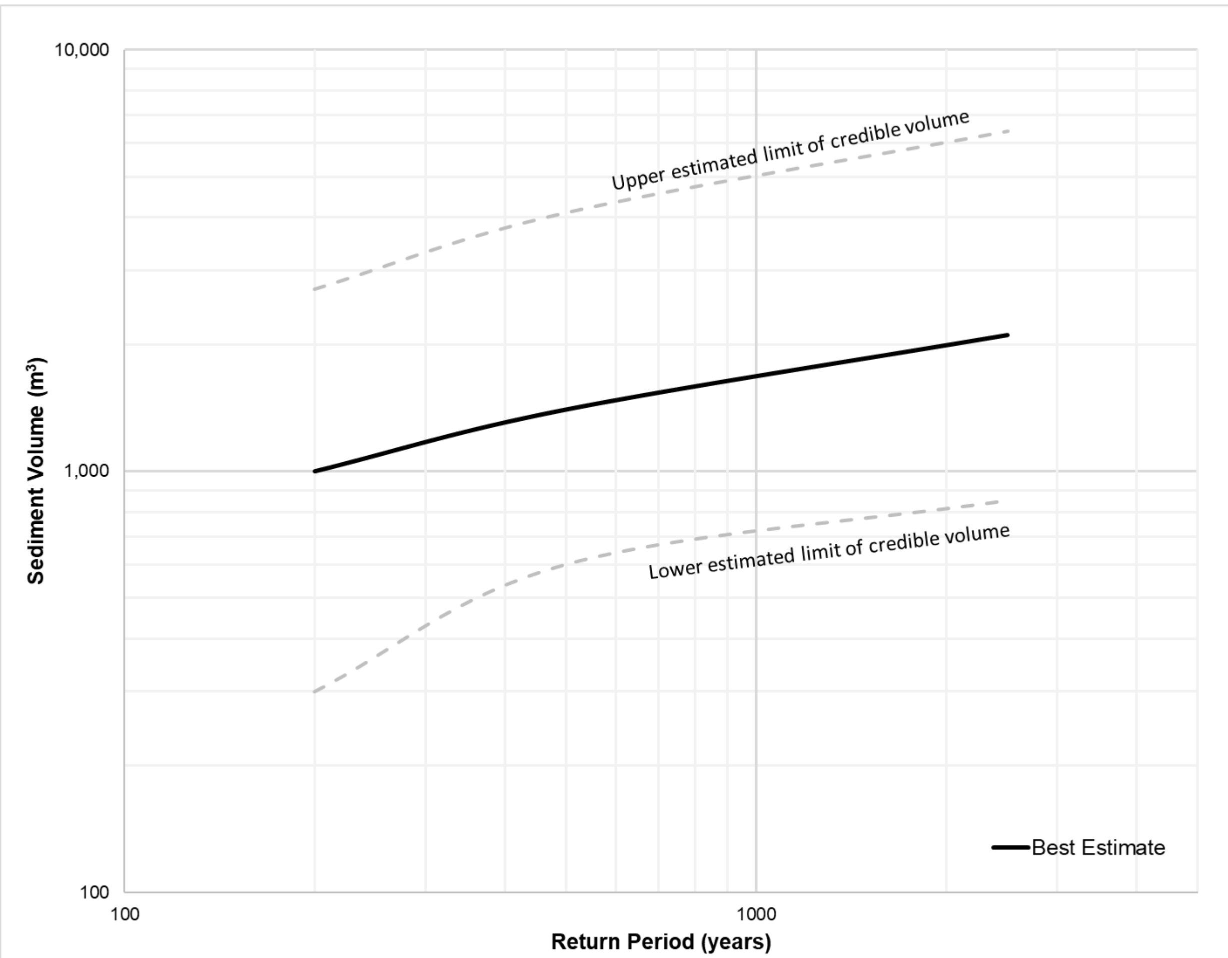


Figure D-4. Gravel Creek best estimate F-M curve derived from F-M model ensemble.

### D.5.3.1. Regional Fan Debris Flood Frequency-Magnitude Analysis

In areas where comprehensive studies on debris flood or debris flow frequencies and magnitude have been conducted, a normalization procedure based on fan area or fan volume can be applied to generate an approximate F-M at other sites without the need for in-depth field investigation.

This methodology was first applied by Jakob et al. (2016), who compiled nine detailed debris-flow hazard- and risk assessments completed by BGC and Cordilleran Geoscience over a period of approximately 15 years in southwest BC and later updated with data from the Bow Valley near Canmore (Jakob et al., 2020) (Figure D-5). For each of these projects, an F-M curve had been established using a variety of methods. Jakob et al. (2020) normalized the individual F-M curves by fan area and plotted them on the same graph. A best-fit line was plotted, and a predictive equation extracted.

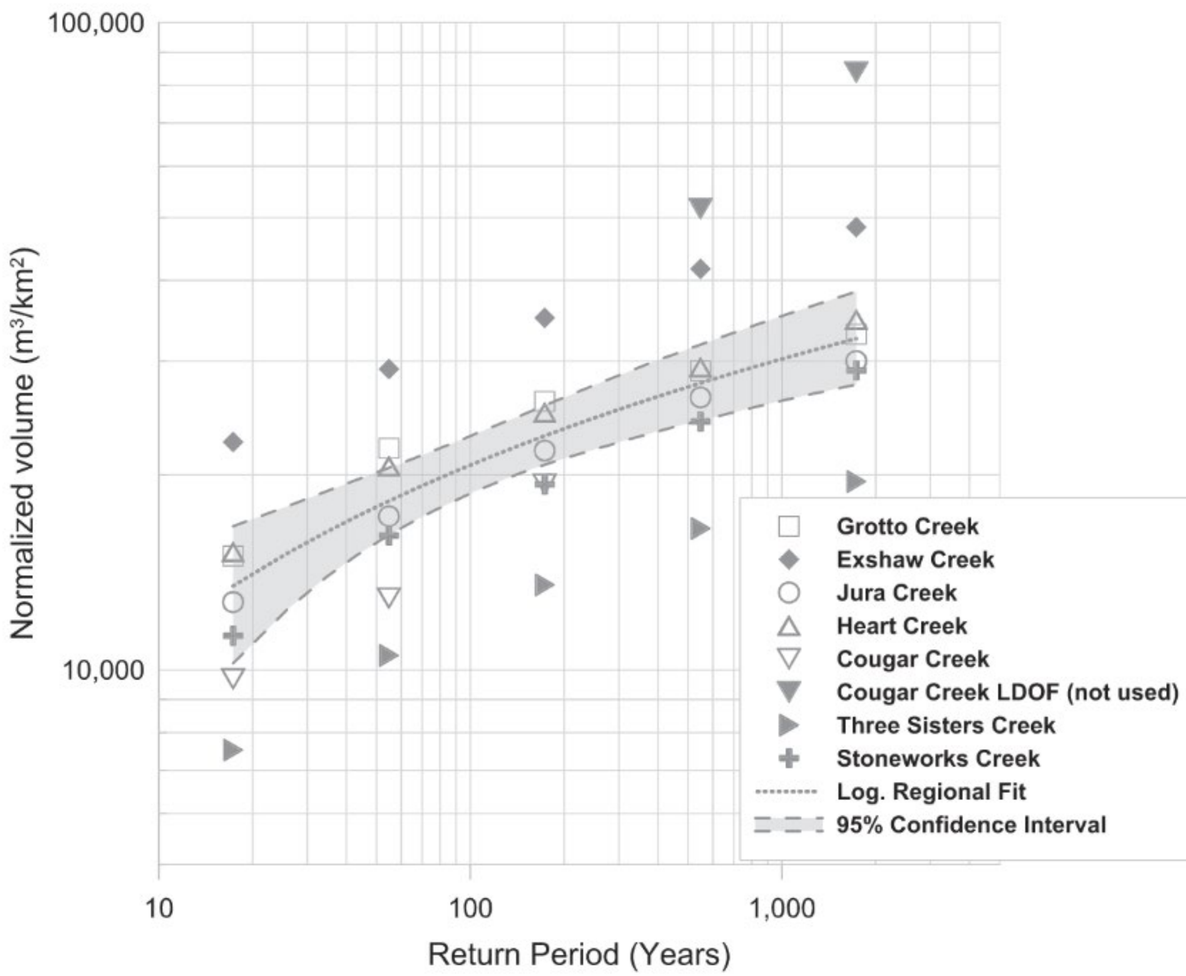


**Figure D-5. Regional debris flood frequency-magnitude data normalized by fan area for seven detailed studies in the Bow Valley, AB. From Jakob et al. (2020).**

BGC used the F-M equation for the southwestern BC and Bow Valley debris-flood creeks for application to the study creeks. Debris-flood and debris-flow prone creeks with similar characteristics to the study creeks (watershed area, fan areas) were included in the analysis.

The resulting, fan-normalized relationships for each creek are summarized in Equations D-3, D-4, and D-5.

Daisy Ck.: $V_{NAf} = 60322\ln(T) - 220346$ [Eq. D-3]

Thistle Ck,: $V_{NAf} = 22594\ln(T) - 72394$ [Eq. D-4]

Grave Ck.l: $V_{NAf} = 30214\ln(T) - 104297$ [Eq. D-5]

where $V_{NAf}$ is the normalized sediment volumes associated with fan areas and watershed areas and $T$ is the return period. The equations above allow the user to choose any return period (T) and calculate the corresponding debris-flood or debris-flow volume, as appropriate.

#### D.5.3.2. Debris Flood Sediment Volume Estimates from Empirical Rainfall-Sediment Transport Relations

Prediction of bedload transport can be important for hazard assessments and engineering applications although knowledge on sediment transport is still limited, particularly from a modeling perspective. Furthermore, few sediment transport studies have been completed for steep (> 5%) mountain creeks, and as noted by Hassan et al. (2005), sediment transport in such channels may be quite different from low-gradient channels. Hillslope processes are linked to channel processes with some channels being supply-limited while others being supply-unlimited (Jakob & Bovis, 1996; Rickenmann, 2005). As pointed out by Church and Zimmermann (2007), steep mountain creeks can display a multitude of grain sizes, variable sediment sources, and rough and structured stream beds with a step-pool morphology. Large boulders (keystones), woody debris and occasional bedrock sections further create significant variation in channel geometry, flow velocity and roughness, all of which render theoretical or flume-derived sediment transport equations questionable (Gomi & Sidle, 2003). These channel characteristics apply to the study creeks.

During August 21 to 23, 2005 severe flooding occurred in a large area of northern Switzerland with significant morphological changes in stream channels (Jäggi, 2007). This event was associated with more than 200 mm of rain within three days with corresponding return periods exceeding 100 years. As many mountain creek hazards have been mitigated by catchment basins, the sediment volumes could be determined. A database was created with 33 debris flows and 39 fluvial sediment transport events, details of which are reported in Rickenmann and Koschni (2010). These authors used a variety of transport movement equations to compare modeled and predicted sediment transport volumes including those by Rickenmann (2001), Rickenmann and McArdell (2007), Hunziker and Jäggi (2002), Recking et al. (2008), and D'Agostino et al. (1996). Rickenmann and Koschni (2010) found reasonable agreements between modeled and measured sediment volumes for channels with less than 5% gradient using the Meyer-Peter and Müller equations. In contrast, for steeper channels, the observed sediment volumes transported by fluvial processes are over-predicted by bedload equations developed for steep channels.

Given the value of the Rickenmann and Koschni (2010) database, BGC analyzed the data further. First, BGC separated the debris-flow events from the mostly fluvial transport data. Watersheds with very large areas and correspondingly low gradients (< 1%) were also deleted from the dataset. These deletions provided a final dataset of 36 cases. Multivariate regression analysis was then applied to the log-transformed dataset to determine sediment volumes based on catchment area, rainfall volume, runoff coefficient, surface runoff and channel gradient. This analysis yielded the two following formulae:

$$logV_S = 0.753logV_R - 0.553,\ R^2 = 0.79 \quad \text{[Eq. D-6]}$$

$$logV_S = -1.55 + 0.877logV_R + 0.019S,\ R^2 = 0.81 \quad \text{[Eq. D-7]}$$

where $V_S$ is the total sediment volume displaced and $V_R$ is the total rainfall. The difference between the two formulae is the inclusion of channel slope $S$ in Equation D-7. However, since the increase in variance is very small (2%), the effect of slope appears small. Neglecting slope would not be appropriate had the entire dataset been used as that also includes debris flows. Therefore, the formula presented above is only appropriate for debris floods with channel gradients from approximately 2 to 24%.

In addition to the Swiss dataset, BGC created a dataset with 14 creeks in the Bow Valley[2] that experienced debris floods during a June 2013 storm (i.e., BGC, October 31, 2014). Sediment volumes for these events were estimated by comparing 2008 or 2009 LiDAR to 2013 LiDAR (pre- and post-event LiDAR).

Both the Swiss and Bow Valley data were log transformed and a linear regression was applied to the combined data which resulted in Equation D-8, which shows very little difference from the Swiss dataset regression. This combined regression was used in further analyses.

$$logV_S = 0.740logV_R - 0.4624,\ R^2 = 0.78 \quad \text{[Eq. D-8]}$$

where $V_S$ is the total sediment volume displaced and $V_R$ is the rainfall volume. The regression analysis of the combined data is shown in Figure D-6 below. For the Bow Valley dataset a snowmelt contribution was added to the rainfall volume (i.e., rainfall + snowmelt = available water), as a shallow snowpack was present in mid to upper reaches of the watersheds.

As illustrated by Figure D-6, the rainfall-sediment relation observed in the Bow Valley correlates well with the Swiss dataset. This observation suggests that a relationship between runoff and sediment mobilized is location independent (as long as a quasi-unlimited sediment supply is present), as similar results were seen in the Rocky Mountains as in the Alps. While this relation appears to be location independent, it has not been verified for temporal independence. It is still unknown as to whether this relation holds for different storms of different magnitudes for individual creeks.

[2] This analysis was restricted to the general vicinity of Canmore and Exshaw.

#### D.5.3.2.1 Application to Study Creeks

BGC estimated debris-flood volumes with the following workflow:

1. Using the 24 hour precipitation totals generated for the study area (Section D.3.1).
2. The 24-hour precipitation values were then multiplied with the watershed area of the study creeks to arrive at a total volume of rain falling onto the watersheds in a 24-hour period.
3. To allow for orographic contribution, BGC added a 20% multiplier to the rainfall totals.
4. To allow for snowmelt contribution, BGC added 20% water equivalent over half of the watershed. This value can vary depending on the timing of a given storm (i.e., if snow prevails, at what elevation and at what water equivalent) and snow water equivalent (i.e., how wet the snow is at the time of the rainstorm).
5. The final step was to use Equation D-7 to estimate the debris flood sediment volumes for each return period class. BGC used this equation which includes slope as the study creeks are all steeper than 24%.

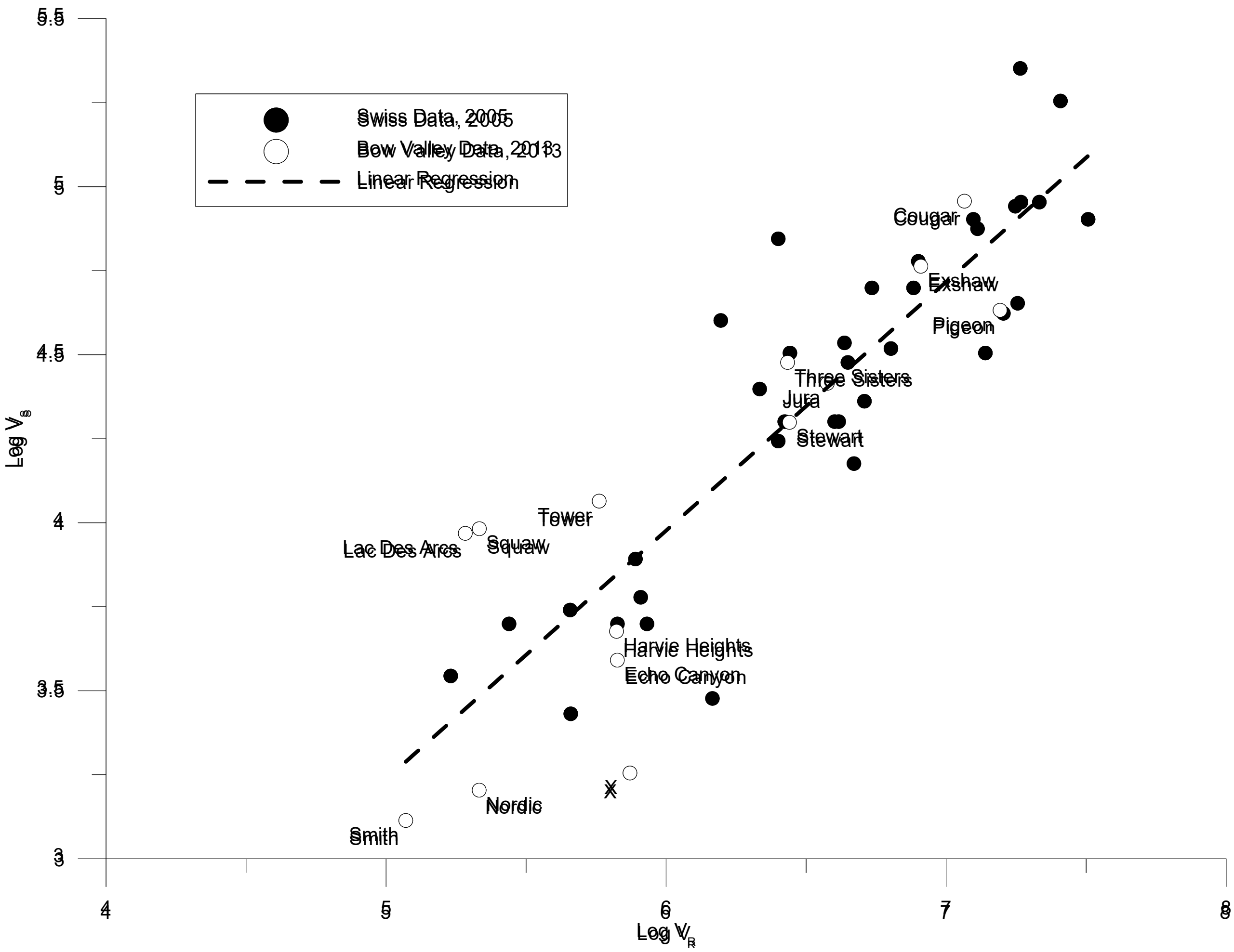


**Figure D-6. Log transformed sediment ($V_S$) and available water ($V_R$) data from the Swiss and Bow Valley datasets complied by Rickenmann and Koschni (2010) and BGC, respectively.**

### D.5.3.3. Empirical Bedload Transport Analysis

BGC leveraged the same concept to estimate debris volumes as was applied to determine the onset of debris floods based on threshold discharge for mobilization of the $D_{84}$ (Section D.5.1). The process can be summarized as follows:

1. Determine the critical shear stress required for bed mobilization (Equation D-1).
2. Use average channel dimensions and Manning's equation[3] to determine the debris flood discharge that corresponds with the critical shear stress.
3. Use the hydrographs (Section D.4.3) associated with a specific representative return period to calculate the amount of time that the flow exceeded the discharge threshold.
4. Select an appropriate sediment transport equation to calculate sediment discharge based on stream power.
5. Calculate sediment volume based on the estimated sediment discharge (4.) multiplied by the duration over which the critical shear stress occurs.

BGC used the Rickenmann (2001) bedload transport rate $q_b$, is defined as:

$$q_b = 12.6(\frac{D_{90}}{D_{30}})^{0.2} \cdot (q - q_c) \cdot S^{2.0} \cdot (s - 1)^{-1.6} \quad \text{[Eq. D-9]}$$

where $q_b$ is the bedload transport rate per unit channel width ($m^3/s/m$), $q$ is unit discharge ($m^3/s/m$), $q_c$ is the critical unit discharge at initiation of bedload transport, and $s$ is the ratio of solid to fluid density. For simplification, setting $(D_{90}/D_{30})^{0.2} = 1.05$ and $s = 2.68$ yields:

$$q_b = 5.8(q - q_c) \cdot S^{2.0} \quad \text{[Eq. D-10]}$$

Equation D-10 is based on 252 flume laboratory experiments. Observations on bedload transport in steep experimental streams are considered as a reference condition, which defines maximum transport rates ("transport capacity") for the idealized case of a uniform bed material, no morphological features, and hence no significant form roughness effects. Rickenmann (2001) then compared this empirical formula with bedload transport data from 19 mountain streams. This comparison showed that most of the smaller and steeper streams tended to have a lower bedload transport efficiency than larger streams. Rickenmann attributed this reduction in transport efficiency to an increase in flow resistance, as all the lower efficiency streams are grouped within the range of relative flow depths[3] smaller than 4 to 6. However, he also noted that lower efficiencies may be related to having flows near critical conditions for the beginning of sediment transport, which prevailed for many events on mountain streams analyzed in his study (i.e., only partial sediment transport occurred and full bed mobilization did not occur).

[3] Relative flow depth is defined as $h/D_{90}$, where $h$ is flow depth and $D_{90}$ is the grain size for which 90% of the surface bed material is finer by weight.

Given this variance from idealized conditions, Rickenmann (2001) provides the following alternative equation for bedload transport:

$$G_E = AS^{2.0}V_{re} \qquad \text{[Eq. D-11]}$$

where $G_E$ is the total bedload volume per flood events and the effective runoff volume, $V_{re}$, is the integral of the discharge above the critical discharge at initiation of bedload motion ($Q$-$Q_c$). The parameter $A$ represents bedload efficiency, which is defined by the deviation of observed transport rates from those predicted by Equation D-10.

The Rickenmann (2001) relationship is applicable for creeks with gradients 3% ≤ S ≤ 20%. All of BGC's study creek gradients exceed these values. BGC applied the relationship to Thistle and Gravel creeks which have lower gradient than Daisy Creek. The resultant volume estimates should be considered conservative given Rickenmann's observations of lower transport efficiencies in steeper channels.

## D.6. DEBRIS-FLOW ASSESSMENT

This section outlines the methodology to assess debris-flow frequency and magnitude at Daisy Creek.

### D.6.1. Debris-Flow Frequency

This section discusses the methods employed to estimate debris-flow frequency at Daisy Creek.

#### D.6.1.1. Air Photo Interpretation

BGC did not identify any evidence of debris-flows that reached the proposed development area in the air photo record from 1932 to 2003 (Section D.2.2.1).

#### D.6.1.2. Dendrogeomorphology

BGC identified and dated two trees with impact scars interpreted to be from past debris flow events on Daisy Creek in the north channel upstream of the main logging road (elevation 440-460 m). Other trees near the channel did either not show scars or were too young to be useful. Details from the two trees are summarized in Table D-12.

**Table D-12. Daisy Creek dendrogeomorphology sample details.**

| Sample | Location (UTM 10) | Elevation (m) | Tree Type | Age of Impact (years) | Photo Appendix | Notes |
|---|---|---|---|---|---|---|
| D-DF-01 | 486224, 5494868 | 445 | Douglas Fir | 104 | Photo 6 | Key tree on boulder lobe. |
| D-DF-02 | 486180, 5494845 | 430 | Douglas Fir (Stump) | 135 ± 5 | Photo 7 | Stump logged in 2016. |

### D.6.1.3. Stratigraphic Section and Radiocarbon Dating

Assessment of stratigraphic sections allow estimation of the thickness of past debris flows/debris floods, which are typically distinct from overlying and underlying deposits. It also permits sampling of datable organic materials found in paleosols (old soil layers) and embedded within the debris-flow deposits. An approximate age can then be assigned to the deposit. These sections can be created using excavator-assisted test trenching, occur as road cuts, or be found naturally such as along channel banks.

Radiocarbon dating involves measuring the amount of the radio isotope $^{14}C$ preserved in organic materials and using the rate of radioactive decay to calculate the age of a sample. This method requires the deposition and preservation of organic materials within the sedimentary stratigraphy of the fan. The age range that this method can assess is from approximately 45,000 years to several decades. As such, the method is applicable to the time scale of post-glacial fan formation in western Canada.

During BGC's field assessment on May 11, 2022 an eroded bank at Daisy Creek was discovered on its right (north) bank, approximately 250 m downstream of Highway 99 (Figure D-7) which served as a section to describe materials and stratigraphy and obtain organic samples in paleosols (ancient soils built up between consecutive debris flows).

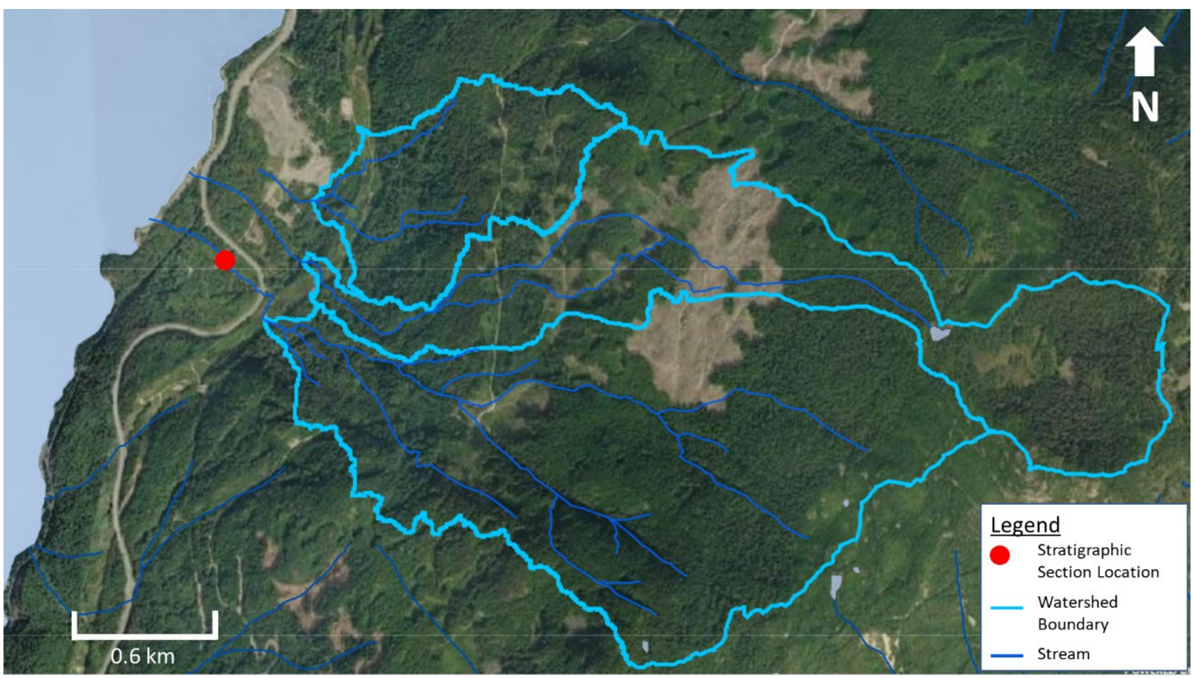


**Figure D-7. Stratigraphic section location. ESRI World Imagery, 2022.**

BGC identified four deposits within the section. The approximate delineations of these layers are shown in Figure D-8.

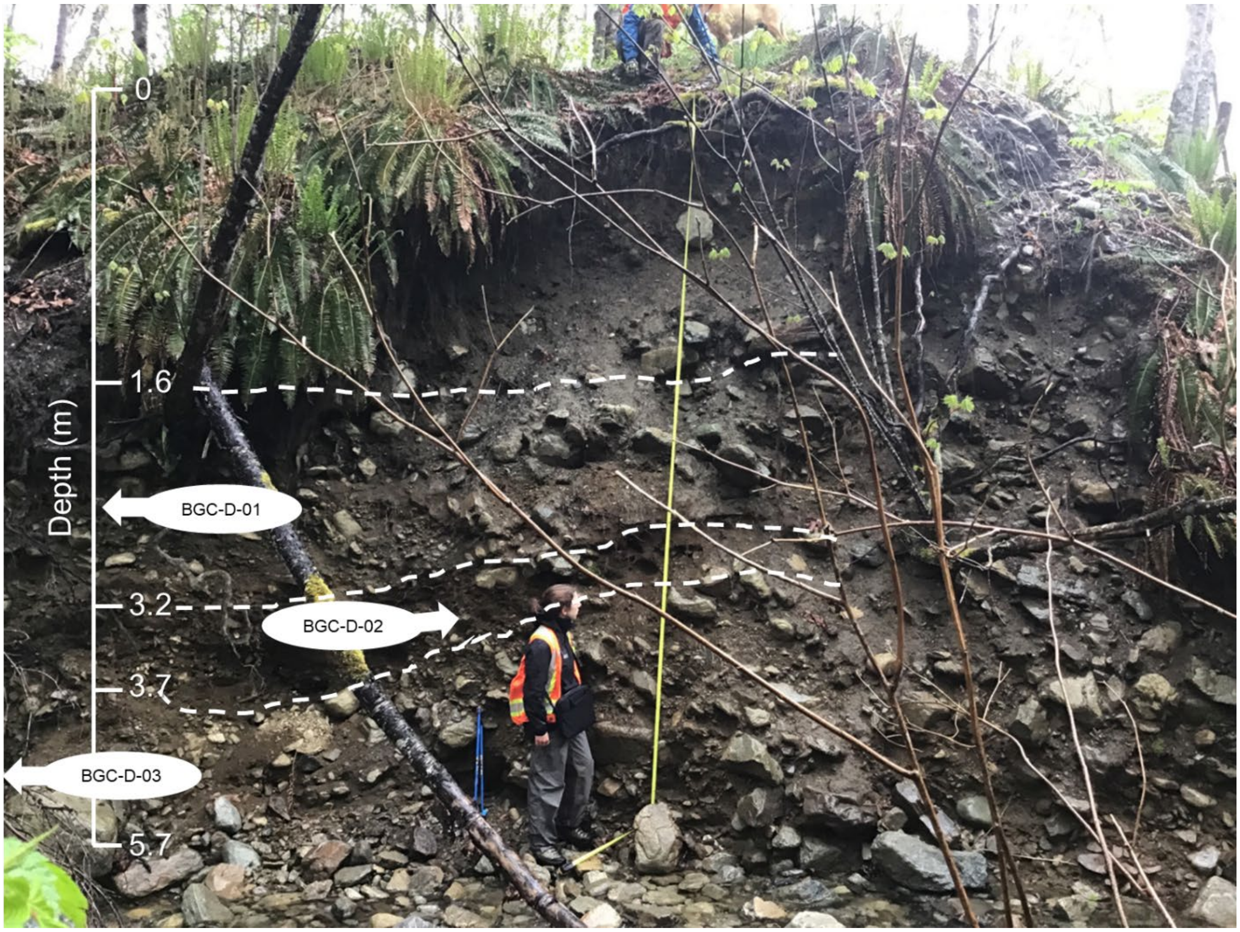


**Figure D-8. Stratigraphic section on the right (north) bank of Daisy Creek, approximately 250 m downstream from Highway 99. The approximate extent of the depositional layers is shown in white, as well as the approximate location of sediment sample collection. BGC photo: May 11, 2022.**

BGC interpreted the lower three deposits (Figure D-8) to be remnants of historical debris flows. BGC collected sediment samples (BGC-D-01, BGC-D-02, and BGC-D-03) from paleosols overlying each of these units. BGC did not sample the uppermost layer as it was likely placed and modified by anthropogenic activity, as judged by the soil texture and size.

The samples were sent to Beta Analytics Testing Laboratory (Miami, Florida) for radiocarbon dating of the organic sediments present. The results are presented in Table D-13, with the full report attached to the end of this appendix.

**Table D-13. Radiocarbon dating results, accurate to within two standard deviations (Beta Analytics Testing Laboratory, June 6, 2022).**

| Sample | Age (Years) | Date Range (Calendar Years) |
|---|---|---|
| BGC-D-01 | 990 – 820 | 1032 - 1202 Common Era (CE) |
| BGC-D-02 | 2063 – 1898 | 41 Before Common Era (BCE) -124 CE |
| BGC-D-03 | 2843 – 2790 | 821 - 768 BCE |

The dates of these past events are well outside of the historical record and BGC did not identify evidence of more recent debris flows reaching the proposed development area from air photos. The level of anthropogenic modification on the fan area within the proposed development limits the potential to collect tree ring samples for dating as the trees have largely been removed or are young second growth that is not amenable to dendrogeomorphological analysis. Collectively, this suggest that debris flows pose a credible hazard to the proposed development; however, the historic frequency of such events is very low.

This analysis is limited to dating of samples collected from a single location and can therefore not be considered representative of the entire fan, as geomorphological activity on the fan varies considerably through time and space.

### D.6.2. Sediment Volume Estimates

Estimating debris-flow sediment volumes is important for two reasons: sediment volumes are an important input to numerical modeling as larger debris flows will travel further, have thicker flow depth and are more destructive; and any mitigation measures that contain debris need to be based on estimates of debris volumes for different return periods so that such measures can be sized appropriately.

BGC employed a method ensemble consisting of four independent semi-empirical techniques to estimate debris-flow sediment volumes for baseline (unburned) conditions on Daisy Creek:

- An empirical method relating fan area to debris-flow F-M
- An empirical method relating the channel recharge rate to sediment volume
- An empirical method that develops a scaled F-M relationship based on an analogue watershed (Charles Creek)
- An estimate of total volumes based on channel yield estimates collected during the June 8, 2022 field traverse.

This ensemble of methods is supplemented with analysis of post-wildfire debris flows (Section D.6.2.5). All analyses consider climate change impacts to the end of the century (2100). As BGC does not have equal confidence in all techniques, a confidence level was assigned a corresponding weighted average used to generate the best estimate. The results are summarized in Table D-14 and shown graphically in Figure D-9. The following subsections describe the methods applied for each technique.

**Table D-14. Model ensemble to estimate sediment volumes under baseline (unburned) conditions per representative return period at Daisy Creek.**

| Representative Return Period (years) | Model Ensemble for Sediment Volume ($m^3$) | | | | Best Estimate |
|---|---|---|---|---|---|
| | Regional (Jakob et al., 2020) | Channel recharge (Jakob et al., 2005) | Charles Creek Analogue (Jakob & Nolde, 2022) | Yield Rate | |
| Confidence | Low | Low-Medium | Medium-High | Medium | Weighted Average |
| Rationale | Uncertainty about fan delineation | Few data points on which equations are based | Charles Ck. may be bordering on supply-unlimited | Debris thickness is estimated, not measured | |
| Weighting Factor | 1 | 1.5 | 2.5 | 2 | |
| 20 | 0 | 0 | 0 | 0 | 0 |
| 50 | 1,000 | 1,000 | 2,000 | 0 | 1,000 |
| 200 | 11,000 | 5,000 | 8,000 | 9,000 | 8,000 |
| 500 | 23,000 | 7,000 | 13,000 | 13,000 | 13,000 |
| 2500 | 38,000 | 8,000 | 18,000 | 21,000 | 20,000 |
| 5000 | 49,000 | 9,000 | 22,000 | 24,000 | 24,000 |

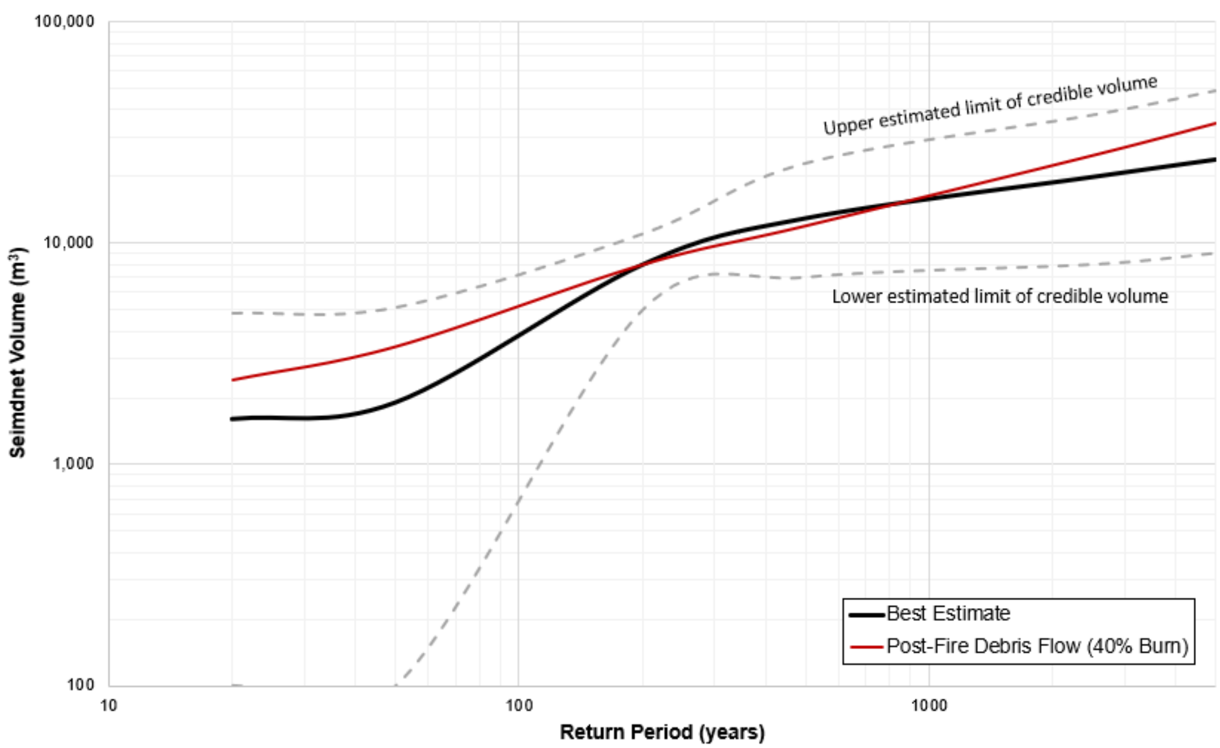


**Figure D-9. Frequency-magnitude relationships derived from methods used for the Daisy Creek debris-flow model ensemble.**

### D.6.2.1. Regional Fan Debris-Flow Frequency-Magnitude Analysis

This method is outlined in Section D.5.3.1 for application to debris floods. The same methodology is applicable to debris flows, when appropriate comparative creeks are selected (e.g., Figure D-10) to develop a predictive equation. Equation D-3 is the predictive equation developed and applied by BGC for Daisy Creek.

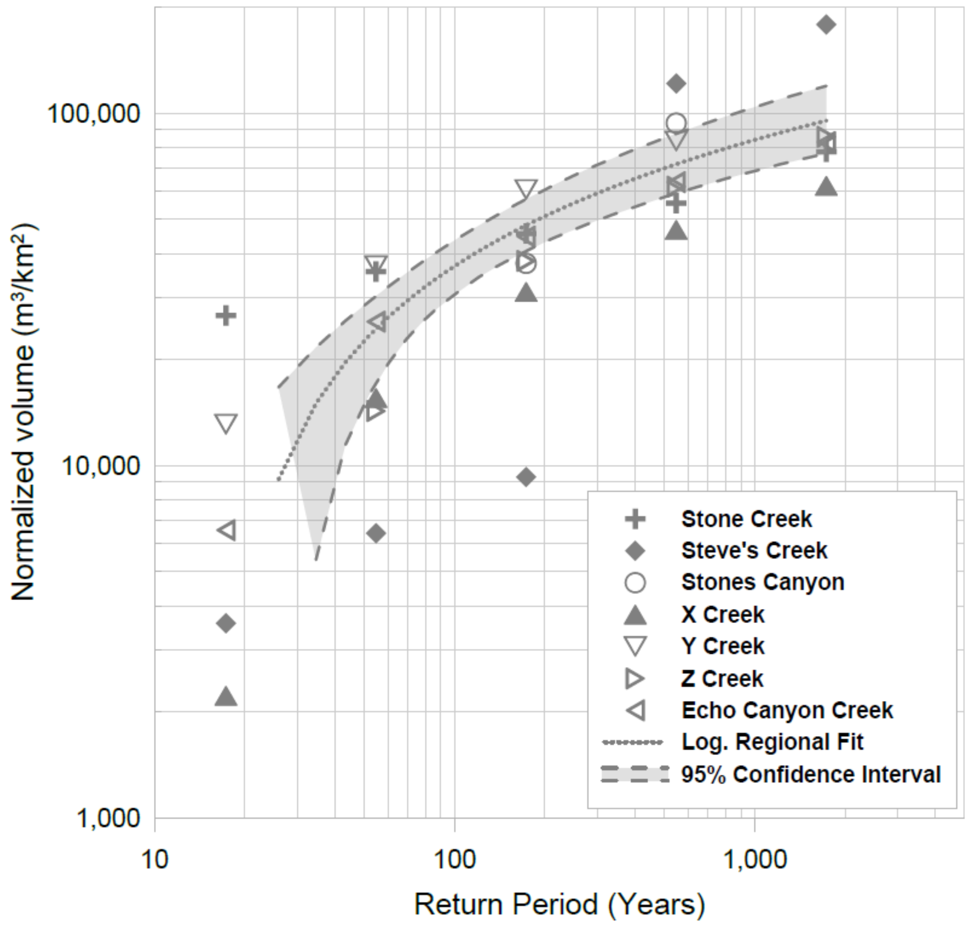


**Figure D-10. Regional debris flow frequency-magnitude data normalized by fan area for seven detailed studies in the Bow Valley, AB. From Jakob et al. (2020).**

### D.6.2.2. Channel Recharge

Jakob et al. (2005) developed a relationship to estimate debris-flow sediment volume based on the time elapsed since the last debris flow ($t_e$) and a normalized channel recharge rate ($R_t$) (Equation D-12).

$$R_t = 0.23t_e^{-0.58} \qquad \text{[Eq. D-12]}$$

By multiplying the recharge rate by channel length, a total sediment volume for in-channel entrainment is developed. On Daisy Creek, the most recent evidence of debris flows observed by BGC was the tree-ring sample from the impacted tree on the north channel at 104 years ago (Table D-12). For simplicity, BGC used a time elapsed ($t_e$) of 100 years.

BGC supplemented this with estimation of point source failures on channel side walls or within the watershed with the potential to contribute to total debris-flow volume. BGC mapped the areal extent of potential source areas using the 2019 lidar. An estimated failure depth[4] of 0.75 m was used to generate estimated point source failure volumes.

To build an F-M relationship for Daisy Creek, BGC applied the logic outlined in Table D-15. This logic considers the nature of the Daisy Creek watershed which is supply-limited, meaning it takes time for the channel to recharge with sediment between consecutive debris flows. As a result, for higher return periods, BGC expects that the in-channel sediment volume will be similar to the 100-year return period sediment volume. Further, since not all point source failures are likely to fail simultaneously for smaller storms, BGC applied a scaling by return period.

**Table D-15. Channel recharge rate assumptions applied at Daisy Creek. These assumptions are based on air photograph interpretation and field observations.**

| Representative Return Period (years) | Channel Recharge Rate Assumptions |
|---|---|
| 20 | No point source failures |
| 50 | No point source failures |
| 200 | 100-year channel recharge volume estimate plus half (1/2) of all reasonably conceivable point source failure volumes. |
| 500 | 100-year channel recharge volume estimate plus 2/3 of all point source failure volumes. |
| 2,500 | 100-year channel recharge volume estimate plus all point source failure volumes. |
| 5,000 | 100-year channel recharge volume estimate plus all point source failure volumes. |

### D.6.2.3. Charles Creek Analogue

Jakob (1996) developed a method to predict debris-flow sediment volumes using geomorphic indicators (watershed relief, active contributing area) for creek analogues. At Daisy Creek, BGC leveraged a well-studied watershed, Charles Creek, located approximately 20 km south of Daisy Creek, as the analogue. Charles Creek is a reasonable proxy to Daisy Creek given the close geographic location, similar site geology, and the fact that they are both supply-limited watersheds, although Charles Creek has substantially more sediment stored in the form of talus slopes. This implies that while not entirely supply-unlimited, renewed debris-flow activity is likely even shortly after debris flows occurred.

On Charles Creek a detailed database of debris-flow events from 1969 (53-year record) exists. Using these events, BGC developed a cumulative magnitude-frequency curve (CMF) using the statistical methods outlined in Jakob (2012) and Jakob and Nolde (2022). BGC then used the

[4] BGC considers 0.75 m depth to be characteristic of till veneers over bedrock within southern BC.

computed scaling factor to adjust the Charles Creek CMF to Daisy Creek using the following methodology:

1. Map out the area actively contributing debris $(A_C)$ in both watersheds. This includes both the creek channels and tributaries and slopes that actively contribute debris to the system. BGC mapped the active sediment contribution area for each watershed using a lidar-derived DEM.
2. Calculate the proportion of watershed actively contributing debris $(A_{\%})$ using the active area and total watershed area for each creek.
3. Measure to the total watershed relief $(Z_T)$ for each creek.
4. Calculate the average debris-flow magnitude $(V)$ using Equation D-13 (Bovis & Jakob, 1999) for each creek.

$$\log V = 0.48 + 2.00Z_T + 0.10A_{\%} \quad \text{[Eq. D-13]}$$

5. Calculate a ratio (scaling factor) of the *V* for each creek.

BGC multiplied the Charles Creek CMF by the scaling factor to develop a CMF relationship for Daisy Creek. After plotting the Daisy Creek CMF, BGC fit a logarithmic curve-fit trendline which was used to determine the sediment volume for the representative return periods of interest.

#### D.6.2.4. Yield Rate

BGC estimated the average yield rate (amount of sediment per meter of channel) during the Daisy Creek channel hike on June 7, 2022. During this hike, BGC recorded a range of available sediment volumes for representative channel reaches from the fan apex to the top of the 2016 cutblock (Figure 2-3 in the main body of the report). BGC estimated channel yield from the top of the cutblock to the channel headwaters based on lidar, field observations, and informed judgement from previous studies on dozens of similar creeks. BGC also measured channel reach slopes using the lidar-derived DEM. All reaches with slopes ≤ 15° were identified as mostly depositional and were not included in the total sediment volume estimates. The resultant sediment volumes are summarized in Table D-16.

**Table D-16. Summary of channel yield rate estimates on Daisy Creek.**

| Channel | Sediment Volume ($m^3$) | |
|---|---|---|
| | Range | Best Estimate |
| Main Channel (fan apex to confluence downstream of logging road) and north channel (upstream of logging road) | 7,500 - 22,500 | 15,000 |
| South channel (upstream of logging road) | 5,000 - 19,000 | 12,000 |
| **Total** | **12,500 - 41,500** | **27,000** |

Notes:

1. Sediment volumes rounded to nearest 500 $m^3$.

As was done with the channel recharge method (Section D.6.2.2), BGC employed assumptions to apply the channel yield estimate to develop an F-M relationship (Table D-17).

**Table D-17. Channel yield rate assumptions applied at Daisy Creek.**

| Representative Return Period (years) | Channel Recharge Rate Assumptions |
|---|---|
| 20 | No debris flows. |
| 50 | Debris flow initiates on north channel, deposits in depositional reaches upstream of the fan apex. |
| 200 | Debris flow initiates on north channel, plus half of all reasonably conceivable point source failure volumes. Half of the total volume deposits in the depositional reaches upstream of the fan apex. |
| 500 | Debris flow initiates on north channel plus 2/3 of all point source failure volumes. One third (1/3) of the total volume deposits in the depositional reaches upstream of the fan apex. |
| 2,500 | Debris flows initiate on both channels and all point sources fail. One third (1/3) of the total volume deposits in the depositional reaches upstream of the fan apex. |
| 5,000 | Debris flows initiate on both channels and all point sources fail. One quarter (1/4) of the total volume deposits in the depositional reaches upstream of the fan apex. |

### D.6.2.5. Post-wildfire (climate-change adjusted)

BGC estimated post-wildfire debris-flow volumes for Daisy Creek using an empirical model developed to predict post-wildfire debris-flow volumes in in southern California and calibrated to British Columbia with an adjustment factor developed for fires near Lytton, BC.

Climate-adjusted IDF curves for rainfall intensity and burn probability modeling were used in this empirical model to predict fire frequency and calculate the probability of debris-flow occurrence in the 2 years following a fire, which is when slopes are generally most susceptible to post-wildfire effects (Cannon and Gartner, 2005; Staley et al., 2020; De Graff et at., 2015). Estimated post-fire debris-flow volumes consider multiple burn scenarios that affect different proportions of the watershed.

Empirical models for predicting post-wildfire debris-flow volumes (e.g., Cannon et al., 2010; Gartner et al., 2014) can be used to assess hazards posed by debris flows following wildfires. The Gartner et al. (2014) model employed in this study is used by the United States Geological Survey (USGS) for emergency assessments of post-wildfire debris-flow hazards. The model is applicable for up to two years following a wildfire, after which plant re-growth and/or source area sediment depletion render it less reliable. The inputs for the model include:

- The contributing watershed area burned at moderate- and high severity
- The relief of the contributing watershed area
- The storm rainfall intensity measured over a 15-minute duration.

The Gartner et al. (2014) model was developed using data from southern California and has not been tested in southern British Columbia (B.C.). To evaluate the applicability of the model in southern B.C., BGC compared predicted post-wildfire volumes to volumes of previously recorded post-wildfire debris flows near Creston, B.C. (Jordan, 2015) and to the Lytton Creek Fire area in 2021. These comparisons illustrated that the Gartner et al. (2014) model overpredicts debris flow volumes in BC by a factor of 2 to 5. As a result, on Daisy Creek, BGC used scaling factors of 2 to 4 to generate a range of predicted sediment volumes.

Currently, IDF curves are developed with historical data assuming that the same processes will determine future rainfall patterns and generate similar IDF curves. This assumption is not valid under changing climate conditions. Therefore, BGC used a climate-adjusted IDF for this assessment to provide a better representation of expected storm intensities to the end of century (2100). These data were retrieved using the web-based IDF_CC Tool version 6.0, developed by the University of Western Ontario (Simonovic et al., 2015). The tool combines historical data based on observed precipitation with global circulation models (GCMs) for future scenarios. The Squamish Airport station (ECCC station 10476F0) was selected, which is the closest weather station to the study area with at least 10 years of data, considered to be the minimum number of years of record to generate IDF curves.

A time period of 2060 to 2100 and the PCIC – Bias Corrected (CMIP6) – All models (averaged) were selected to generate the IDF. The SSP5.85 scenario[5] was used, which applies a radiative forcing of 8.5 W/m$^2$ by the year 2100 and represents the upper boundary of the range of scenarios currently described in the literature. The rainfall intensity values for the selected model are shown in Table D-3. BGC used the 15-minute rainfall intensity values in Table D-18 in the Gartner et al. (2014) model. Of note is that the 24-hour rainfall intensities of Table D-18 are very similar to the climate-change adjusted values calculated by BGC (i.e., Table D-4).

[5] SSP stands for Shared Socio-economic Pathways. SSP5.85 represents the high end of the range of future pathways, corresponding to RCP8.5.

**Table D-18. Precipitation intensity rates (mm/hr) for different return periods (2 years to 50 years) and at different durations (5 min to 24 hours) under a radiative climate forcing of 8.5 W/m$^2$). Values are generated from the IDF_CC Tool (Simonovic et al., 2015).**

| Rainfall Duration | Return Period (years) | | | | | |
|---|---|---|---|---|---|---|
| | 2 | 5 | 10 | 20 | 25 | 50 |
| 5 min | 31 | 53 | 74 | 101 | 110 | 149 |
| 10 min | 24 | 37 | 50 | 65 | 71 | 93 |
| 15 min | 21 | 31 | 39 | 49 | 53 | 66 |
| 30 min | 17 | 22 | 26 | 30 | 32 | 37 |
| 1 h | 14 | 18 | 20 | 23 | 24 | 29 |
| 2 h | 12 | 15 | 17 | 19 | 19 | 22 |
| 6 h | 9 | 11 | 13 | 15 | 15 | 17 |
| 12 h | 8 | 10 | 11 | 12 | 13 | 14 |
| 24 h | 6 | 8 | 9 | 10 | 10 | 11 |

Notes:

1. Rainfall intensity values rounded up to the nearest 1 mm.

The wildfire frequency in the watershed is also needed to estimate probabilities of post-fire debris-flow occurrence in the 2 years following a fire, when burned basins are most sensitive to post-wildfire effects. BGC used provincial burn probability mapping from the BC Wildfire Service. The mapping is based on the Burn-P3 simulation model developed based on observed historical databases by Parisien et al. (2005) for Canada Wildfire. The probability of burn in the Daisy Creek watershed is mapped as 0.3% for 2050-2100. BGC then applied the following equation to determine the combined probability of debris-flow occurrence in the 2 years post-fire.

$$P_C = 1 - \left(1 - \frac{1}{T}\right)^n * P_B \qquad \text{[Eq. D-14]}$$

where $P_C$ is the combined probability, T is the desired return period, n is the number of years to assess (in this case, 2 years), and $P_B$ is the burn probability (in this case, 0.003). The inverse of the combined probability provides the post-fire debris-flow return period. Different burn proportions (e.g., 20%, 40%, and 60% of total watershed area burned to moderate to high severity) were then applied to the Gartner et al. (2014) volume model as a sensitivity study (given that burn area is unpredictable) to estimate sediment volumes. Using a power-law relationship fit to the derived data, BGC calculated the post-fire debris-flow volumes under climate change conditions. The results are shown graphically in Figure D-11 and summarized in Table D-19. BGC selected a 40% watershed burned area to represent the best-estimate of post-fire debris-flow volumes at Daisy Creek.

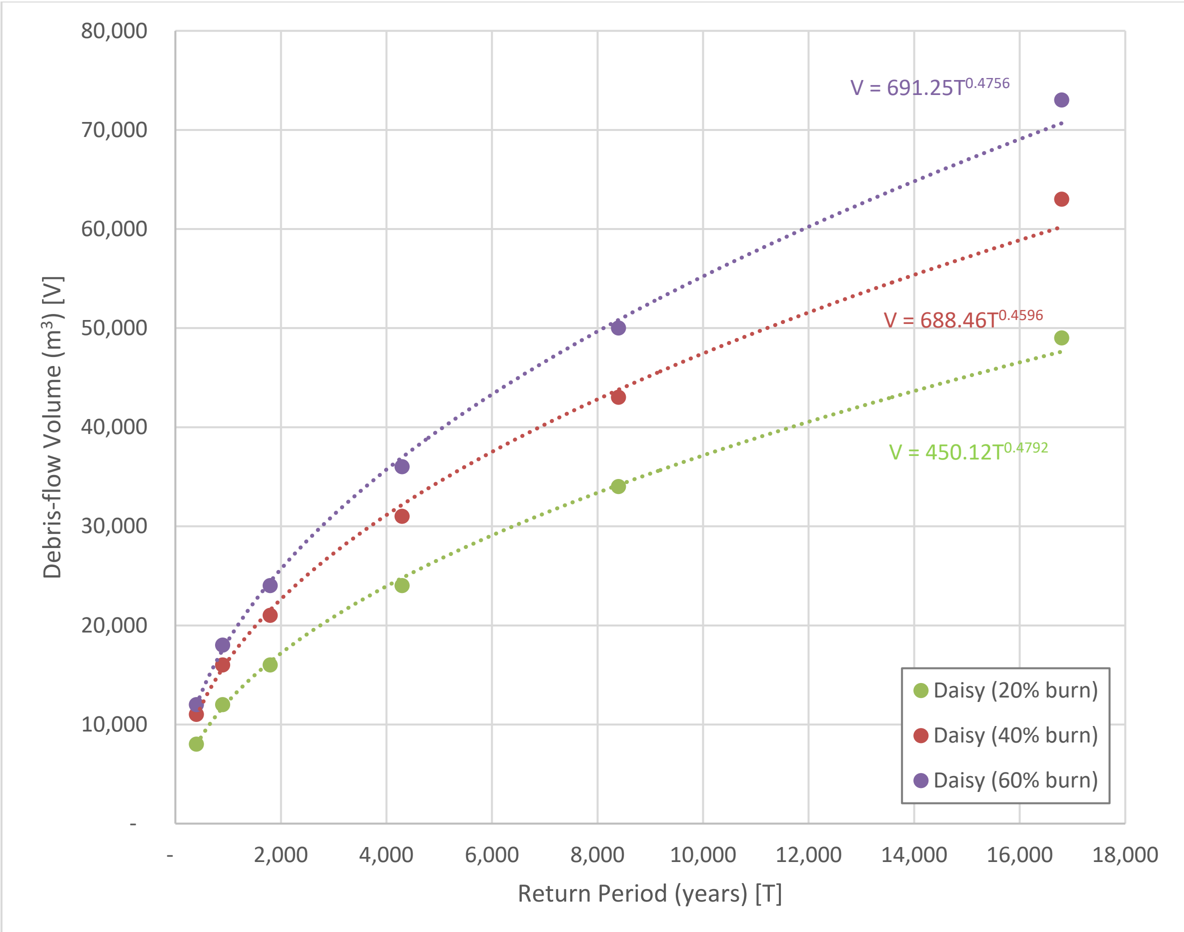


**Figure D-11. Relationship between post-fire debris-flow volume and fire-adjusted return period given probability of occurrence in the next 2 years, under climate change conditions. Different burn scenarios are provided for varying proportion of watershed burned to a moderate to high severity (20% to 60%).**

**Table D-19. Post-fire debris-flow volume and fire-adjusted return period given probability of occurrence in the next 2 years. Values are calculated under climate change conditions for different burn scenarios of proportion of watershed burned to a moderate to high severity.**

| Return Period (years) | Post-fire Debris-flow Volume ($m^3$) | | |
|---|---|---|---|
| | 20% burn | 40% burn | 60% burn |
| 20 | 2,000 | 3,000 | 3,000 |
| 50 | 3,000 | 4,000 | 4,000 |
| 200 | 6,000 | 8,000 | 9,000 |
| 500 | 9,000 | 12,000 | 13,000 |
| 2,500 | 19,000 | 25,000 | 29,000 |
| 5,000 | 27,000 | 35,000 | 40,000 |

### D.6.3. Peak Discharge Estimates

#### D.6.3.1. Debris-Flow Peak Discharge

Debris-flow peak discharge was reconstituted using empirical relationships that relate the estimated debris-flow volumes to peak discharges for the same event (Bovis & Jakob, 1999; Mizuyama et al., 1992).

Bovis and Jakob (1999) provide empirical correlations between peak discharge and debris-flow volume based on observations of 33 debris flow basins in southwestern British Columbia (Figure D-12). Mizuyama et al. (1992) similarly provide empirical correlations based on observations on creeks in Japan and Alberta. These relationships were constructed for “muddy” debris flows and “granular” debris flows. Muddy debris flows are those with a relatively fine-grained matrix as found from volcanic source areas or fine-grained sedimentary rocks, while granular debris flows are those typical for granitic source areas with large clasts embedded in the flow which slow the flow through friction thus creating large surge fronts.

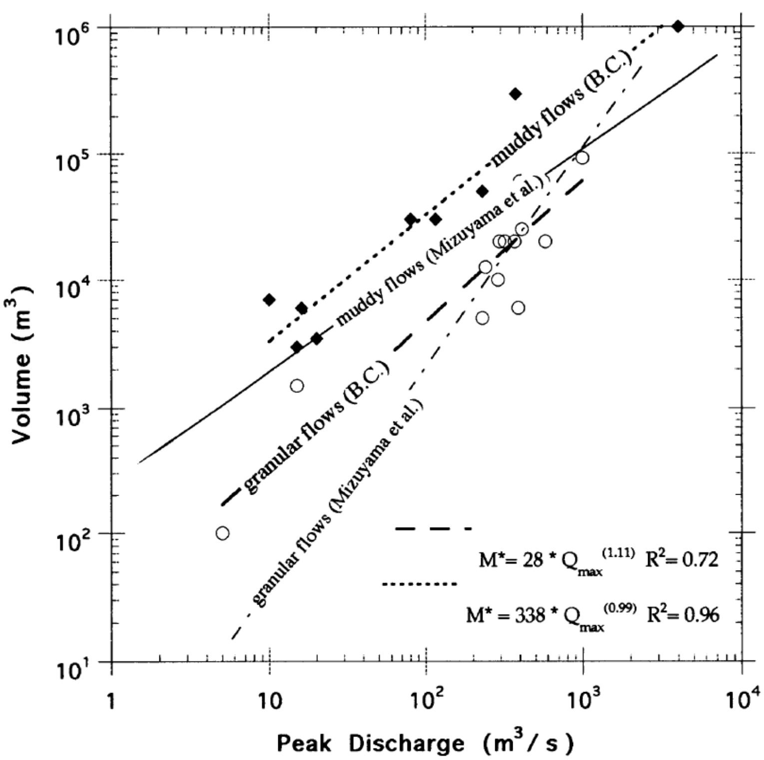


**Figure D-12. Bovis and Jakob (1999) relationship between peak discharge and volume for British Columbia, with comparison regressions computed by Mizuyama et al. (1992).**

Debris flows on Daisy Creek are derived from competent, quartz-dioritic intrusive rocks (Bellefontaine et al., 1994) and therefore BGC selected to use the relationships for granular flows (Equations D-15, D-16)

$$Q_{granular\ (Bovis\,\&\,Jakob)} = 0.105 \cdot (V)^{0.83} \qquad \text{[Eq. D-15]}$$

$$Q_{granular\ (Mizuyama\ et\ al.)} = 0.135 \cdot (V)^{0.78} \qquad \text{[Eq. D-16]}$$

BGC averaged the peak discharge derived from Bovis & Jakob (1999) and Mizuyama et al. (1992) for the best estimate of peak discharge for the representative return periods considered on Daisy Creek, as summarized in Table D-20. Peak discharge and total debris-flow volume were then input to the numerical modelling together with rheological parameters as outlined in Appendix E.

**Table D-20. Best estimate of debris-flow peak discharge and sediment volume on Daisy Creek to the end of the century (2100).**

| Representative Return Period (years) | Baseline | | Post-Wildfire | |
|---|---|---|---|---|
| | Sediment Volume (m³) | Peak Discharge (m³/s) | Sediment Volume (m³) | Peak Discharge (m³/s) |
| 20 | - | - | 2,400 | 80 |
| 50 | 400 | 10 | 3,400 | 100 |
| 200 | 8,000 | 170 | 8,000 | 170 |
| 500 | 13,000 | 250 | 12,000 | 230 |
| 2,500 | 20,000 | 350 | 25,000 | 420 |
| 5,000 | 24,000 | 410 | 35,000 | 550 |

# APPENDIX E
# NUMERICAL MODELLING

## E.1. INTRODUCTION

Numerical modeling is a fundamental step in steep creek hazard and risk assessments. It uses computer models to simulate a fluid that approximates the potential real debris-floods and debris-flows. This allows designation of hazard zones (Appendix F) and will guide eventual mitigation efforts. This appendix describes the software package and methodology applied for the numerical modelling of steep creek hazards on Daisy, Thistle, and Gravel creeks.

## E.2. SOFTWARE DESCRIPTION

BGC used the readily available HEC-RAS software developed by the US Army Corps of Engineers (Version 6.2) for modelling. The HEC-RAS software for two-dimensional (2D) modelling uses an irregular mesh to simulate the flow of water over terrain. Irregular meshes are useful for development of numerically efficient 2D models to allow refinement of the model in locations where the flow is changing rapidly and/or where additional resolution is desired. With 2D models, the objective is to define a model with sufficient accuracy and resolution, but at the same time minimize model runtime.

HEC-RAS uses lidar-generated topography as an input. Additional processing is sometimes needed to digitally remove bridge decks and ensure the existing channel profile is maintained under bridges. Similarly, HEC-RAS allows integration of culverts to the model domain. Digital elevation models (DEM) derived from the lidar only capture the water surface. In shallow debris-flood prone creeks, the need for bathymetry not accounted by the lidar dataset is likely negligible. In lakes and larger mainstem rivers, the terrain should be modified to include estimated bathymetry at the downstream boundary (lake, river, ocean, reservoir). In these cases, the model domain can be extended approximately 500 m past the shoreline to ensure that the boundary condition does not affect the discharge on the fan.

The default cell geometries created by HEC-RAS are rectangular but other geometries can be developed to transition between different refinement areas (varying cell size or breaklines). Within HEC-RAS, a 2D mesh is generated based on the following inputs:

- The model perimeter (the model domain or extent of the model).
- Refinement areas to define sub-domains where the mesh properties (e.g., mesh resolution) are adjusted.
- Breaklines to align the mesh with terrain features which influence the flow such as dikes, stream channel banks, roadways, terraces, and embankments. HEC-RAS provides options to adjust the mesh resolution along breaklines, if the modeler chooses.

From these inputs, HEC-RAS generates a mesh consisting of computational points at the cell centroid and the faces of the cells. The mesh then needs to be cleaned and checked for errors such as a cell having more than 8 faces and large cells in the mesh that may be created when the breaklines are enforced. The general mesh for each site is developed with a site-specific grid size and additional breaklines refine spatial discretization to capture important topographic features, such as the stream channel banks, roadways, and other infrastructure. Refinement areas are used with a higher resolution grid along the stream channels, avulsion paths, and in areas of overland flooding to provide adequate model resolution and detail.

HEC-RAS includes modelling capabilities for Newtonian (clearwater floods, debris floods) and non-Newtonian (debris flows) fluids. Non-Newtonian fluids are those whose viscosity changes when force is exerted on the fluid making it more liquid or more solid. Ketchup or mayonnaise are examples of non-Newtonian fluids. The capability to model all steep creek process types in the study area was a main driver to select HEC-RAS as the modelling package for this assessment.

## E.3. MODEL SCENARIOS

The first step in numerical modelling is to define hazard scenarios for the representative return periods considered in the assessment. The following subsections outline the hazard scenarios selected for the study creeks. As the results of the numerical modelling will subsequently be integrated into a risk assessment, a conditional probability is assigned to each hazard scenario. When there is only one hazard scenario at a given return period, it has a conditional probability of 100%. When there are multiple hazard scenarios for a given return period, the total of the conditional probabilities of all the scenarios must sum to 100%. The respective conditional probabilities are based partially on analysis knowing the capacity of culverts and comparing those to the estimated peak flows for the different hazard scenarios, and partially on judgment. The latter is based on the team’s experience in similar projects where detailed post-event forensics demonstrated how mitigation works functioned or how culverts performed, for example, in creeks with significant wood loading. Slight changes in conditional probabilities are unlikely to affect the principal risk assessment results.

### E.3.1. Thistle Creek and Gravel Creek

Thistle and Gravel creeks are adjacent to one another and BGC classified them both as flood and debris flood prone. BGC modelled these two creeks in the same model domain with individual inflow conditions for each creek. Modelled floods and debris floods were used to gain an understanding of potential depths, velocities, and inundated areas from Thistle and Gravel creeks.

Six scenarios were modelled as outlined in Table E-1.

**Table E-1. Thistle- and Gravel creek model scenarios.**

| Representative Return Period (years) | Process | Scenario Description | Conditional Probability (%) |
|---|---|---|---|
| 20 | Flood | Thistle box culvert below Highway 99 clear, all other Highway 99 culverts blocked. Road crossing through proposed development clear. | 100 |
| 50 | Thistle: Debris Flood<br>Gravel: Flood | Thistle box culvert below Highway 99 clear, all other Highway 99 culverts blocked. Road crossing through proposed development clear. | 100 |
| 200 | Debris Flood | Thistle box culvert below Highway 99 clear, all other Highway 99 culverts blocked. Road crossing through proposed development clear. | 100 |
| 500 | Debris Flood | Thistle box culvert below Highway 99 clear, all other Highway 99 culverts blocked. Road crossing through proposed development clear. | 100 |
| 2,500 | Debris Flood | Thistle box culvert below Highway 99 clear, all other Highway 99 culverts blocked. Road crossing through proposed development clear. | 80 |
| | | All culverts blocked. | 20 |

Notes:

1. The culverts below Highway 99 all have small diameters (≤ 30 cm) with the exception of the main Thistle Creek culvert. BGC assumed that the smaller culverts would block during a flood or debris-flood event.
2. BGC assumed that the road crossing Thistle and Gravel creeks through the proposed development would be designed with sufficient capacity to convey the peak discharges associated with flood and debris-flood events on these creeks and was left clear in the modelling. BGC did not increase the channel size through the crossings, only left the channel open (i.e., did not include bridge deck or culvert).

### E.3.2. Daisy Creek

BGC modelled Daisy Creek independently of Thistle and Gravel creeks, as it is susceptible to debris-floods and debris-flows and events on Daisy Creek are expected to have limited interaction with Thistle or Gravel creeks. BGC used a two-phase model to simulate the coarse front and muddy afterflow characteristic of debris flows (Appendix C) as described in Section 1.2. Modelled debris floods and debris flows were used to gain an understanding of potential depths, velocities, and areas potentially inundated by Daisy Creek.

Thirteen scenarios were modelled as outlined in Table E-2.

**Table E-2. Daisy Creek model scenarios.**

| Return Period (years) | Process | Scenario Description | Conditional Probability (%) |
|---|---|---|---|
| 20 | Debris Flood | All culverts clear and function as intended. | 60 |
| | | Debris basin overflow, Highway 99 culvert clear, others blocked. | 40 |
| | Debris Flow | ***Post-Wildfire Conditions:*** *Not modelled as debris basin has sufficient capacity and peak discharge of both coarse front and muddy after flow is lower than bulked debris flood.* | N/A |
| 50 | Debris Flow | ***Baseline Conditions:*** *Not modelled. Majority of sediment expected to be deposited upstream of basin.* | 30 |
| | | **Post-Wildfire Conditions:** All culverts clear and function as intended. | 10 |
| | Debris Flood | All culverts clear and function as intended. | 20 |
| | | Debris basin overflow, Highway 99 culvert clear, others blocked. | 40 |
| 200 (1) | Debris Flow | **Baseline, Post-Wildfire Conditions**: All culverts clear and function as intended. | 50 |
| | | **Baseline, Post-Wildfire Conditions:** Debris basin outlet main culvert blocks. Railway culvert blocks. Basin overflow, Hwy 99 culverts clear and function as intended. | 50 |
| 500 (1,2) | Debris Flow | **Baseline, Post-Wildfire Conditions:** Debris basin outlet main culvert blocks. Railway culvert blocks. Basin overflow, Hwy 99 culverts clear and function as intended. | 40 |
| | | **Baseline, Post-Wildfire Conditions:** All culverts block. | 60 |
| 2,500 | Debris Flow | **Baseline Conditions:** All culverts block. | 50 |
| | | **Post-Wildfire Conditions:** All culverts block. | 50 |
| 5,000 | Debris Flow | **Baseline Conditions**: All culverts block. | 50 |
| | | **Post-Wildfire Conditions:** All culverts block. | 50 |

Notes:

1. For the 200-year and 500-year, the debris-flow baseline and post-wildfire conditions are modelled as a single scenario as they have the same, or very similar, sediment volumes and peak discharges.
2. The coarse front is expected to block both debris basin culverts, so the debris basin culverts are blocked for the muddy after flow.
3. All scenarios assume that the crossing infrastructure in development is sufficiently sized to convey flow within the channel. BGC did not modify the channel dimensions, only left the channel open (i.e., did not add a bridge deck or culvert).

## E.4. MODEL SELECTION AND MODIFICATION

### E.4.1. Floods

BGC modelled floods with the clear-water hydrographs developed using HEC HMS modelling (Appendix D). These events were modelled using Newtonian conditions over the full duration of the hydrographs.

### E.4.2. Debris Floods

BGC modelled debris floods using hydrographs developed in HEC HMS modelling that were bulked to account for the increased sediment concentration associate with debris floods (Appendix D). These events were modelled using Newtonian conditions over the full duration of the hydrographs (Thistle and Gravel creeks where significant ponding associated with the events is anticipated) or beyond the peak of the hydrograph until steady state was reached (Daisy Creek).

### E.4.3. Debris Flows

Debris flows were modelled using the "Bingham" rheological model, which is parameterized by the dynamic viscosity[1] of the flow and the yield stress[2]. A material's rheology defines how it behaves under stress. Clear water has a linear stress-strain relationship and deforms under any stress that is applied. A "Bingham" fluid also has a linear stress-strain relationship but requires that a certain threshold of stress is applied before the fluid deforms, in other words, it behaves more like warm ketchup than water when flowing downhill.

The model was split to simulate a quasi-two-phase flow. Debris flows are often characterized by a rigid more viscous portion and a more liquid afterflow. The more rigid plug (hereafter referred to as the 'coarse front') consists of large boulders and often trees that slow the flow through frictional resistance. Once that load has been deposited where the channel loses confinement, the more liquid, and often faster afterflow (hereafter referred to as the 'muddy afterflow') overshoots or bypasses the freshly deposited coarse front. This phenomenon is not included in a single rheology model. Multi-rheological models exist but are not yet readily available in a format easily applicable to consulting projects. To model debris flows as realistically as possible, BGC split the model into a more viscous and less viscous flow phase.

The coarse front (the more viscous phase) was modelled based on the frequency – magnitude relationship and associated peak flows discussed in Appendix D. The simulation was ended when the hydrograph was complete, and the deposit of the coarse front was added to the base topography to allow a realistic representation of the obstruction caused by this phase of flow. The muddy afterflow phase was then run over this altered topography until steady state was reached.

[1] Dynamic viscosity is the resistance to movement of one layer of a fluid over another.

[2] A fluid yield stress is a characteristic whereby the material does not flow unless the applied stress exceeds a certain value greater than zero. The yield stress is therefore defined as the stress that must be applied to the sample before it starts to flow.

### E.4.4. Model Geometry

The domain (the area included in the model run) for each model was selected to include the entire fan extent and a fringe of the Pacific Ocean so that debris floods and debris flows can outflow beyond the fan-delta boundaries. In this manner any overland flooding including avulsions are captured within the domain. Detailed topographic data of the channels and floodplain were available from high resolution lidar flown June 18, 2019. This lidar was used to generate a high-resolution digital elevation model (DEM) for the model terrain. It is assumed that water depths in the channels were low, or the channel was dry at the time the lidar was flown and the channel topography was reasonably well-represented without requiring additional survey. Terrain modifications were made as necessary to account for topographic features such as concrete barriers or ditches/berms observed during field work. All bridge decks were removed, as it was assumed that all bridges will be designed to accommodate the modelled events.

The general mesh for each site was developed with a 2 m grid, and additional break lines were used to refine its spatial discretization to capture important topographic features, such as the stream channel, and roadways.

### E.4.5. Model Roughness

The values used for hydraulic roughness in the HEC-RAS 2D models are represented by Manning's roughness coefficients (Manning's *n*). The roughness coefficient defines the frictional resistance of the terrain to flow. Channels, fan surfaces, and roads should be assigned unique Manning's *n* values. These can be estimated using the empirical equations of Jarrett (1984) and Zimmerman (2010), which were developed for steep creeks of varying slopes. Additionally, several authors have proposed that, in mobile-bed rivers, channel adjustment limits Froude numbers from exceeding 1, except for short distances or short periods of time (e.g., Piton, 2019; Jarrett, 1984; Grant, 1997). Creek morphology varies between steep creeks, so unique values for each creek need to be selected to provide defensible results for each location. Appropriate in-channel Manning's *n* values are selected using cross-sections measured along creeks and bed material grain size sampling along with channel slope estimates from lidar. The calculated values can vary along the length of a channel, but a typical Manning's *n* value can be selected for each stream within the range calculated and that maintains a Froude number below 1 (i.e., subcritical flow) along the channel except in particularly steep or constricted sections (e.g., bridges) under 1 in 20-year flood conditions. Floodplain values can be estimated through associating different land cover types with different values of Manning's *n*.

For the channel, Manning's *n* values were estimated using the empirical equations of Jarrett (1984) that were developed for steep creeks of varying slopes. These Manning's n values were tested through a sensitivity analysis (Section E.4.8)

The floodplain values were estimated through associating different land cover types with different values of Manning's n as summarized in Table E-3.

**Table E-3. Assumed Manning's n-values for the Thistle, Gravel and Daisy Creek debris flood and debris-flow modeling.**

| Land Cover Layer | Manning's n |
|---|---|
| Channel | 0.08 |
| Road | 0.011 |
| Railway | 0.07 |
| Riparian | 0.07 |
| Gravel Pit | 0.025 |
| Beach | 0.025 |
| Other | 0.07 |

## E.4.6. Boundary Conditions

For all modelled scenarios, the downstream boundary condition was set to a Stage Hydrograph along Howe Sound. The stage was held steady at -2 m (the approximate water surface elevation at the time the lidar was flown) throughout all simulations.

An upstream boundary condition of inflow hydrographs was applied to each creek.

### E.4.6.1. Inflow Hydrographs

#### E.4.6.1.1 Floods and Debris Floods

Inflow hydrographs for debris-flood modelling on Thistle- Gravel and Daisy creeks were developed through rainfall-runoff modelling using the software HEC HMS, as described in Appendix D.

#### E.4.6.1.2 Debris Flows

The upstream boundary condition to each debris flow model is a flow hydrograph shaped roughly like a triangle with the rising limb of the hydrograph being 1/6 of the total flow hydrograph duration as informed by doctoral thesis research on debris-flow behaviour. The simplified flow hydrographs are bulked and thus include sediment in the flow assuming a constant sediment volumetric concentration (Cv) of approximately 50%, which is typical for debris flows. The triangular flow hydrograph shape and duration is set to transport the estimated volume of sediment/debris associated with each return period peak flow being modelled.

## E.4.7. Rheology Calibration

Ideally, the rheological parameters of the debris flow model would be calibrated and validated with observed events. Because there are no documented debris flows on Daisy Creek, the rheological parameters were calibrated using engineering/geoscientific judgement.

A low gradient (< 15°) reach was noted in the Daisy Creek channel approximately 300 m above the fan apex. Here substantial sediment from previous debris flows had deposited which implies that future debris flows would likely do the same. Hence the rheological model would need to be calibrated to simulate deposition in this reach.

The rheological parameters of the coarse front phase were calibrated by varying first the yield strength and then the dynamic viscosity of the modelled 1 in 200-year event. The yield strength was varied between 100 and 2500 Pa, and the dynamic viscosity was varied between 1 and 500 Pa*s. The rheological parameters of the muddy afterflow phase were calibrated to allow flow across the entire fan reaching Howe Sound, which would be expected for such flow phase. The calibrated rheological input parameters used for modelled debris flows in this assessment are listed in Table E-4.

**Table E-4. Final model rheological parameters following model calibration.**

| Model Phase | Rheological Parameter | Value |
|---|---|---|
| Coarse Front | Yield Stress, $\tau_y$ | 5000 |
| | Dynamic Viscosity, $\mu_m$ | 500 |
| Muddy Afterflow | Yield Stress, $\tau_y$ | 100 |
| | Dynamic Viscosity, $\mu_m$ | 1 |

### E.4.8. Model Sensitivity and Parametrization

Sensitivity modeling consists of identifying the model input parameters that are uncertain (i.e., cannot be directly measured or calculated) to examine the extent to which the parameters affect model outcome. The uncertain parameters of the model include, but are not limited to:

- The roughness coefficient, Manning's n.
- The volume concentration of sediment in the flow over the duration of the hydrograph.
- The rheological parameters: dynamic viscosity and yield stress of the fluid flow.
- The stage (ocean level) set at the downstream boundary condition.

A sensitivity analysis was completed by varying the parameters listed above, and comparing depositional area, depths, and velocities between model variations. Morphological clues and geoscientific reasoning were used to select the most realistic model parameters. The sensitivity parameters and results are presented in Table E-5.

**Table E-5. Model sensitivity.**

| Parameter | Variance | Model Sensitivity | Notes |
|---|---|---|---|
| Manning's roughness coefficient | +/- 20% | Low | The modelled flow area, depth and velocity were largely unaffected by this change, indicating that the model results are not sensitive to the selected roughness coefficient. |
| Volumetric concentration of sediment in flow | +/-25% | Medium | The model was somewhat sensitive to the volumetric concentration of sediment in the flow. Varying the volumetric concentration of sediment from 25% to 75% impacted the velocity, depth, flow area, and deposition volume contained within the debris basin. The volumetric concentration of sediment in flows was left at 50%. |
| Rheology (dynamic viscosity and yield strength) | Credible minimum to credible maximum (reference Section E.4.7) | Medium | The model was also sensitive to the dynamic viscosity and yield stress of the fluid flow, see Section E.4.7. |
| Downstream boundary condition | +1 m | Low | The downstream boundary condition was set to the ocean level at the time the lidar was flown. The level was increased by 1 m to test the sensitivity of the model to the downstream boundary condition, and evaluate the impact of sea level rise on the hazard.<br>This had little impact on the modelled depth, velocity, or flow area. Highway 99 serves as a barrier between the creeks and the ocean. It is therefore not anticipated that sea level rise would influence the model results until the ocean level exceeds the height of the Highway 99 road surface. At the outlet of Thistle and Gravel creeks, Highway 99 is currently approximately 8 m above sea level |

### E.4.9. Model Limitations

The numerical model has several limitations which may create discrepancies between modelled and real events.

- Actual debris-flow rheology and surge sequencing (single vs. multiple surges) cannot be predicted with certainty, as rheology may vary depending on debris-flow triggering (in-channel vs. triggered by a debris avalanche) or grain sizes (high proportion of ash in post-fire debris flows vs. "normal" debris flows).
- There is uncertainty in the precise flow behavior of each modelled scenario as each scenario has the potential for channel aggradation, bank erosion, scour, bridge and/ or channel blockages, highway erosion, and existing fences that could influence the flow path and its impact force. The debris-flow model also does not account for possible debris basin failure.

- The model cannot foresee human response to debris floods or debris flows. For debris flows, due to their short duration, human interference will matter little. By the time heavy machinery arrives at site the event will very likely be over. For debris floods which may occur over the course of many hours, human interference will be important. This may include excavations of existing channels, removing debris underneath bridges, bridge removal or placement of riprap.

### E.4.10. Summary

BGC used a 2D hydrodynamic model that is suited for debris-flood and debris-flow modeling to simulate those processes for the volume classes that have been identified in this study. Debris flows were modelled through a quasi two-phase approach, with a viscous coarse front and a low viscosity muddy afterflow. The model is most sensitive to sediment volume concentration and rheological parameters. BGC is confident that a reasonable representation of possible debris-flood and debris-flow runouts for the different return periods considered has been achieved.

# APPENDIX F
# HAZARD MAPPING

## F.1. INTRODUCTION

A composite hazard map represents the hazard at a site from the aggregate of many hazard scenarios. In other words, for any location in the study area, it describes how often and how intense a debris flood or debris flow could be. The map is drawn using an index called the "impact force probability ($P_{Fi}$)", which combines estimates of hazard intensity and probability of occurrence for various scenarios. The $P_{Fi}$ calculation, assumptions, and limitations are documented in this Appendix. The composite hazard map is provided in Drawing 06. This approach complies with the provincial landslide assessment guidelines provided by Engineers and Geoscientists BC (EGBC) (in press).

## F.2. IMPACT FORCE PROBABILITY CALCULATION

The $P_{Fi}$ is the annual probability of impact forces from geohazards at a given location. It is calculated as a product of the impact force per meter flow width and the respective probability of occurrence and summed for all hazard scenarios considered. The $P_{Fi}$ calculation is completed spatially across the numerical modelling domain resulting in a gridded $P_{Fi}$, which is used to generate a composite hazard map (see Section F.4). The equation used to calculate $P_{Fi}$ at a location $j$ is:

$$P_{Fi,j} = \sum_{i=1}^{n} P(H)_i \times \rho_{i,j} \times {v_{i,j}}^2 \times d_{i,j} \qquad \text{[Eq. F-1]}$$

where $P(H)$ is the annual probability of the scenario (years$^{-1}$), $\rho$ is the fluid density (kg/m$^3$), $v$ is average flow velocity (m/s), and $d$ is the average flow depth (m) for $i$ hazard scenarios considered (Jakob et al., 2022). The $P_{Fi}$ units are in Newtons per metre per year (N/m per year). The equation applies to rapid flow-type landslides such as debris flows and debris floods.

### F.2.1. Intensity

The $v^2 \times d$ term in Eq. F-1 is known as the flow intensity (m$^3$/s$^2$) and has been correlated to building damage (Jakob et al., 2012)Table F-1. The average flow intensity for a given area is estimated spatially across the study area for each hazard scenario with numerical modelling completed for this assessment. Intensity values are estimated from HEC-RAS modelling.

**Table F-1. Hazard intensity descriptions and vulnerability of persons in homes when impacted by debris flows or debris floods. Note flow intensity is not the same as $P_{Fi}$.**

| Flow Intensity ($m^3/s^2$) | Building Damage Potential | Description |
|---|---|---|
| < 1 | Minor | Slow flowing shallow and deep water with little or no debris. High likelihood of water damage. Potentially dangerous to people in buildings, on foot or in vehicles in areas with higher water depths. |
| 1 to 3 | Moderate | Slow flowing shallow and deep flow with minor debris. High likelihood of sedimentation and water damage. Potentially dangerous to people in buildings, on foot or in vehicles in areas with higher water depths. |
| 3 to 10 | Major | Potentially fast flowing but mostly shallow water with debris. High likelihood of building structure damage and high likelihood of major sediment and/or water damage. Potentially dangerous to people on the first floor or in the basement of buildings, on foot or in vehicles. |
| 10 to 30 | Extensive | Fast flowing and deep water and debris. High likelihood of extensive building structure damage and severe sediment and water damage. Very dangerous to people in buildings, on foot or in vehicles. |
| 30 to 100 | Severe | Very fast flowing and deep water and debris. High likelihood of severe building structure damage and sever sediment and water damage. Extremely dangerous to people in buildings, on foot or in vehicles. |
| >100 | Total Destruction | Very fast flowing and deep water and debris. Very high likelihood of total building destruction. Extremely dangerous to people in buildings, on foot or in vehicles |

## F.2.2. Probability

The $P(H)$ term in Eq. F-1 for this assessment is the probability of each assessed return period multiplied by a conditional probability of the scenario occurring. The probability of each return period is calculated as the difference between the probability of the lower bound ($L_i$) and upper ($U_i$) bound return periods:

$$Probability = \frac{1}{L_i} - \frac{1}{U_i} \quad \text{[Eq. F-2]}$$

A conditional probability of a hazard scenario describes the relative likelihood that the specific scenario occurs given a hazard of a certain return period occurs. Conditional probabilities must sum to 1 for each return period. If only one scenario is assessed for a given return period, the conditional probability for that scenario is 1. In this assessment, conditional probabilities are assigned using professional judgement. Probabilities for each modelled scenario are listed in Appendix E.

## F.2.3. Density

For $\rho$ in Eq.F-1, a density of 2,000 kg/m$^3$ was assumed for debris flows, 1,300 kg/m$^3$ for debris floods, and 1,000 kg/m$^3$ for floods (Kwan, 2012).

## F.3. MODELLED SCENARIOS

BGC numerically modelled 13 scenarios at Daisy Creek and 6 scenarios at Thistle and Gravel creeks. The scenarios were selected to represent various return periods, flood processes, burn conditions, and culvert blockages. Details of numerical modelling are provided in Appendix E.

## F.4. INTERPRETED COMPOSITE HAZARD MAP

Interpreted composite hazard polygons were manually drawn for the hazard categories listed in Table F-2 using the gridded $P_{Fi}$ (raw results from the $P_{Fi}$ calculation), topography, and expert judgement. $P_{Fi}$ outputs are further interpreted and smoothed manually into distinct polygons for the purposes of land-use decision making. Composite hazard rating categories are defined in Table F-2.

**Table F-2. Composite hazard rating categories, modified from provincial landslide assessment guidelines provided by EGBC (in press).**

| Composite Hazard Rating | Approximate Range of $P_{Fi}$ (N/m per year) | Hazard and Consequence Description Given Impact to Standard Wood Frame Building |
|---|---|---|
| Very Low | < 1 | Hazard is very rare or of minor intensity and does not constitute a credible life-loss risk but can cause nuisance building damage |
| Low | 1 to 10 | Hazard is rare or of moderate intensity and is unlikely to lead to life loss, but will cause building damage |
| Moderate | 10 to 100 | Hazard likely occurs within a person's lifetime or of substantial intensity and may lead to life loss and considerable building damage |
| High | 100 to 1,000 | Hazard occurs frequently and/or with very high intensity and is likely to lead to life loss and requires building reconstruction |
| Very High | >10,000 | Hazard occurs frequently and/or with extreme intensity and is very likely to lead to life loss and total building destruction |

## F.5. LIMITATIONS

The composite hazard map is based on BGC's current understanding of steep creek hazards and topography at the site. The map should be reviewed periodically and revised if a potential change in the hazard is suspected, when new information emerges or changed conditions are observed. New information could be related to the magnitude and frequency of steep creek hazards and flow mobility and behaviour. Changed conditions could include, but are not limited to, vegetation removal in the watershed, forest fire, large slope instability, mitigation works, or changes to topographic features on the fan.

Hazard polygons are interpreted from raw modelling results using the $P_{Fi}$ calculation. The composite hazard map does not provide information on the frequency of debris floods or debris flows at specific locations, nor does it allow interpretation of site-specific impact forces. This information, if required, can be determined from the numerical modelling results for specific hazard scenarios.

# PHOTOGRAPHS

DECEMBER 2022

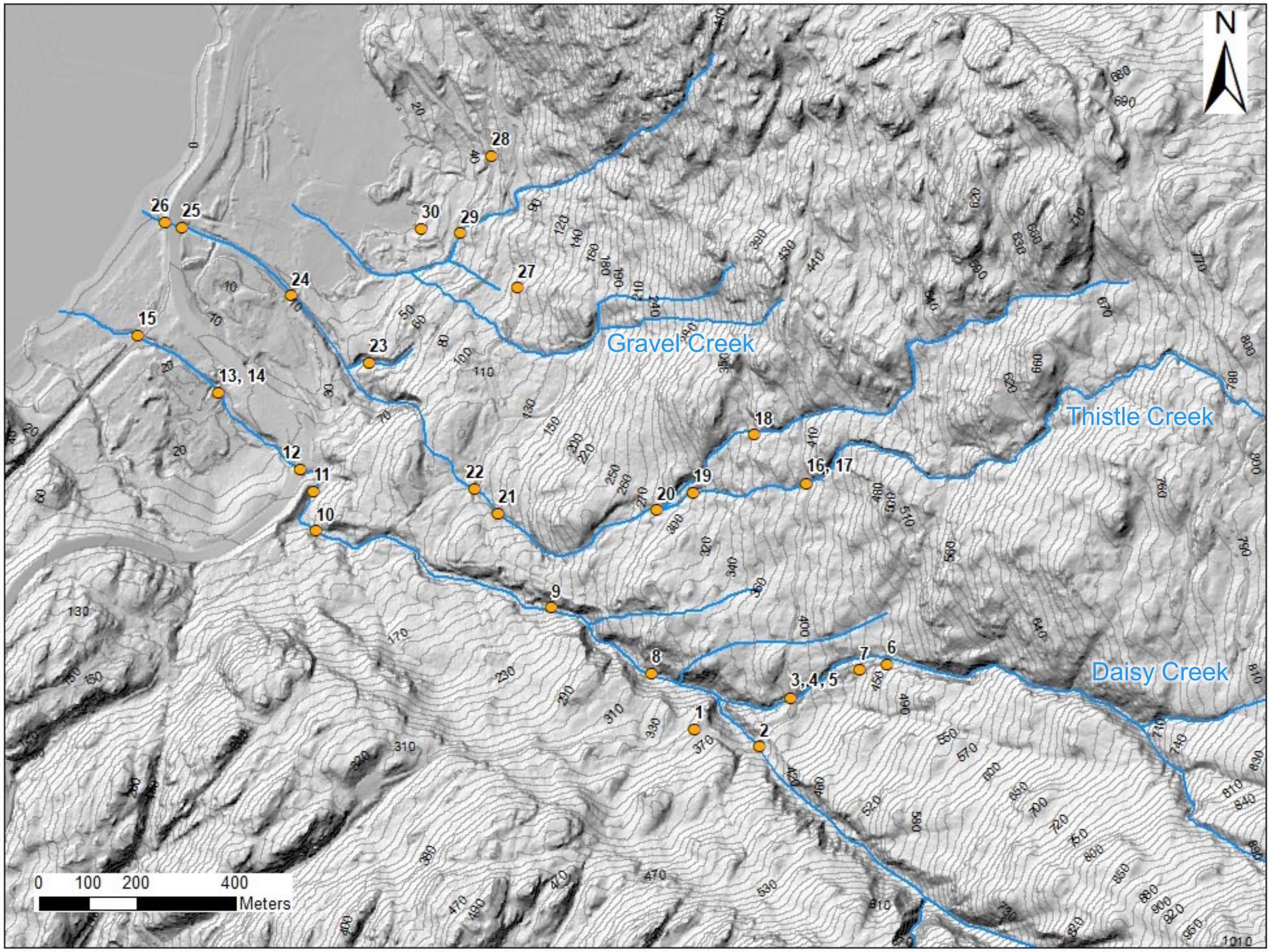


NOTES
1. THIS FIGURE SHOULD BE READ IN CONJUNCTION WITH BGC'S REPORT TITLED 'DAISY, THISTLE, AND GRAVEL CREEKS HAZARD AND RISK ASSESSMENT' AND DATED DECEMBER 2022.
2. BASE TOPOGRAPHIC DATA BASED ON LIDAR PROVIDED BY GEOBC AND DATED JUNE 18, 2019. CONTOUR INTERVAL IS 10 m.
3. CREEKS DIGITIZED BY BGC.
4. PHOTOS TAKEN BY BGC DURING FIELD VISITS ON JUNE 16, 2020; MAY 11, 2022; AND JUNE 7, 2022.

| PREPARED BY: | FIGURE TITLE: | | |
| --- | --- | --- | --- |
| LCH | PHOTO LOCATION MAP | | |
| CHECKED BY: SZ | CLIENT: TIGERBAY DEVELOPMENT CORP. | | |
| APPROVED BY: LCH | SCALE: AS SHOWN | PROJECT NO: 2143002 | FIGURE NO: PHOTOS |

0 5 10 mm in ANSI A sized paper

**BGC ENGINEERING INC.**

**Photo 1. Daisy Creek**

South tributary logging road crossing. Logging slash is evident in channel downstream of crossing.

Photo: BGC, June 7, 2022

**Photo 2. Daisy Creek**

South tributary logging road crossing. Looking downstream.  Bridge deck is 9.5 m long and 6.5 m wide. Bridge is 1.5 m above stream bed. Bridge is DSQ #3148 in BC MOF system.

Photo: BGC, June 7, 2022


**Photo 3. Daisy Creek**

Looking upstream from north tributary logging road crossing.

Photo: BGC, June 7, 2022

**Photo 4. Daisy Creek**

North tributary logging road crossing. Bridge deck is 11.4 m long and 4.3 m wide. Bridge deck is 3 m above the creek bed. Bridge is DSQ #3149 in BC MOF system.

Photo: BGC, June 7, 2022

**Photo 5. Daisy Creek**

Looking downstream from north tributary logging road crossing.

Photo: BGC, June 7, 2022

**Photo 6. Daisy Creek**

Scarred fir tree on top of boulder lobe sampled for dendrochronology analysis (D-DF-01). Elevation 460 m.

Photo: BGC, June 7, 2022

**Photo 7. Daisy Creek**

Scarred tree stump used for dendrochronological analysis. Elevation 440 m.

Photo: BGC, June 7, 2022

**Photo 8. Daisy Creek**

Looking upstream at typical erosional reach (Elevation 270 m).

Photo: BGC, June 7, 2022.

**Photo 9. Daisy Creek**

On right (north) bank looking to left (south) bank at elevation 195 m within approximately 40 m wide depositional reach.

Photo: BGC, June 7, 2022.


**Photo 10. Daisy Creek**

Fault observed at Daisy Creek debris basin inlet.

Photo: BGC, May 11, 2022.


**Photo 11. Daisy Creek**

Daisy Creek debris basin outlet. Culvert grillage cut or broken.

Photo: BGC, May 11, 2022.

**Photo 12. Daisy Creek**

Daisy Creek culvert below Highway 99. Culvert is 3.47 m by 2.23 m oval corrugated steep pipe.

Photo: BGC, May 11, 2022.


**Photo 13. Daisy Creek**

Daisy Creek blocked culvert inlet within developed area.

Photo: BGC, May 11, 2022.


**Photo 14. Daisy Creek**

Looking upstream from blocked culvert inlet within developed area.

Photo: BGC, May 11, 2022.

**Photo 15. Daisy Creek**

Looking downstream at CN Rail crossing.

Photo: BGC, May 11, 2022.

**Photo 16. Thistle Creek**

Looking upstream from logging road on southern channel. Elevation 400 m.

Photo: BGC, June 7, 2022.

**Photo 17. Thistle Creek**

Culvert inlet on south channel. The corrugated steel pipe (CSP) is 2000 mm diameter (DSQ-3151 in MOF system). Elevation 400 m.

Photo: BGC, June 7, 2022.

**Photo 18. Thistle Creek**

Bedrock controlled step-pool morphology on northern channel. Channel width is 2-4 m. Elevation 360 m.

Photo: BGC, June 7, 2022.

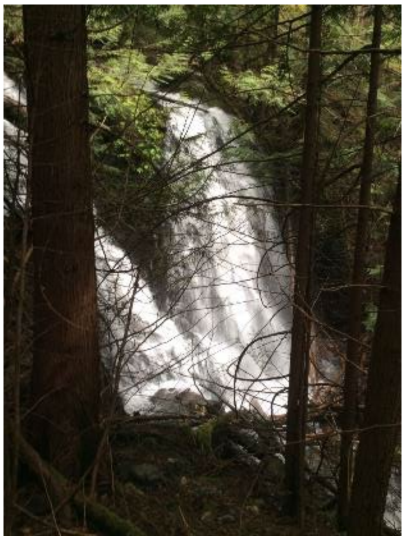

**Photo 19. Thistle Creek**

Looking upstream at southern Thistle Creek channel at approximately 8 m high bedrock waterfall. Elevation 300 m.

Photo: BGC, June 7, 2022.

**Photo 20. Thistle Creek**

Looking upstream at concrete retention structure at approximate elevation 280 m. Structure is approximately 7.5 m wide and up to 4 m tall.

Photo: BGC, June 7, 2022.

**Photo 21. Thistle Creek**

Looking downstream at Thistle Creek channel from approximately 150 m elevation.

Photo: BGC, June 7, 2022.

**Photo 22. Thistle Creek**

Looking upstream at Thistle Creek channel from logging road crossing at approximately 125 m elevation.

Photo: BGC, June 7, 2022.

**Photo 23. Thistle Creek**

Thistle Creek tributary. Standing on right (north) bank looking to left (south) valley slope at approximately 38 m elevation.

Photo: BGC, May 11, 2022.


**Photo 24. Thistle Creek**

Looking downstream at Thistle Creek bridge within proposed development area. Bridge is approximately 10 m wide and bridge low chord is 1.65 m above the channel. BGC expects this bridge to be replaced as part of the proposed development.

Photo: BGC, May 11, 2022.

**Photo 25. Thistle Creek**

Highway 99 and CN Rail concrete box culvert inlet**.** Culvert opening is 3 m wide by 2.2 m with a 1.8 m tall headwall and wingwalls at approximately 45°.

Photo: BGC, August 10, 2020.

v

**Photo 26. Thistle Creek**

Highway 99 and CN Rail concrete box culvert outlet**.**

Photo: BGC, May 11, 2022.

**Photo 27. Gravel Creek**

Bedrock outcrop in Gravel Creek watershed.

Photo: BGC, June 16, 2020.

**Photo 28. Gravel Creek**

Looking north at erosion along logging / access road.

Photo: BGC, June 16, 2020.

**Photo 29. Gravel Creek**

Increased erosion along and across logging / access road. Looking southwest to proposed development area.

Photo: BGC, June 7, 2022.

**Photo 30. Gravel Creek**

Highly erodible raised delta sediments in the proposed development. Interbeds of sand and gravel visible.

Photo: BGC, June 16, 2020.

# DRAWINGS

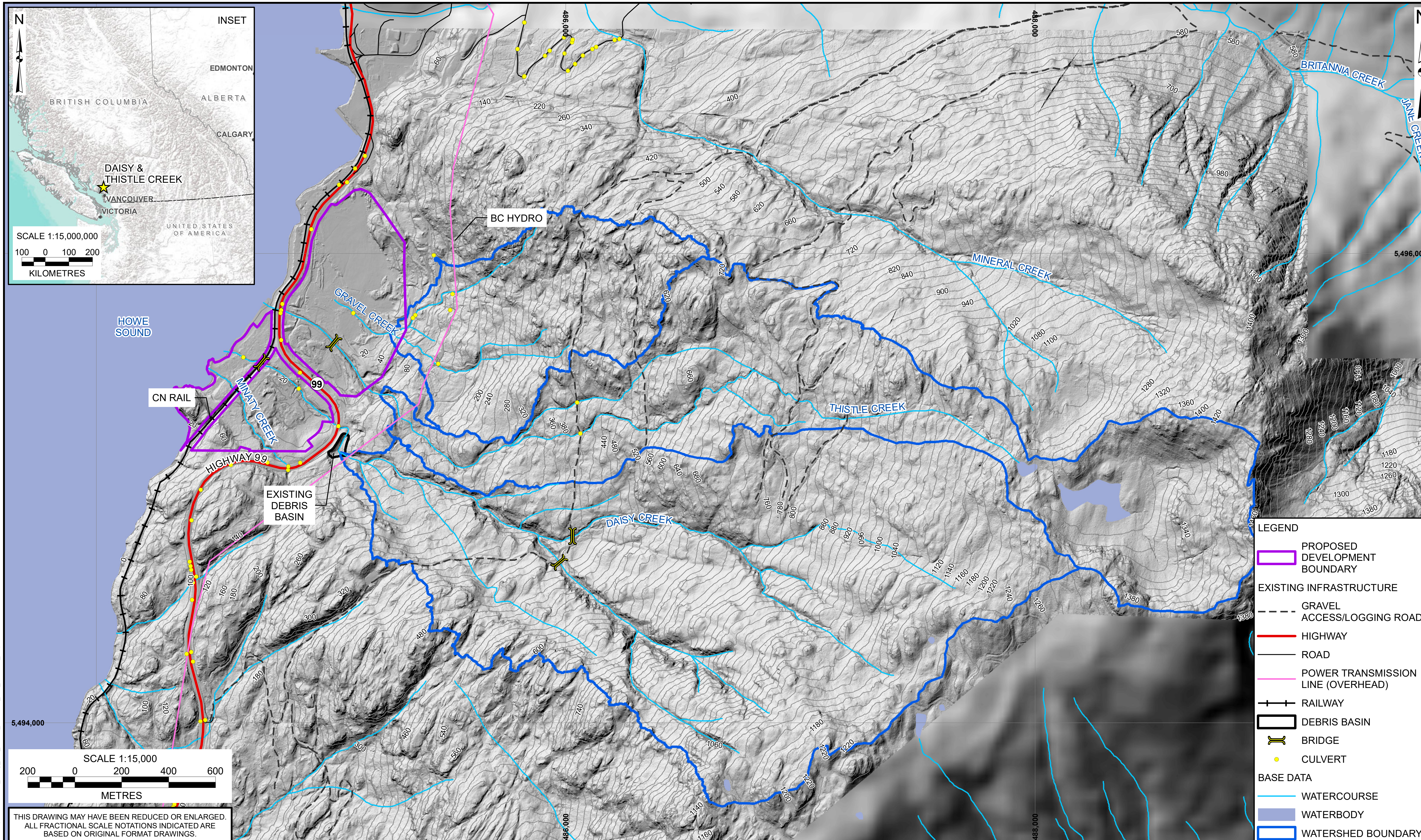


X:\Projects\2143002\GIS\Production\Report\20220429_Daisy_and_Thistle_Creek\01_Site_Location_Map.mxd

NOTES:
1. ALL DIMENSIONS ARE IN METRES UNLESS OTHERWISE NOTED.
2. THIS DRAWING MUST BE READ IN CONJUNCTION WITH BGC'S REPORT TITLED "DAISY, THISTLE, AND GRAVEL CREEKS HAZARD AND RISK ASSESSMENT", AND DATED DECEMBER 2022.
3. BASE TOPOGRAPHIC DATA BASED ON LIDAR PROVIDED BY THE GEOBC, DATED JUNE 18, 2019. CONTOUR INTERVAL IS 20 m. DEM TO THE EAST IS CDED FROM GEOBASE, DATED FEBRUARY 20, 2012.
4. BASE TOPOGRAPHIC MAPPING FROM CANVEC. STREAM LINES WERE MODIFIED BY BGC BASED ON LIDAR, AERIAL IMAGERY, AND FIELD OBSERVATIONS.
5. BGC REFERS TO "MINATY CREEK" FOR CONSISTENCY BUT NOTES THAT IT IS NOT PART OF A PUBLIC DATASET.
6. WATERSHED BOUNDARIES AND BRIDGES DIGITIZED BY BGC.
7. CULVERT DATA PROVIDED BY MOTI ALONG HIGHWAY 99 AND UPDATED WITH BGC FIELD OBSERVATIONS WITHIN PROPOSED DEVELOPMENT AND WATERSHEDS.
8. COORDINATE SYSTEM IS NAD 1983 UTM ZONE 10N. VERTICAL DATUM IS UNKNOWN.
9. UNLESS BGC AGREES OTHERWISE IN WRITING, THIS DRAWING SHALL NOT BE MODIFIED OR USED FOR ANY PURPOSE OTHER THAN THE PURPOSE FOR WHICH BGC GENERATED IT. BGC SHALL HAVE NO LIABILITY FOR ANY DAMAGES OR LOSS ARISING IN ANY WAY FROM ANY USE OR MODIFICATION OF THIS DOCUMENT NOT AUTHORIZED BY BGC. ANY USE OF OR RELIANCE UPON THIS DOCUMENT OR ITS CONTENT BY THIRD PARTIES SHALL BE AT SUCH THIRD PARTIES' SOLE RISK.

| | |
|---|---|
| SCALE: | 1:15,000 |
| DATE: | DEC 2022 |
| DRAWN: | CM |
| REVIEW: | HKW |
| APPROVED: | LCH |

CLIENT: TIGER BAY DEVELOPMENT CORP

BGC

PROJECT: DAISY, THISTLE, AND GRAVEL CREEKS HAZARD AND RISK ASSESSMENT

TITLE: OVERVIEW MAP

PROJECT No.: 2143002

DWG No: 01

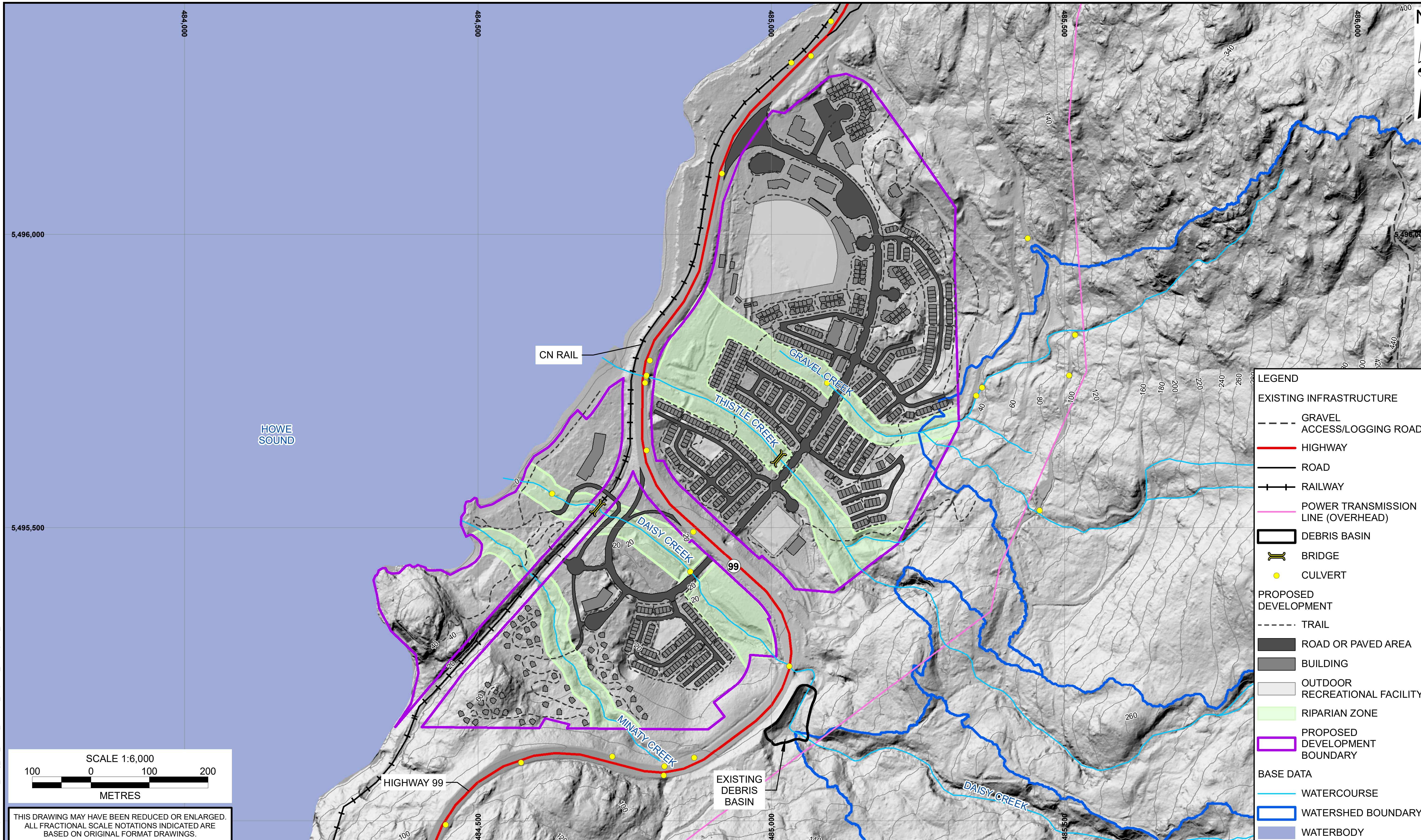


NOTES:
1. ALL DIMENSIONS ARE IN METRES UNLESS OTHERWISE NOTED.
2. THIS DRAWING MUST BE READ IN CONJUNCTION WITH BGC'S REPORT TITLED "DAISY, THISTLE, AND GRAVEL CREEKS HAZARD AND RISK ASSESSMENT", AND DATED DECEMBER 2022.
3. BASE TOPOGRAPHIC DATA BASED ON LIDAR PROVIDED BY THE GEOBC, DATED JUNE 18, 2019. CONTOUR INTERVAL IS 20 m.
4. BASE TOPOGRAPHIC MAPPING FROM CANVEC. STREAM LINES WERE MODIFIED BY BGC BASED ON LIDAR, AERIAL IMAGERY, AND FIELD OBSERVATIONS.
5. BGC REFERS TO "MINATY CREEK" FOR CONSISTENCY BUT NOTES THAT IT IS NOT PART OF A PUBLIC DATASET.
6. PROPOSED DEVELOPMENT DIGITIZED BY BGC BASED ON DWG PROVIDED BY TIGERBAY DEVELOPMENT ON APRIL 1, 2022.
7. WATERSHED BOUNDARIES AND BRIDGES DIGITIZED BY BGC.
8. CULVERT DATA PROVIDED BY MOTI ALONG HIGHWAY 99 AND UPDATED WITH BGC FIELD OBSERVATIONS WITHIN PROPOSED DEVELOPMENT AND WATERSHEDS.
9. COORDINATE SYSTEM IS NAD 1983 UTM ZONE 10N. VERTICAL DATUM IS UNKNOWN.
10. UNLESS BGC AGREES OTHERWISE IN WRITING, THIS DRAWING SHALL NOT BE MODIFIED OR USED FOR ANY PURPOSE OTHER THAN THE PURPOSE FOR WHICH BGC GENERATED IT. BGC SHALL HAVE NO LIABILITY FOR ANY DAMAGES OR LOSS ARISING IN ANY WAY FROM ANY USE OR MODIFICATION OF THIS DOCUMENT NOT AUTHORIZED BY BGC. ANY USE OF OR RELIANCE UPON THIS DOCUMENT OR ITS CONTENT BY THIRD PARTIES SHALL BE AT SUCH THIRD PARTIES' SOLE RISK.

| | |
|---|---|
| SCALE: | 1:6,000 |
| DATE: | DEC 2022 |
| DRAWN: | CM |
| REVIEW: | HKW |
| APPROVED: | LCH |

CLIENT: TIGER BAY DEVELOPMENT CORP

PROJECT: DAISY, THISTLE, AND GRAVEL CREEKS HAZARD AND RISK ASSESSMENT

TITLE: PROPOSED DEVELOPMENT AREA

PROJECT No.: 2143002
DWG No: 02

X:\Projects\2143002\GIS\Production\Report\20220429_Daisy_and_Thistle_Creek\02_Proposed_Development_Area.mxd

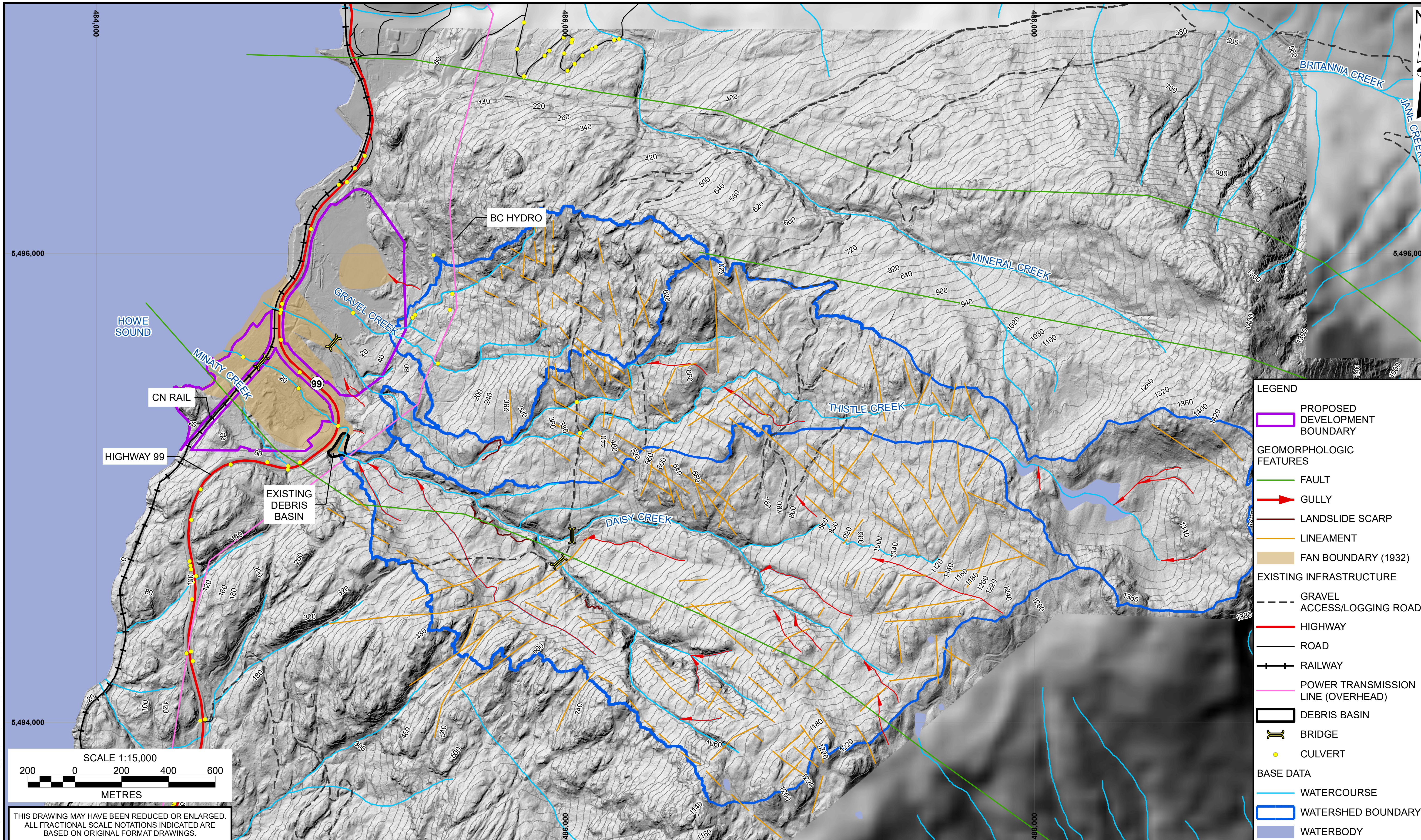


NOTES:
1. ALL DIMENSIONS ARE IN METRES UNLESS OTHERWISE NOTED.
2. THIS DRAWING MUST BE READ IN CONJUNCTION WITH BGC'S REPORT TITLED "DAISY, THISTLE, AND GRAVEL CREEKS HAZARD AND RISK ASSESSMENT", AND DATED DECEMBER 2022.
3. BASE TOPOGRAPHIC DATA BASED ON LIDAR PROVIDED BY THE GEOBC, DATED JUNE 18, 2019. CONTOUR INTERVAL IS 20 m. DEM TO THE EAST IS CDED FROM GEOBASE, DATED FEBRUARY 20, 2012.
4. BASE TOPOGRAPHIC MAPPING FROM CANVEC. STREAM LINES WERE MODIFIED BY BGC BASED ON LIDAR, AERIAL IMAGERY, AND FIELD OBSERVATIONS.
5. BGC REFERS TO "MINATY CREEK" FOR CONSISTENCY BUT NOTES THAT IT IS NOT PART OF A PUBLIC DATASET.
6. FAULTS FROM BC GEOLOGICAL SURVEY (CUI ET AL., 2017).
7. WATERSHED BOUNDARIES, FAN BOUNDARY, AND BRIDGES DIGITIZED BY BGC.
8. CULVERT DATA PROVIDED BY MOTI ALONG HIGHWAY 99 AND UPDATED WITH BGC FIELD OBSERVATIONS WITHIN PROPOSED DEVELOPMENT AND WATERSHEDS.
9. COORDINATE SYSTEM IS NAD 1983 UTM ZONE 10N. VERTICAL DATUM IS UNKNOWN.
10. UNLESS BGC AGREES OTHERWISE IN WRITING, THIS DRAWING SHALL NOT BE MODIFIED OR USED FOR ANY PURPOSE OTHER THAN THE PURPOSE FOR WHICH BGC GENERATED IT. BGC SHALL HAVE NO LIABILITY FOR ANY DAMAGES OR LOSS ARISING IN ANY WAY FROM ANY USE OR MODIFICATION OF THIS DOCUMENT NOT AUTHORIZED BY BGC. ANY USE OF OR RELIANCE UPON THIS DOCUMENT OR ITS CONTENT BY THIRD PARTIES SHALL BE AT SUCH THIRD PARTIES' SOLE RISK.

| | |
|---|---|
| SCALE: | 1:15,000 |
| DATE: | DEC 2022 |
| DRAWN: | CM |
| REVIEW: | HKW |
| APPROVED: | LCH |

CLIENT: TIGER BAY DEVELOPMENT CORP

BGC

PROJECT: DAISY, THISTLE, AND GRAVEL CREEKS HAZARD AND RISK ASSESSMENT

TITLE: GEOMORPHOLOGIC MAP

| PROJECT No.: | DWG No: |
|---|---|
| 2143002 | 03 |

X:\Projects\2143002\GIS\Production\Report\20220429_Daisy_and_Thistle_Creek\03_Geomorphological_Map.mxd

N

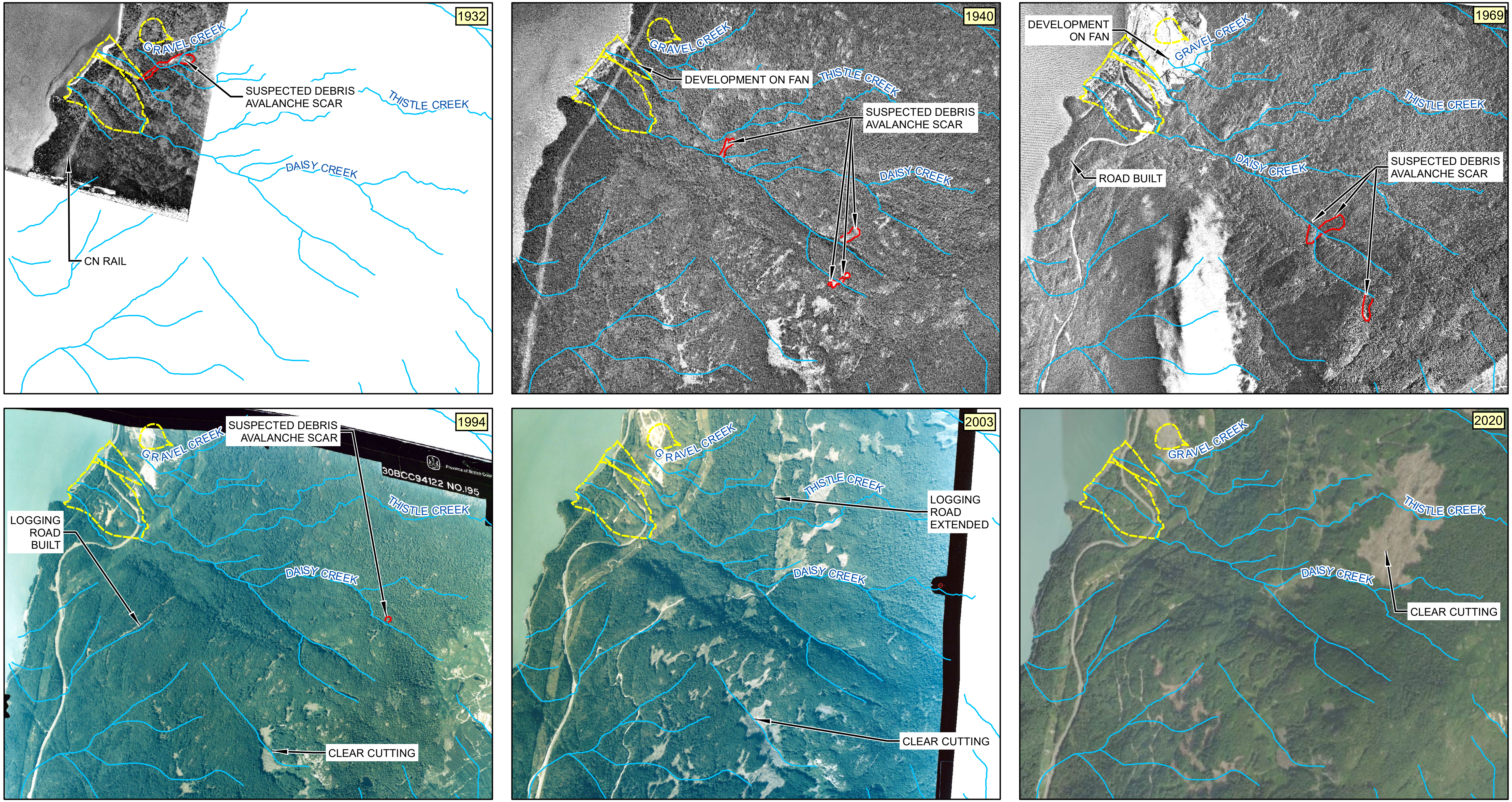


SCALE 1:30,000

250 0 250 500 750 1,000

METRES

THIS DRAWING MAY HAVE BEEN REDUCED OR ENLARGED. ALL FRACTIONAL SCALE NOTATIONS INDICATED ARE BASED ON ORIGINAL FORMAT DRAWINGS.

LEGEND

- HAZARD FEATURE
- WATERCOURSE
- APPROXIMATE FAN AREA (1932)

NOTES:

1. ALL DIMENSIONS ARE IN METRES UNLESS OTHERWISE NOTED.
2. THIS DRAWING MUST BE READ IN CONJUNCTION WITH BGC'S REPORT TITLED "DAISY, THISTLE, AND GRAVEL CREEKS HAZARD AND RISK ASSESSMENT", AND DATED DECEMBER 2022.
3. THE 1932 AIR PHOTO IS FROM THE NATIONAL AIR PHOTO LIBRARY. THE 1940, 1969, 1994, AND 2003 AIR PHOTOS ARE FROM THE UBC GEOGRAPHIC INFORMATION CENTRE. THE 2020 IMAGERY IS ESRI WORLD IMAGERY.
4. APPROXIMATE FAN AREA (1932) DIGITIZED BY BGC.
5. COORDINATE SYSTEM IS NAD 1983 UTM ZONE 11N. VERTICAL DATUM IS UNKNOWN.
6. UNLESS BGC AGREES OTHERWISE IN WRITING, THIS DRAWING SHALL NOT BE MODIFIED OR USED FOR ANY PURPOSE OTHER THAN THE PURPOSE FOR WHICH BGC GENERATED IT. BGC SHALL HAVE NO LIABILITY FOR ANY DAMAGES OR LOSS ARISING IN ANY WAY FROM ANY USE OR MODIFICATION OF THIS DOCUMENT NOT AUTHORIZED BY BGC. ANY USE OF OR RELIANCE UPON THIS DOCUMENT OR ITS CONTENT BY THIRD PARTIES SHALL BE AT SUCH THIRD PARTIES' SOLE RISK.

| | |
|---|---|
| SCALE: | 1:30,000 |
| DATE: | DEC 2022 |
| DRAWN: | CM |
| REVIEW: | HKW |
| APPROVED: | LCH |

CLIENT: TIGER BAY DEVELOPMENT CORP

BGC

PROJECT: DAISY, THISTLE, AND GRAVEL CREEKS HAZARD AND RISK ASSESSMENT

TITLE: AIR PHOTO COMPARISON

PROJECT No.: 2143002

DWG No: 04

X:\Projects\2143002\GIS\Production\Report\20220429_Daisy_and_Thistle_Creek\04_AirPhotoComparison.mxd

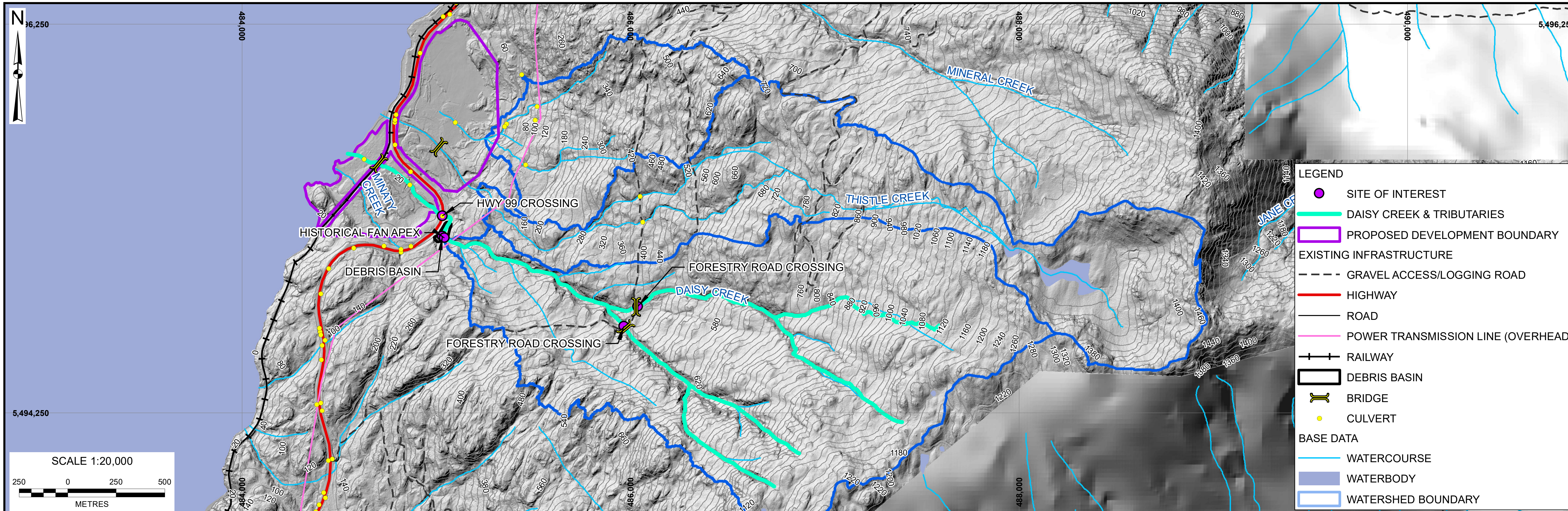


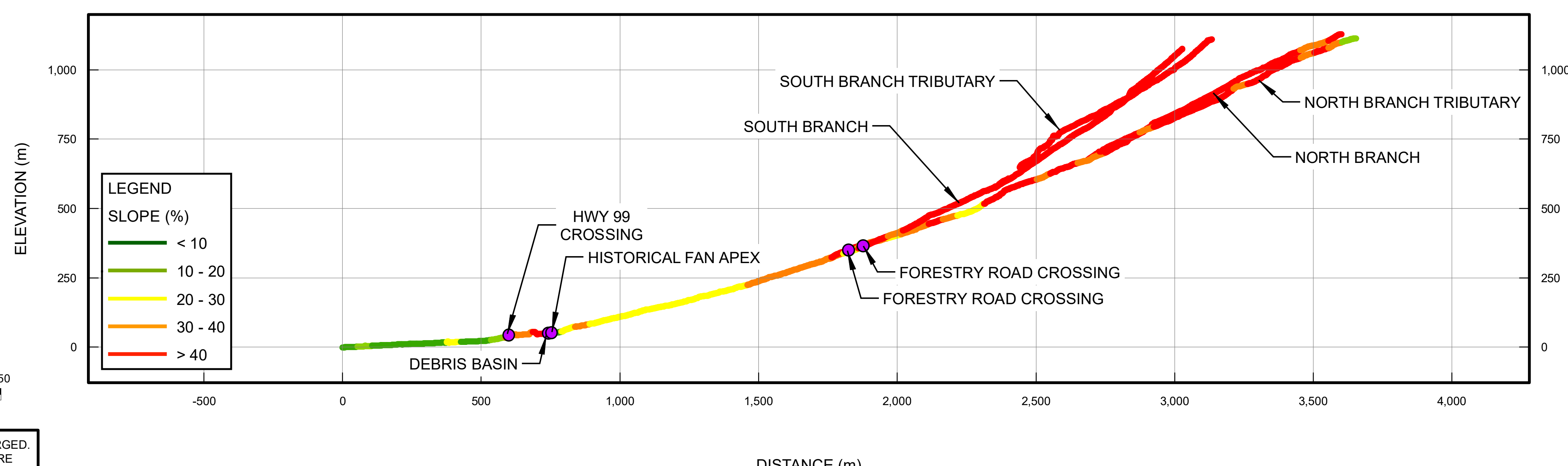


SCALE 1:20,000

250 0 250 500 750

METRES

THIS DRAWING MAY HAVE BEEN REDUCED OR ENLARGED. ALL FRACTIONAL SCALE NOTATIONS INDICATED ARE BASED ON ORIGINAL FORMAT DRAWINGS.

NOTES:
1. ALL DIMENSIONS ARE IN METRES UNLESS OTHERWISE NOTED.
2. THIS DRAWING MUST BE READ IN CONJUNCTION WITH BGC'S REPORT TITLED "DAISY, THISTLE, AND GRAVEL CREEKS HAZARD AND RISK ASSESSMENT", AND DATED DECEMBER 2022.
3. BASE TOPOGRAPHIC DATA BASED ON LIDAR PROVIDED BY THE GEOBC, DATED JUNE 18, 2019. DEM TO THE EAST IS CDED FROM GEOBASE, DATED FEBRUARY 20, 2012.
4. BASE TOPOGRAPHIC MAPPING FROM CANVEC. STREAM LINES WERE MODIFIED BY BGC BASED ON LIDAR, AERIAL IMAGERY, AND FIELD OBSERVATIONS.
5. BGC REFERS TO "MINATY CREEK" FOR CONSISTENCY BUT NOTES THAT IT IS NOT PART OF A PUBLIC DATASET.
6. WATERSHED BOUNDARIES AND BRIDGES DIGITIZED BY BGC.
7. CULVERT DATA PROVIDED BY MOTI ALONG HIGHWAY 99 AND UPDATED WITH BGC FIELD OBSERVATIONS WITHIN PROPOSED DEVELOPMENT AND WATERSHEDS.
8. COORDINATE SYSTEM IS NAD 1983 UTM ZONE 10N. VERTICAL DATUM IS UNKNOWN.
9. UNLESS BGC AGREES OTHERWISE IN WRITING, THIS DRAWING SHALL NOT BE MODIFIED OR USED FOR ANY PURPOSE OTHER THAN THE PURPOSE FOR WHICH BGC GENERATED IT. BGC SHALL HAVE NO LIABILITY FOR ANY DAMAGES OR LOSS ARISING IN ANY WAY FROM ANY USE OR MODIFICATION OF THIS DOCUMENT NOT AUTHORIZED BY BGC. ANY USE OF OR RELIANCE UPON THIS DOCUMENT OR ITS CONTENT BY THIRD PARTIES SHALL BE AT SUCH THIRD PARTIES' SOLE RISK.

| | |
|---|---|
| SCALE: | 1:20,000 |
| DATE: | DEC 2022 |
| DRAWN: | CM |
| REVIEW: | HKW |
| APPROVED: | LCH |

CLIENT: TIGER BAY DEVELOPMENT CORP

BGC

PROJECT: DAISY, THISTLE, AND GRAVEL CREEKS HAZARD AND RISK ASSESSMENT

TITLE: CHANNEL PROFILE - DAISY CREEK

PROJECT No.: 2143002

DWG No: 05a

X:\Projects\2143002\GIS\Production\Report\20220429_Daisy_and_Thistle_Creek\05a_Daisy_Creek_Profile.mxd

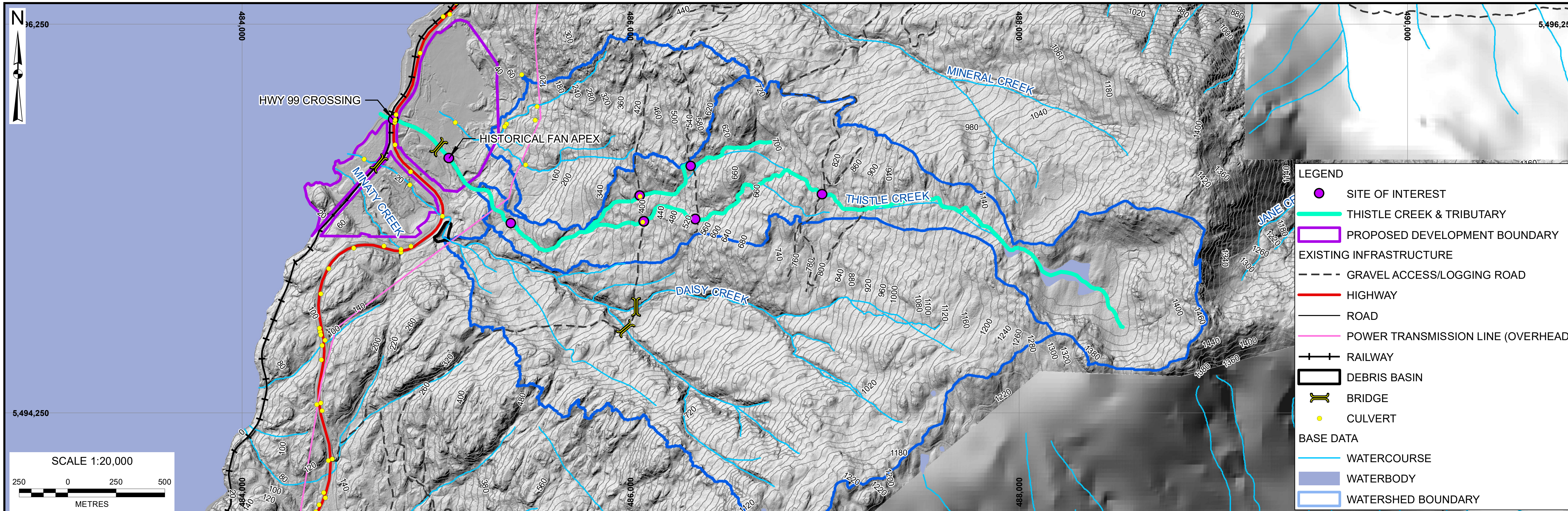


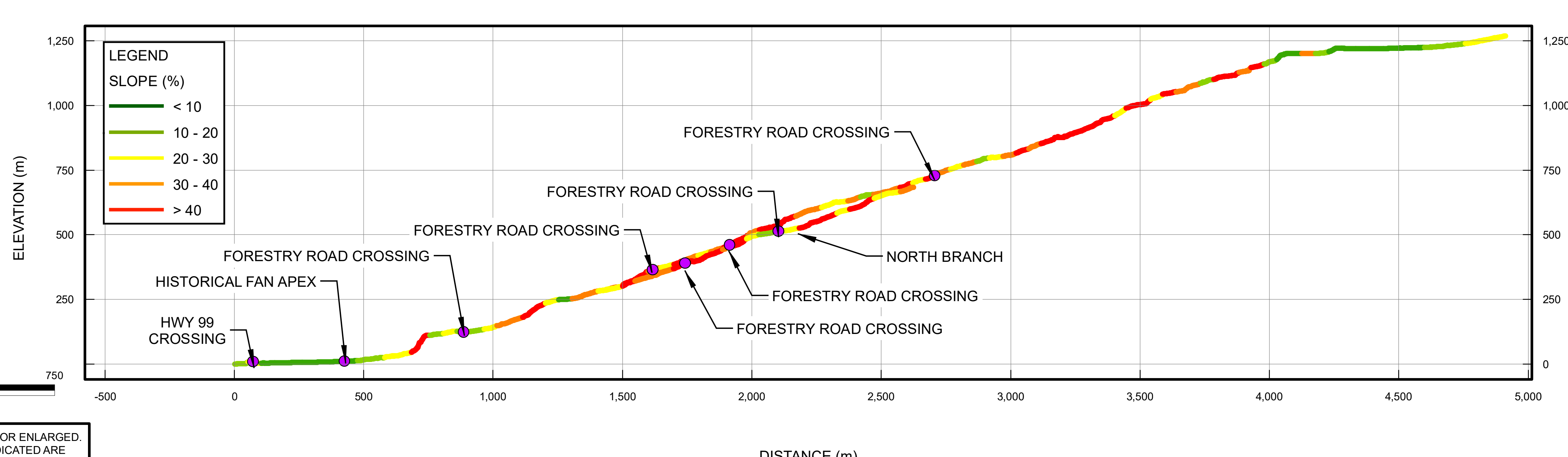


THIS DRAWING MAY HAVE BEEN REDUCED OR ENLARGED. ALL FRACTIONAL SCALE NOTATIONS INDICATED ARE BASED ON ORIGINAL FORMAT DRAWINGS.

NOTES:
1. ALL DIMENSIONS ARE IN METRES UNLESS OTHERWISE NOTED.
2. THIS DRAWING MUST BE READ IN CONJUNCTION WITH BGC'S REPORT TITLED "DAISY, THISTLE, AND GRAVEL CREEKS HAZARD AND RISK ASSESSMENT", AND DATED DECEMBER 2022.
3. BASE TOPOGRAPHIC DATA BASED ON LIDAR PROVIDED BY THE GEOBC, DATED JUNE 18, 2019. DEM TO THE EAST IS CDED FROM GEOBASE, DATED FEBRUARY 20, 2012.
4. BASE TOPOGRAPHIC MAPPING FROM CANVEC. STREAM LINES WERE MODIFIED BY BGC BASED ON LIDAR, AERIAL IMAGERY, AND FIELD OBSERVATIONS.
5. BGC REFERS TO "MINATY CREEK" FOR CONSISTENCY BUT NOTES THAT IT IS NOT PART OF A PUBLIC DATASET.
6. WATERSHED BOUNDARIES AND BRIDGES DIGITIZED BY BGC.
7. CULVERT DATA PROVIDED BY MOTI ALONG HIGHWAY 99 AND UPDATED WITH BGC FIELD OBSERVATIONS WITHIN PROPOSED DEVELOPMENT AND WATERSHEDS.
8. COORDINATE SYSTEM IS NAD 1983 UTM ZONE 10N. VERTICAL DATUM IS UNKNOWN.
9. UNLESS BGC AGREES OTHERWISE IN WRITING, THIS DRAWING SHALL NOT BE MODIFIED OR USED FOR ANY PURPOSE OTHER THAN THE PURPOSE FOR WHICH BGC GENERATED IT. BGC SHALL HAVE NO LIABILITY FOR ANY DAMAGES OR LOSS ARISING IN ANY WAY FROM ANY USE OR MODIFICATION OF THIS DOCUMENT NOT AUTHORIZED BY BGC. ANY USE OF OR RELIANCE UPON THIS DOCUMENT OR ITS CONTENT BY THIRD PARTIES SHALL BE AT SUCH THIRD PARTIES' SOLE RISK.

| | |
|---|---|
| SCALE: | 1:20,000 |
| DATE: | DEC 2022 |
| DRAWN: | CM |
| REVIEW: | HKW |
| APPROVED: | LCH |

CLIENT: TIGER BAY DEVELOPMENT CORP

PROJECT: DAISY, THISTLE, AND GRAVEL CREEKS HAZARD AND RISK ASSESSMENT

TITLE: CHANNEL PROFILE - THISTLE CREEK

PROJECT No.: 2143002

DWG No: 05b

X:\Projects\2143002\GIS\Production\Report\20220429_Daisy_and_Thistle_Creek\05b_Thistle_Creek_Profile.mxd

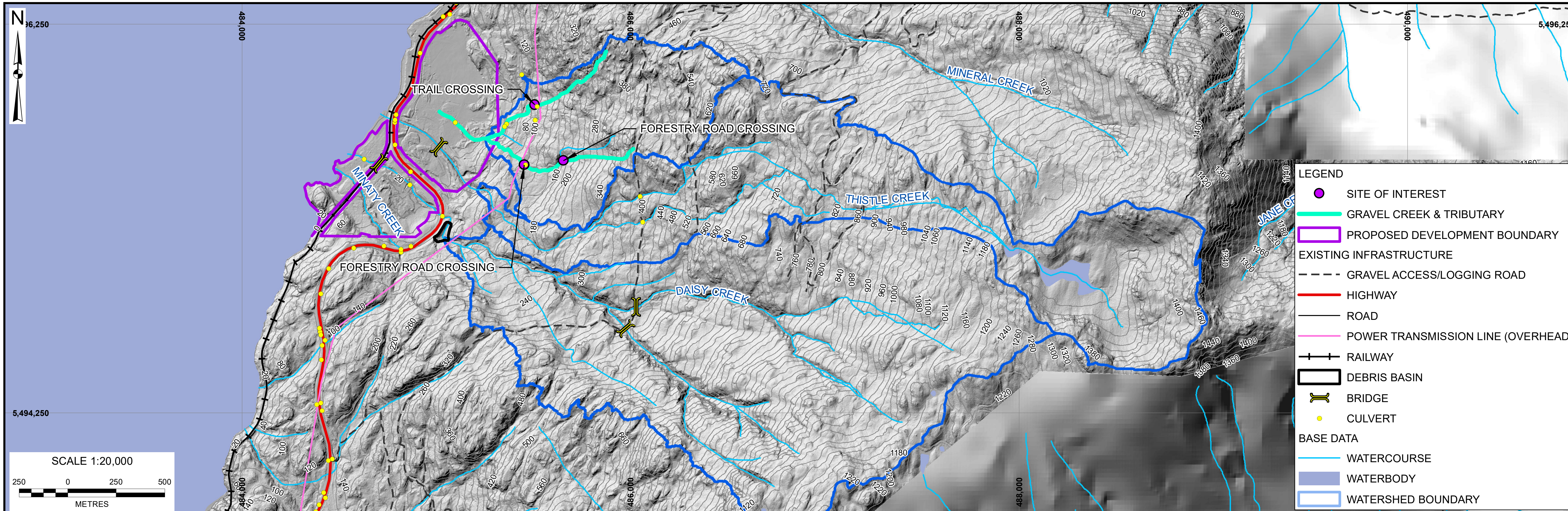


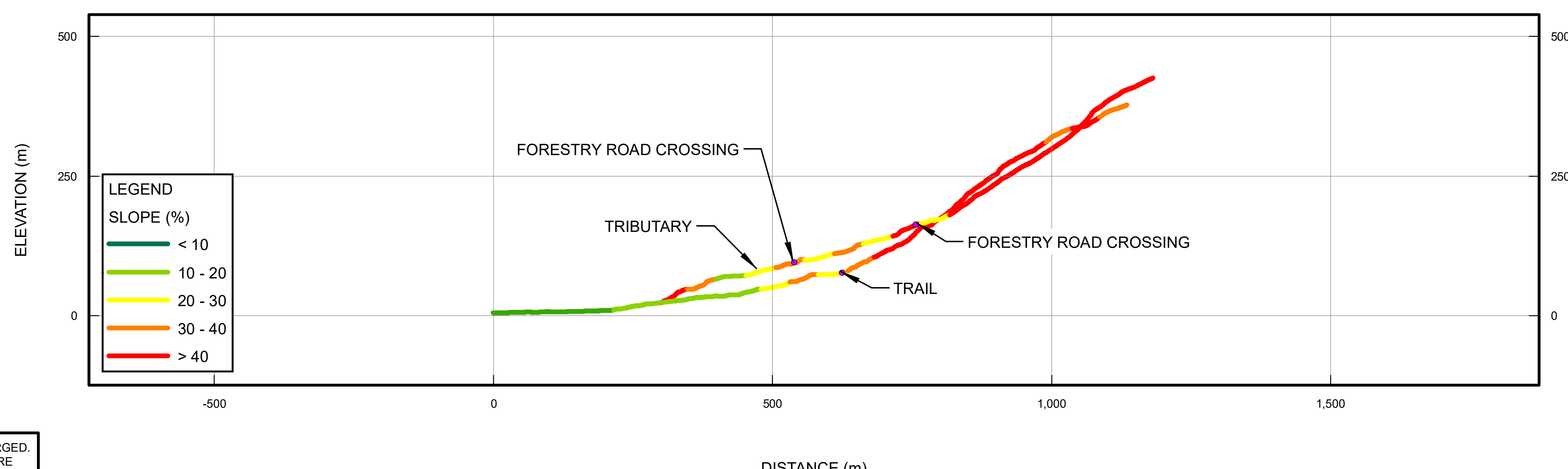


SCALE 1:10,000

100 0 100 200 300

METRES

THIS DRAWING MAY HAVE BEEN REDUCED OR ENLARGED. ALL FRACTIONAL SCALE NOTATIONS INDICATED ARE BASED ON ORIGINAL FORMAT DRAWINGS.

NOTES:
1. ALL DIMENSIONS ARE IN METRES UNLESS OTHERWISE NOTED.
2. THIS DRAWING MUST BE READ IN CONJUNCTION WITH BGC'S REPORT TITLED "DAISY, THISTLE, AND GRAVEL CREEKS HAZARD AND RISK ASSESSMENT", AND DATED DECEMBER 2022.
3. BASE TOPOGRAPHIC DATA BASED ON LIDAR PROVIDED BY THE GEOBC, DATED JUNE 18, 2019. DEM TO THE EAST IS CDED FROM GEOBASE, DATED FEBRUARY 20, 2012.
4. BASE TOPOGRAPHIC MAPPING FROM CANVEC. STREAM LINES WERE MODIFIED BY BGC BASED ON LIDAR, AERIAL IMAGERY, AND FIELD OBSERVATIONS.
5. BGC REFERS TO "MINATY CREEK" FOR CONSISTENCY BUT NOTES THAT IT IS NOT PART OF A PUBLIC DATASET.
6. WATERSHED BOUNDARIES AND BRIDGES DIGITIZED BY BGC.
7. CULVERT DATA PROVIDED BY MOTI ALONG HIGHWAY 99 AND UPDATED WITH BGC FIELD OBSERVATIONS WITHIN PROPOSED DEVELOPMENT AND WATERSHEDS.
8. COORDINATE SYSTEM IS NAD 1983 UTM ZONE 10N. VERTICAL DATUM IS UNKNOWN.
9. UNLESS BGC AGREES OTHERWISE IN WRITING, THIS DRAWING SHALL NOT BE MODIFIED OR USED FOR ANY PURPOSE OTHER THAN THE PURPOSE FOR WHICH BGC GENERATED IT. BGC SHALL HAVE NO LIABILITY FOR ANY DAMAGES OR LOSS ARISING IN ANY WAY FROM ANY USE OR MODIFICATION OF THIS DOCUMENT NOT AUTHORIZED BY BGC. ANY USE OF OR RELIANCE UPON THIS DOCUMENT OR ITS CONTENT BY THIRD PARTIES SHALL BE AT SUCH THIRD PARTIES' SOLE RISK.

| | |
|---|---|
| SCALE: | 1:20,000 |
| DATE: | DEC 2022 |
| DRAWN: | CM |
| REVIEW: | HKW |
| APPROVED: | LCH |

CLIENT: TIGER BAY DEVELOPMENT CORP

BGC

PROJECT: DAISY, THISTLE, AND GRAVEL CREEKS HAZARD AND RISK ASSESSMENT

TITLE: CHANNEL PROFILE - GRAVEL CREEK

PROJECT No.: 2143002

DWG No: 05c

X:\Projects\2143\002\GIS\Production\Report\20220429_Daisy_and_Thistle_Creek\05c_Gravel_Creek_Profile.mxd

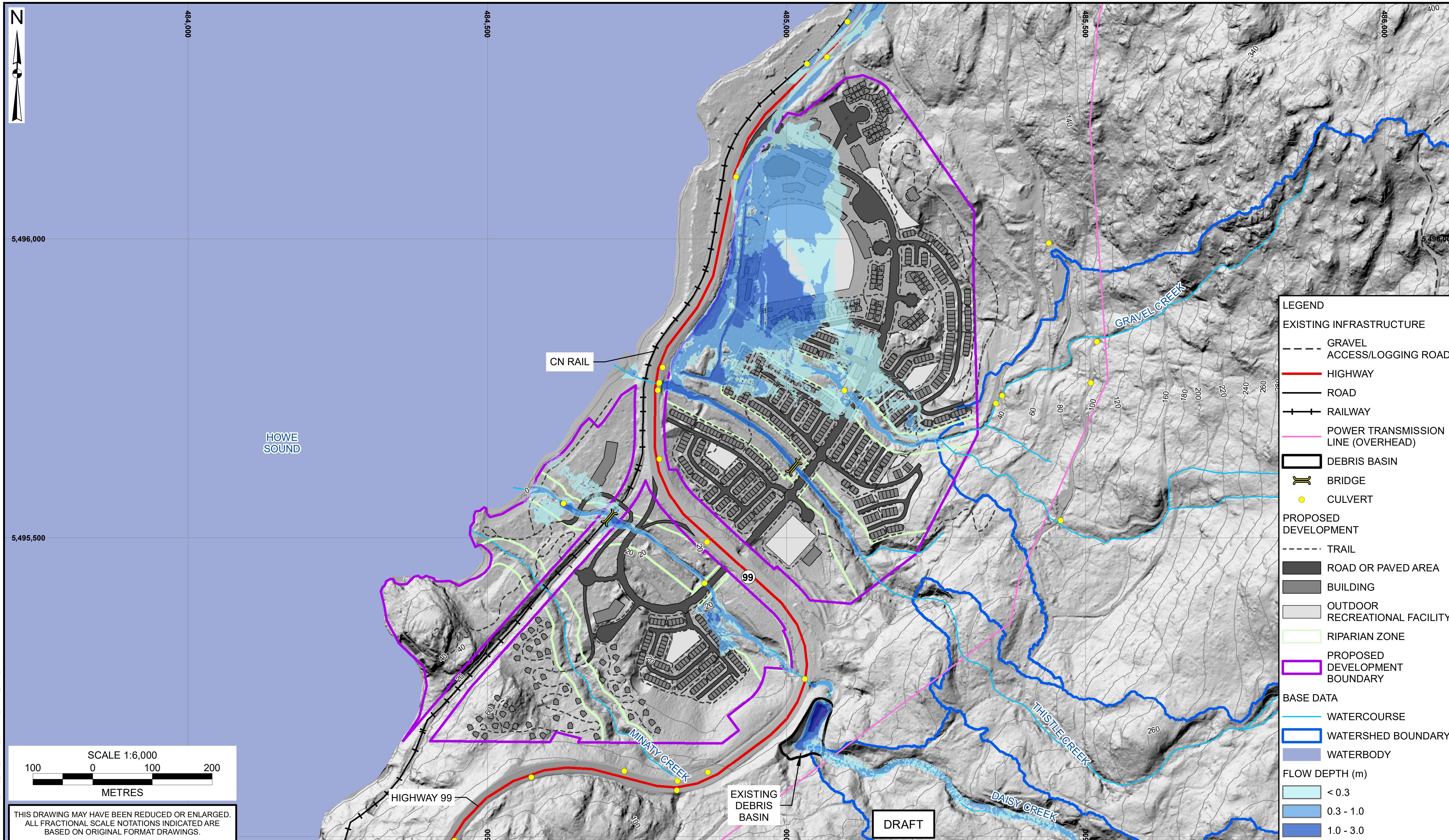


THIS DRAWING MAY HAVE BEEN REDUCED OR ENLARGED. ALL FRACTIONAL SCALE NOTATIONS INDICATED ARE BASED ON ORIGINAL FORMAT DRAWINGS.

NOTES:
1. ALL DIMENSIONS ARE IN METRES UNLESS OTHERWISE NOTED.
2. THIS DRAWING MUST BE READ IN CONJUNCTION WITH BGC'S REPORT TITLED "DAISY, THISTLE, AND GRAVEL CREEKS HAZARD AND RISK ASSESSMENT", AND DATED DECEMBER 2022.
3. BASE TOPOGRAPHIC DATA BASED ON LIDAR PROVIDED BY THE GEOBC, DATED JUNE 18, 2019. CONTOUR INTERVAL IS 20 m.
4. BASE TOPOGRAPHIC MAPPING FROM CANVEC. STREAM LINES WERE MODIFIED BY BGC BASED ON LIDAR, AERIAL IMAGERY, AND FIELD OBSERVATIONS.
5. BGC REFERS TO "MINATY CREEK" FOR CONSISTENCY BUT NOTES THAT IT IS NOT PART OF A PUBLIC DATASET.
6. FLOW DEPTHS SHOWN ARE THE MAXIMUM DEPTH FOR ANY 200-YEAR RETURN PERIOD HAZARD SCENARIO BASED ON NUMERICAL MODELLING COMPLETED BY BGC, AS DESCRIBED IN THE ACCOMPANYING REPORT.
7. PROPOSED DEVELOPMENT DIGITIZED BY BGC BASED ON DWG PROVIDED BY TIGERBAY DEVELOPMENT ON APRIL 1, 2022.
8. THIS MAP DOES NOT ACCOUNT FOR AUXILLARY HAZARDS SUCH AS ROAD EMBANKMENT EROSION, CREEK BANK FAILURES, OR CHANNELIZATION IN LOOSE SEDIMENTS SHOULD A FLOW DIVERSION OCCUR. IT ALSO DOES NOT ACCOUNT FOR ANY HUMAN INTERFERENCE DURING THE RUNOFF EVENTS.
9. WATERSHED BOUNDARIES AND BRIDGES DIGITIZED BY BGC.
10. CULVERT DATA PROVIDED BY MOTI ALONG HIGHWAY 99 AND UPDATED WITH BGC FIELD OBSERVATIONS WITHIN PROPOSED DEVELOPMENT AND WATERSHEDS.
11. COORDINATE SYSTEM IS NAD 1983 UTM ZONE 10N. VERTICAL DATUM IS UNKNOWN.
12. UNLESS BGC AGREES OTHERWISE IN WRITING, THIS DRAWING SHALL NOT BE MODIFIED OR USED FOR ANY PURPOSE OTHER THAN THE PURPOSE FOR WHICH BGC GENERATED IT. BGC SHALL HAVE NO LIABILITY FOR ANY DAMAGES OR LOSS ARISING IN ANY WAY FROM ANY USE OR MODIFICATION OF THIS DOCUMENT NOT AUTHORIZED BY BGC. ANY USE OF OR RELIANCE UPON THIS DOCUMENT OR ITS CONTENT BY THIRD PARTIES SHALL BE AT SUCH THIRD PARTIES' SOLE RISK.

| | |
|---|---|
| SCALE: | 1:6,000 |
| DATE: | DEC 2022 |
| DRAWN: | CM |
| REVIEW: | SZ |
| APPROVED: | LCH |

CLIENT: TIGER BAY DEVELOPMENT CORP

BGC

PROJECT: DAISY, THISTLE, AND GRAVEL CREEKS HAZARD AND RISK ASSESSMENT

TITLE: 200-YEAR FLOW DEPTH

PROJECT No.: 2143002

DWG No: 06

X:\Projects\2143002\GIS\Production\Report\20220429_Daisy_and_Thistle_Creek\06_200YR_Flow_Depth.mxd

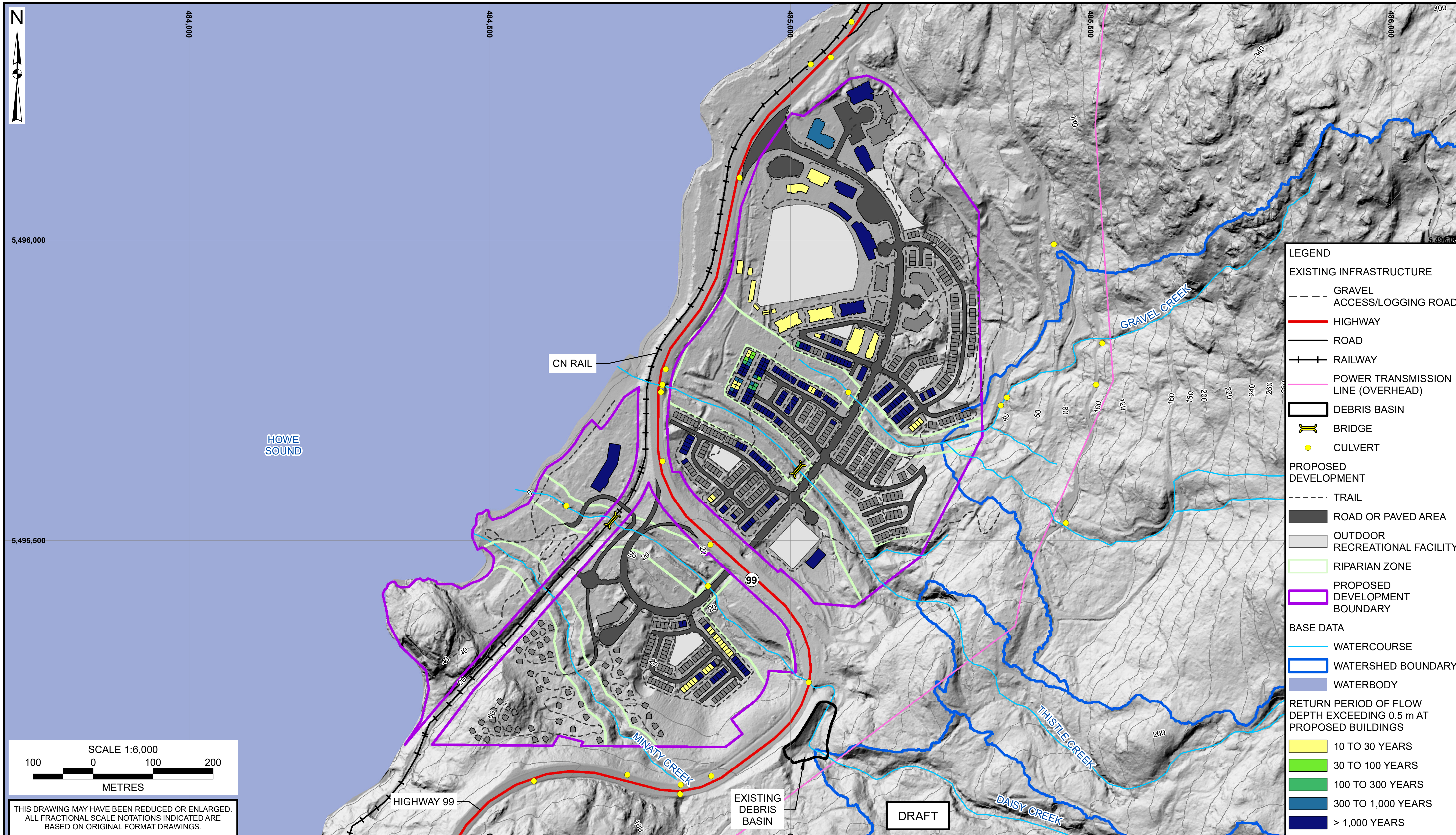


NOTES:
1. ALL DIMENSIONS ARE IN METRES UNLESS OTHERWISE NOTED.
2. THIS DRAWING MUST BE READ IN CONJUNCTION WITH BGC'S REPORT TITLED "DAISY, THISTLE, AND GRAVEL CREEKS HAZARD AND RISK ASSESSMENT", AND DATED DECEMBER 2022.
3. BASE TOPOGRAPHIC DATA BASED ON LIDAR PROVIDED BY THE GEOBC, DATED JUNE 18, 2019. CONTOUR INTERVAL IS 20 m.
4. BASE TOPOGRAPHIC MAPPING FROM CANVEC. STREAM LINES WERE MODIFIED BY BGC BASED ON LIDAR, AERIAL IMAGERY, AND FIELD OBSERVATIONS.
5. BGC REFERS TO "MINATY CREEK" FOR CONSISTENCY BUT NOTES THAT IT IS NOT PART OF A PUBLIC DATASET.
6. BUILDINGS ARE COLOUR CODED TO SHOW THE RETURN PERIOD WHEN FLOW DEPTHS THAT INTERSECT THE BUILDING FOOTPRINT ARE EXPECTED TO EXCEED 0.5 m. FLOW DEPTHS ARE BASED ON NUMERICAL MODELLING OF HAZARD SCENARIOS ON DAISY, THISTLE, AND GRAVEL CREEKS COMPLETED BY BGC, AS DESCRIBED IN THE ACCOMPANYING REPORT.
7. PROPOSED DEVELOPMENT DIGITIZED BY BGC BASED ON DWG PROVIDED BY TIGERBAY DEVELOPMENT ON APRIL 1, 2022.
8. THIS MAP DOES NOT ACCOUNT FOR AUXILLARY HAZARDS SUCH AS ROAD EMBANKMENT EROSION, CREEK BANK FAILURES, OR CHANNELIZATION IN LOOSE SEDIMENTS SHOULD A FLOW DIVERSION OCCUR. IT ALSO DOES NOT ACCOUNT FOR ANY HUMAN INTERFERENCE DURING THE RUNOFF EVENTS.
9. WATERSHED BOUNDARIES AND BRIDGES DIGITIZED BY BGC.
10. CULVERT DATA PROVIDED BY MOTI ALONG HIGHWAY 99 AND UPDATED WITH BGC FIELD OBSERVATIONS WITHIN PROPOSED DEVELOPMENT AND WATERSHEDS.
11. COORDINATE SYSTEM IS NAD 1983 UTM ZONE 10N. VERTICAL DATUM IS UNKNOWN.
12. UNLESS BGC AGREES OTHERWISE IN WRITING, THIS DRAWING SHALL NOT BE MODIFIED OR USED FOR ANY PURPOSE OTHER THAN THE PURPOSE FOR WHICH BGC GENERATED IT. BGC SHALL HAVE NO LIABILITY FOR ANY DAMAGES OR LOSS ARISING IN ANY WAY FROM ANY USE OR MODIFICATION OF THIS DOCUMENT NOT AUTHORIZED BY BGC. ANY USE OF OR RELIANCE UPON THIS DOCUMENT OR ITS CONTENT BY THIRD PARTIES SHALL BE AT SUCH THIRD PARTIES' SOLE RISK.

| | |
|---|---|
| SCALE: | 1:6,000 |
| DATE: | DEC 2022 |
| DRAWN: | CM |
| REVIEW: | SZ |
| APPROVED: | LCH |

CLIENT: TIGER BAY DEVELOPMENT CORP

BGC

PROJECT: DAISY, THISTLE, AND GRAVEL CREEKS HAZARD AND RISK ASSESSMENT

TITLE: BUILDING INUNDATION MAP FLOW DEPTH > 0.5 m

| PROJECT No.: | DWG No: |
|---|---|
| 2143002 | 07 |

X:\Projects\2143\002\GIS\Production\Report\20220429_Daisy_and_Thistle_Creek\07_Building_Inundation_Map.mxd

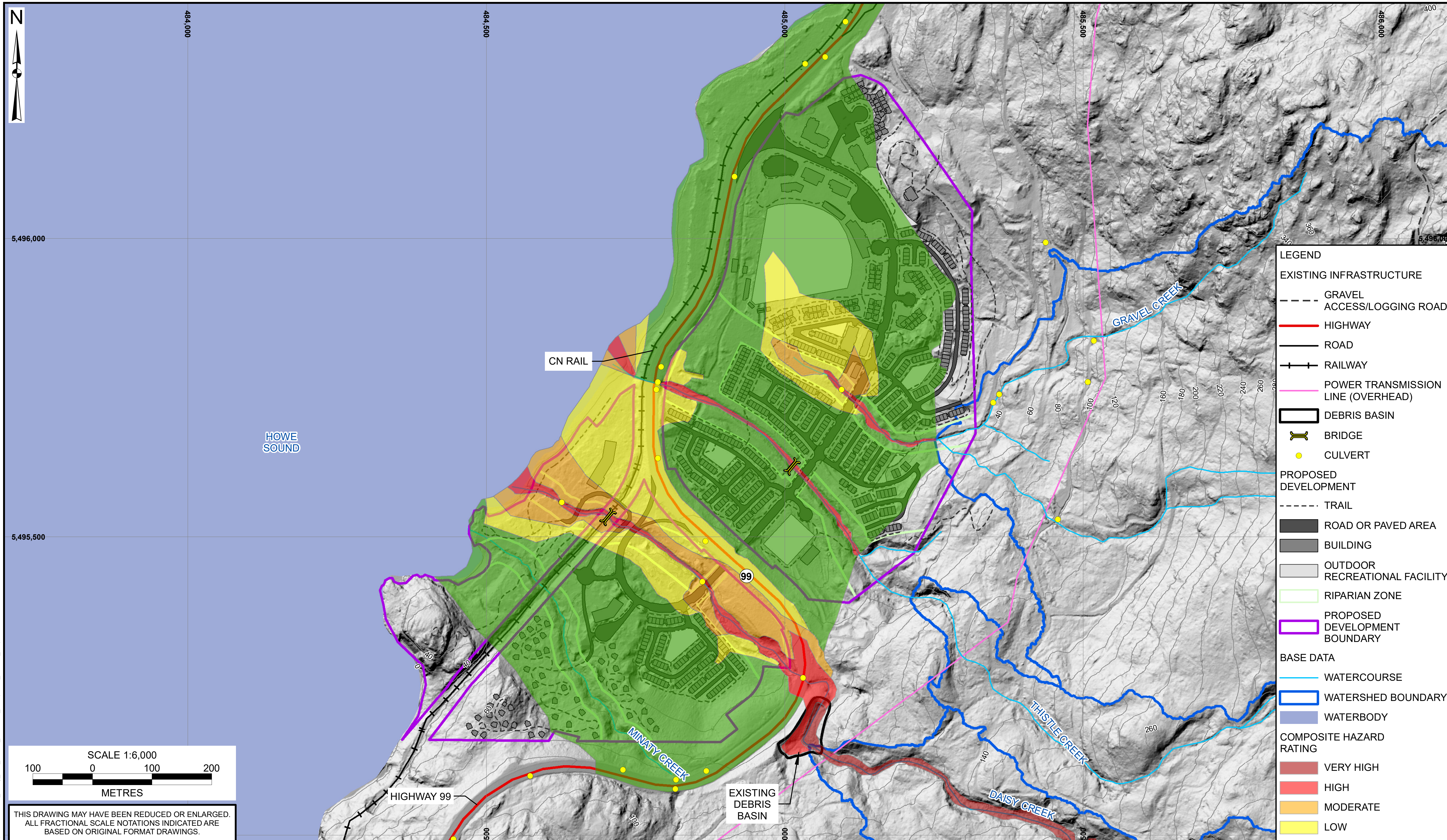


NOTES:
1. ALL DIMENSIONS ARE IN METRES UNLESS OTHERWISE NOTED.
2. THIS DRAWING MUST BE READ IN CONJUNCTION WITH BGC'S REPORT TITLED "DAISY, THISTLE, AND GRAVEL CREEKS HAZARD AND RISK ASSESSMENT", AND DATED DECEMBER 2022.
3. BASE TOPOGRAPHIC DATA BASED ON LIDAR PROVIDED BY THE GEOBC, DATED JUNE 18, 2019. CONTOUR INTERVAL IS 20 m.
4. BASE TOPOGRAPHIC MAPPING FROM CANVEC. STREAM LINES WERE MODIFIED BY BGC BASED ON LIDAR, AERIAL IMAGERY, AND FIELD OBSERVATIONS.
5. BGC REFERS TO "MINATY CREEK" FOR CONSISTENCY BUT NOTES THAT IT IS NOT PART OF A PUBLIC DATASET.
6. COMPOSITE HAZARD RATINGS PORTRAYED ON THIS DRAWNIG ONLY REPRESENT HAZARDS STUDIED WITHIN THE PROPOSED DEVELOPMENT BOUNDARY.
7. PROPOSED DEVELOPMENT DIGITIZED BY BGC BASED ON DWG PROVIDED BY TIGERBAY DEVELOPMENT ON APRIL 1, 2022.
8. THIS MAP DOES NOT ACCOUNT FOR AUXILLARY HAZARDS SUCH AS ROAD EMBANKMENT EROSION, CREEK BANK FAILURES, OR CHANNELIZATION IN LOOSE SEDIMENTS SHOULD A FLOW DIVERSION OCCUR. IT ALSO DOES NOT ACCOUNT FOR ANY HUMAN INTERFERENCE DURING THE RUNOFF EVENTS.
9. WATERSHED BOUNDARIES AND BRIDGES DIGITIZED BY BGC.
10. CULVERT DATA PROVIDED BY MOTI ALONG HIGHWAY 99 AND UPDATED WITH BGC FIELD OBSERVATIONS WITHIN PROPOSED DEVELOPMENT AND WATERSHEDS.
11. COORDINATE SYSTEM IS NAD 1983 UTM ZONE 10N. VERTICAL DATUM IS UNKNOWN.
12. UNLESS BGC AGREES OTHERWISE IN WRITING, THIS DRAWING SHALL NOT BE MODIFIED OR USED FOR ANY PURPOSE OTHER THAN THE PURPOSE FOR WHICH BGC GENERATED IT. BGC SHALL HAVE NO LIABILITY FOR ANY DAMAGES OR LOSS ARISING IN ANY WAY FROM ANY USE OR MODIFICATION OF THIS DOCUMENT NOT AUTHORIZED BY BGC. ANY USE OF OR RELIANCE UPON THIS DOCUMENT OR ITS CONTENT BY THIRD PARTIES SHALL BE AT SUCH THIRD PARTIES' SOLE RISK.

| | |
|---|---|
| SCALE: | 1:6,000 |
| DATE: | DEC 2022 |
| DRAWN: | CM |
| REVIEW: | HKW |
| APPROVED: | LCH |

CLIENT: TIGER BAY DEVELOPMENT CORP

BGC

PROJECT: DAISY, THISTLE, AND GRAVEL CREEKS HAZARD AND RISK ASSESSMENT

TITLE: COMPOSITE HAZARD MAP

PROJECT No.: 2143002

DWG No: 08

X:\Projects\2143002\GIS\Production\Report\20220429_Daisy_and_Thistle_Creek\08_Composite_Hazard_Map.mxd